AD-A191 510 DESIGN MANUAL FOR GEOTEXTILE-RETAINED EARTH WALLS(U) 1/2
DELAWARE UNIV NEWARK DEPT OF CIVIL ENGINEERING
D LESHCHINSKY SEP 85 CE-85-51

UNCLASSIFIED F/G 8/10 NL

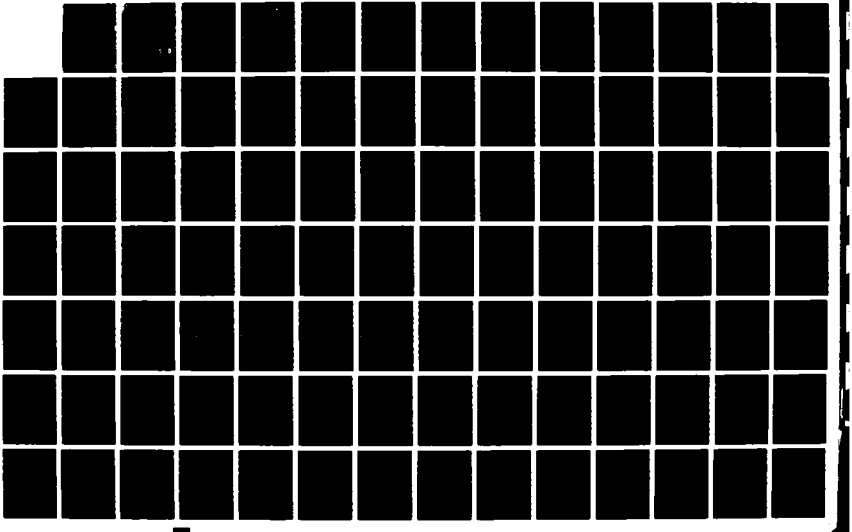

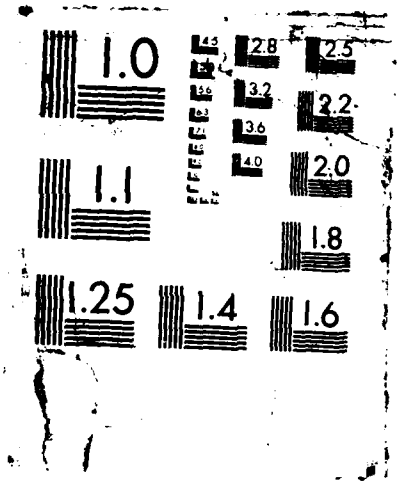
1.0
2.8
2.5
3.2
2.2
3.6
4.0
2.0
1.1
1.8
1.25
1.4
1.6

DESIGN MANUAL FOR GEOTEXTILE-RETAINED EARTH WALLS

By

Dov Leshchinsky

Research Report No. CE-85-51

September 1985

Department of Civil Engineering
University of Delaware
Newark, DE 19716

Prepared for the
US Army Engineer Waterways Experiment Station
Vicksburg, MS 39180

as part of
TM 5-800-8 on ENGINEERING USE OF GEOTEXTILES

TABLE OF CONTENTS

7-1. INTRODUCTION

Soil, especially granular, is relatively strong under compressive stresses. A typical reinforcing material, on the other hand, can carry significant tensile forces. When combined, a reinforced soil is attained. Because of the interaction of the reinforcement and soil, the resulted composite structure possesses higher strength. This extra strength means, for example, that a slope can be built steeper.

Earth reinforcement is an ancient concept used by mankind for about 8000 years. A typical example is the mixture of clay and straw utilized for the construction of dwellings. More details, including an instructive historical overview of earth reinforcement evolution, are given by Jones (1985).

Geotextile, a fabric made of polymer material, was introduced as a soil reinforcing agent in the late 1950s. Since the early 1970s, it has been utilized in the construction of retained soil walls. In these walls, the geotextile sheets are used to wrap compacted soil in layers producing a stable composite structure. Geotextile-retained soil walls somewhat resemble the popular sandbag walls which have been used for some decades. Contrary to sandbag walls, however, geotextile reinforced walls

can be constructed to significant height because of the geotextile's higher strength and a simple mechanized construction procedure.

Some advantages of reinforced walls over conventional concrete walls are:

1. The reinforced wall is flexible, thus it can undergo significant deformation or sustain significant dynamic impacts.
2. The construction of reinforced walls is simple and rapid. This is especially true with geotextile reinforced walls.
3. In many cases the reinforced wall cost-effectiveness compares favorably with conventional walls. Geotextile walls are very competitive.

Some disadvantages are:

1. Excavation behind the reinforced wall may seriously affect its performance.
2. Because of stability requirements the reinforced wall width is typically 0.7 to 0.9 its height. This requires construction space behind the wall face that is 2 to 3 times greater than a conventional concrete wall.

It should be stated that due to limited experience with embedded geotextiles there is still a question regarding its endurance, i.e., its ability to resist chemical and biological

degradation or to resist creep over the long-run (Mitchell (1984)). However, up-to-date performance of geotextiles in walls and other related installations is encouraging.

Applications of geotextile reinforced walls range from construction of temporary road embankments to permanent structures remedying slide problems and widening highways effectively. Such walls can be constructed as noise barriers or even as abutments for secondary bridges. Because of these walls' flexibility, they can be constructed in areas where poor foundation material exists or areas susceptible to earthquake activity.

In section 7-2 a few case histories are presented. Section 7-3 presents briefly the analysis dealing with the internal stability of the geotextile reinforced walls. Section 7-4 deals in detail with the wall design. It covers material selection, and internal and external stability of the wall. Sections 7-5 and 7-6 suggest construction and maintenance procedures.

7-2. CASE HISTORY EXAMPLES

Table 7-1, after Chassie (1984), provides general information regarding some geotextile reinforced walls constructed in the U.S. Notice, however, that project number 8 deals with an allied product (i.e., geogrid), which is beyond the scope of this report (further information about this project is published by Bell et al. (1984) and Szymoniak et al. (1984)). Notice also that projects number 3 and 5 are innovative whereas a sawdust is

Table 7-1. Case history examples (Chassie (1984))

	Project Location and Application	Agency	Year Built	Fabric Type	Backfill	Facing Treatment	Max. Wall Ht. (ft.)	Wall Face Area (ft^2)	Total Cost $/S.F.
1.	Olympic N.F.-Wash.State (retain fill for roadway widening)	USFS	1975	Bidim & Fibertex	Granular Soil	Asphalt Emulsion	18	2,240	$11.80
2.	Gifford Pinchot N.F.-Wash. State (retain fill for roadway widening)	USFS	1980	Fibertex #200	Granular Soil	Asphalt Emulsion	18	925	$28.00
3.	Mt. Baker N.F.-Wash. State (retain fill-roadway widening across slide area)	USFS	1980	SUPAC 5W	Sawdust	Asphalt Emulsion	6	1,750	$29.00
4.	Columbia County-New York State Rte. 22 & 71 (retain fill-slide correction)	New York DOT	1980	Bidim C-34	Crushed Stone	3" Thick Wire Mesh Reinforced Shotcrete	16	3,700 (2 walls)	$30.00
5.	Willamette N.F.-Oregon (retain fill-roadway widening across slide area)	USFS	1981	SUPAC 5W	Sawdust	Asphalt Emulsion	28	2,960	$18.90
6.	I-70 Glenwood Canyon, Colorado (fill retaining walls)	Colorado DOT	1982	Fibertex (Cx 200 & 400) Typar (D3401, D3601) Trevira (H1115, H1127) SUPAC (4P, 6P)	Gravel	2" Thick Wire Mesh Reinforced Shotcrete	15	4,500	$12.50
7.	U.S. 26 - Oregon (temporary widening across slide area)	Oregon DOT	1983	Mirafi 600X	Sandy, Clayey Silt (Native Soil)	None (Temporary wall)	16	6,000	$8.55
8.	Devil's Punch Bowl Slide Correction	Oregon DOT	1983	Tensar SR 2	Crushed Basalt	Sod Facing (Tensar is UV Resistant)	30	3,900	$23.70

NOTES: 1. Cost data tabulated above is the total in-place wall cost which includes the cost of all wall material, backfill, facing treatment, equipment and labor.
2. Walls on projects 2 and 3 were change ordered into project, which may be part of the reason for higher cost.
3. Higher cost of project 4 was due primarily to very high cost of crushed stone backfill used ($24.40/C.Y.).
4. Walls on project 6 were built on clay foundation and have been subjected to over 12 inches differential settlement over a 150 foot length of wall without significant structural distress occurring in wall or shotcrete face.
5. USFS = United States Forest Service, DOT = Department of Transportation.

used as lightweight fill material. This type of fill, however, cannot be considered for a permanent structure primarily because it decomposes with time.

The following are some detailed examples of walls constructed in the U.S.:

Siskiyou National Forest, Oregon (Bell et al. (1975), (1977)): During rain storms in January 1974, large quantities of surface water ran across the Illinois River Road in the vicinity of Snailback Creek in the Siskiyou National Forest. This runoff washed the fill slope and natural slope below and eroded a trough about 35-40 feet wide and 4-6 feet deep. This erosion removed the outside shoulder of the road and approximately two feet of the road surface. Slope reconstruction was judged not to be suited to this location. Considering economics and the requirement of limited construction disturbance of the adjacent areas, a geotextile retained earth wall appeared suited to this location. Such a wall was selected also as an experiment to explore its construction feasibility.

Reconstruction required a wall approximately 10 feet high and 35 feet long. To facilitate construction, the excavation for the wall was ramped down at 1 1/2 to 1 slope at each end. The final wall had a center section 10 feet high and 35 feet long and two end sections each 15 feet long with their height gradually decreasing from 10 feet to zero. The actual wall construction

utilized clean concrete sand as fill. The geotextile, supplied by Crown Zellerbach, was nonwoven, needlepunched, spunbonded polypropylene weighing about one pound per square yard. Its tensile strength, assumed for design, was 65 pounds per inch and its failure elongation is about 165%. Bell et al. (1975) suggest that the ability to undergo very large strains without rupture combined with a nonwoven texture, makes the geotextile resistant to damage during construction. Coarse angular materials may be compacted over it and traveled over if a minimum thickness of twice the maximum particle size or six inches, whichever is greater, is maintained over the geotextile sheet. If a small tear does develop, the nonwoven texture resists enlarging.

The wall was constructed in three days, in mid-December 1978, by a work force which included 4 to 10 laborers and two track-mounted front loaders. The first geotextile sheet was placed directly on the subsoil. A berm of sand, approximately 2 feet wide and 1 foot deep, was placed at the front of the wall with shovels. A small vibrating plate compactor was used to compact the berm to the design layer thickness of 9 inches. The fabric was folded back over the berm. The backfill was placed and spread with the front loader augmented by laborers with shovels and compacted to be in level with the top of the berm. After the third layer was placed in the above manner, burlap bags, filled with sand and placed in a row, were substituted for the

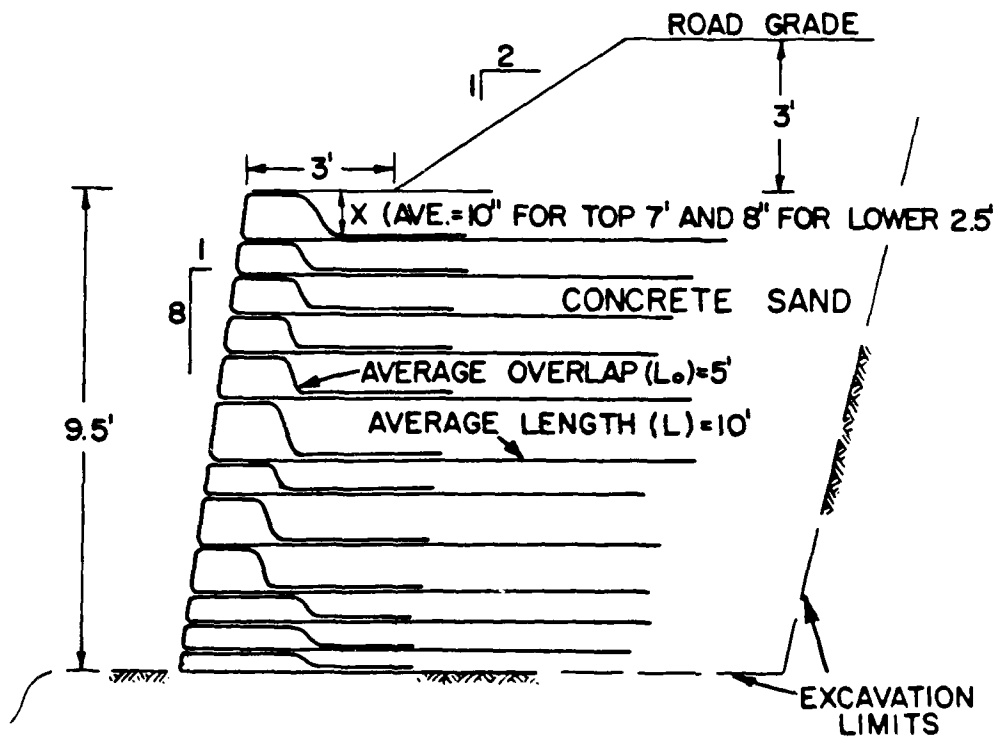

Figure 7-1. Sketch of the as-built Siskuyou wall, Oregon (Bell et al (1975)).

compacted berm. This improved the control of layer thickness, wall batter and speed of construction. A typical section of the completed wall is shown in figure 7-1. Based on at-rest lateral earth pressure (para 7-3-1), Bell et al. (1975) estimated the factor of safety for geotextile tensile strength to be 2.0.

Olympic National Forest, Washington (Mohney (1977), Bell et al. (1977)): This wall was built on the Shelton Ranger District of the Olympic National Forest in June 1975. The purpose of this particular wall was twofold: (1) to evaluate materials and construction methods, and (2) to measure horizontal and vertical movements at various locations in the wall. The wall site is located in steep terrain with 1 1/4:1 side slopes below the road and a 100 foot rock cut adjacent to the site. These conditions necessitated use of a retaining wall to gain additional road width. The site required a wall 166 feet in length and 18.5 feet high at its highest point.

A section through the wall is shown in figure 7-2. The backfill material consisted of an open graded 3" minus crushed rock (locally available). One half of the continuous wall was constructed using nonwoven polyester (weighing 6.8 and 12.0 oz/yd^2; Bidim C-28 and C-38). In the other half, nonwoven polypropylene (weighing 12.4 and 17.7 oz/yd^2; Fibertex) was used. These two geotextiles were selected so that the effect of

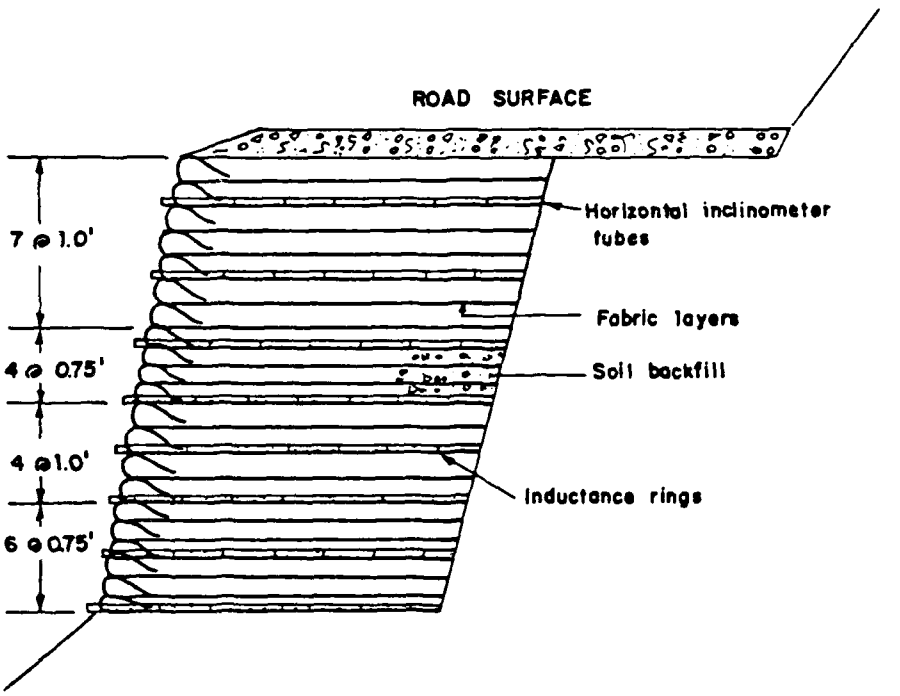

Figure 7-2. Cross-section of Olympic wall, Washington (Mohney (1977))

different stretch properties on the wall performance could be evaluated.

Mohney (1977) reports the following construction sequence. First, the excavation was made and the foundation leveled with a 4 yd^3 track loader. Next, the temporary form system was set in place (e.g., see sec. 7-5) and the first layer of geotextile rolled out. Third, the backfill material was placed and a 2-foot berm compacted at the face with the geotextile folded over the berm. Finally, the backfill was leveled with a JD 450 dozer and compacted with at least two coverages of the loader. This process was repeated for each layer until the final height was reached. The wall was constructed in 12 work days with a supervisor, three laborers and one equipment operator (Bell et al. (1977)).

To protect the wall from ultra-violet radiation, its face was sprayed with CSS 1 asphalt emulsion at a rate of approximately 0.25 gal/yd^2. This was the maximal rate that did not destroy the permeability of the geotextile. Mohney (1977) reports, however, that portions of the asphalt coating appear to have been absorbed into the fibers or have washed off. Chassie (1984) informs that a second layer of asphalt emulsion was applied in 1978.

Vertical and horizontal movements of the wall have been very small. The horizontal movement data shows slight movement

in the outer three feet of the wall. Mohney (1977) suggests that this movement may be due to downhill creep of the foundation soil or redistribution of the backfill material due to differential compaction near the face. Bell et al. (1977), state that there is no evidence of creep in either geotextile in a period of 18 months. They attribute it to their design which was controlled by a few very large live loads (i.e., logging equipment) and, therefore, the sustained dead load produced low-stresses in the fabric. Alternatively, they imply, it is possible that laboratory determination of geotextile stress-strain characteristics are inappropriate since the overburden pressure effects are not accounted for.

Columbia County, New York (Douglas (1982)): Two shallow failures in a side-hill embankment of NY-22 were observed in early 1976. The failures, 125 feet apart, extended to a length of 110 and 150 feet. Subsurface investigation showed that the upper 5 to 10 feet was loose clayey silt, sandy with gravel, overlying similar compact material. Ledge rock was encountered at depth varying from 15 to 25 feet. Indication was that slide occurred within the loose layer primarily due to inadequate drainage. The remedial selected for the slide problem was geotextile reinforced wall because it was the lowest-cost solution meeting all construction requirements (e.g., low future

maintenance, additional shoulder width and safe traffic control during construction).

The design followed the guidelines presented by Steward et al. (1977). A typical cross-section is shown in figure 7-3. The reinforcing geotextile selected was Bidim C-34, a nonwoven, needle-punched, continuous filament polyester with high strength and permeability. The chosen design tensile strength of 75 lb/in width of material represents approximately one-third the grab-test value (ASTM D-1117-69) reported by the manufacturer. Crushed-stone was selected as the fill material because of its high permeability and high internal friction. External stability, dealing with sliding of the wall along its base, was gained by widening the wall and by placing a foundation of 2 feet crushed-stone beneath the first lift. This crushed-stone layer also provided positive drainage for the wall and backfill. In one of the two adjacent construction sites, a separation layer of filter fabric was placed on the backslope of the excavation to prevent contamination of the stone backfill due to side-hill seepage.

Construction was completed in August 1980. Temporary forms were used (see section 7-5 for details). The construction sequence consisted of the following steps which were repeated in order until the wall reached full height:

1. The temporary form system was placed to line and grade.

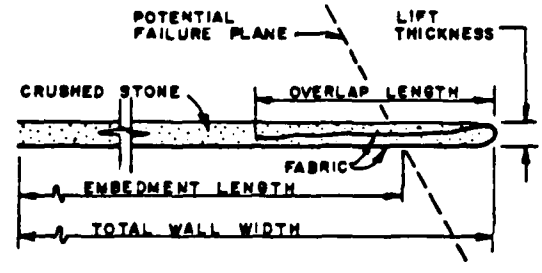

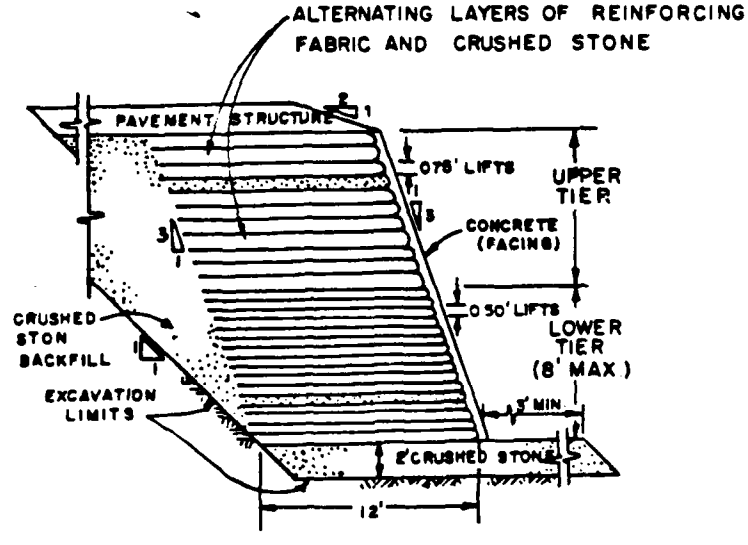

Figure 7-3. Typical section of New York wall (Douglas (1982))

2. The geotextile was positioned and the excess was draped outside the form.
3. Crushed-stone was placed to approximately one-half lift thickness and reached full thickness at the face.
4. The excess geotextile was folded back to overlap the fill, and the fill was completed to full thickness, burying the overlap; and
5. The fill was compacted, and the temporary forms were removed.

The geotextile sheets were placed horizontally, with the long dimension parallel to the centerline. The crushed-stone was dumped from a front-end loader and was back-bladed to its required thickness. When the construction area increased sufficiently, the front-end loader supplied stone and a small bulldozer was used for grading. Compaction of each lift was attained by a hand-guided vibratory compactor and as work area increased, it was replaced by a small ride-on vibratory roller. Douglas (1982) states, "Even when thoroughly compacted, the fabric at the face did not appear highly stressed and could actually be pinched by ordinary finger pressure." This observed phenomenon implies that, apparently, the wall face is not subjected to significant lateral earth pressure, at least when high quality backfill is used.

The maximum allowable exposure time of the geotextiles to ultra-violet (UV) radiation in sunlight was specified as two weeks. For UV protection and protection from vandals, the wall face was covered with a mesh-reinforced, pneumatically projected concrete (see also section 7-5).

The construction of each wall was completed within two weeks (surface areas of 1630 ft^2 and 2100 ft^2). It is interesting to note that the volume of concrete used on the facing exceeded the estimate by 40%, even with the thickness reduced from 3 to 2.5 inches. This increase occurred because of the ribbed surface of the wall and the wall batter formed a shelf between each lift. Douglas (1982) states that the cost of this project compared favorable with that of other alternatives at that site.

The walls were instrumented to investigate vertical and horizontal movements. One year after completion, the foundation settlements of both walls were between 0.25 to 1.32 inch. No foundation lateral movement was detected and horizontal movements within the wall were less than 1/4 inch.

Glenwood Canyon, Colorado (Bell et al. (1983), Barrett (1985)): Construction of this wall was completed during spring 1982. It was designed and constructed by the Colorado Division of Highways in conjunction with project I-70-2(90) in Glenwood Canyon. This canyon is a narrow, steep-walled chasm cut by the

Colorado River through resistant limestone, quartzite and granite. A major constraint in constructing any conventional rigid wall was the compressible deposits creating the foundation material. Laboratory tests indicated a settlement range of 4 to 40 inches, and settlement times of 6 months to 15 years. Surcharging was not possible due to limited space and wick drains were deemed prohibitively expensive. It was decided to use flexible wall and, on an experimental basis, four such types of walls were constructed: Wire Wall, Retained Earth, Reinforced Earth, and geotextile walls.

A primary objective of the Glenwood Canyon test was to determine lower stability limits for a geotextile earth-reinforcement system. This was investigated by designing at, or near, limiting equilibrium on portions of the wall to test the reliability of the selected design procedure given by, for example, Steward et al. (1977). A second objective was to demonstrate that the system could be constructed by a major contractor. A third objective was to demonstrate overall cost-effectiveness of the geotextile reinforcement system when directly compared to other systems. A fourth objective was to investigate the tolerance to differential settlement, and the fifth objective was to demonstrate a facing system that could perform for the design life expectancy of a wall system. A final objective was to demonstrate that the geotextiles' embedment lengths in the lower portion of the wall can be reduced, thus reducing the cost.

The geotextile test wall was approximately 15 feet high and 300 feet long. It was divided into ten 30 feet segments, with a different geotextile or geotextile strength combination used to construct segments 1-8. Segments 9 and 10 were identical to 1 and 2, except the lower geotextile layers were shortened. The segments were designed with different safety factors. Six segments had very low computed safety factors and were expected to creep, possibly to failure. Apparently no vertical joints were used between the segments. Therefore, the movements of various segments were interrelated to a limited extent. Figure 7-4 represents typical cross-sections.

Four nonwoven geotextiles were selected for the tests, each was used in two weights: Fibertex (CZ200, CZ400), Supac (P40z, P60z), Trevira (H 1115, H 1127), and Typar (D3401, D3601). These varieties represent a range of geotextile constructions, polymers, and stress-strain characteristics. None of these geotextiles has particularly high strength. The backfill soil was a free-draining, pit-run, rounded, well-graded, clean sandy gravel. Nearly all particles were less than 6 inch. Approximately 50% passed the 0.75 inch sieve and about 30% passed the No. 4 sieve.

The walls were instrumented so that settlement in the vicinity of the wall could be assessed. Information on horizontal deflection in the foundation soils and vertical deflections of the wall was obtained. Measurements of deflections of the wall

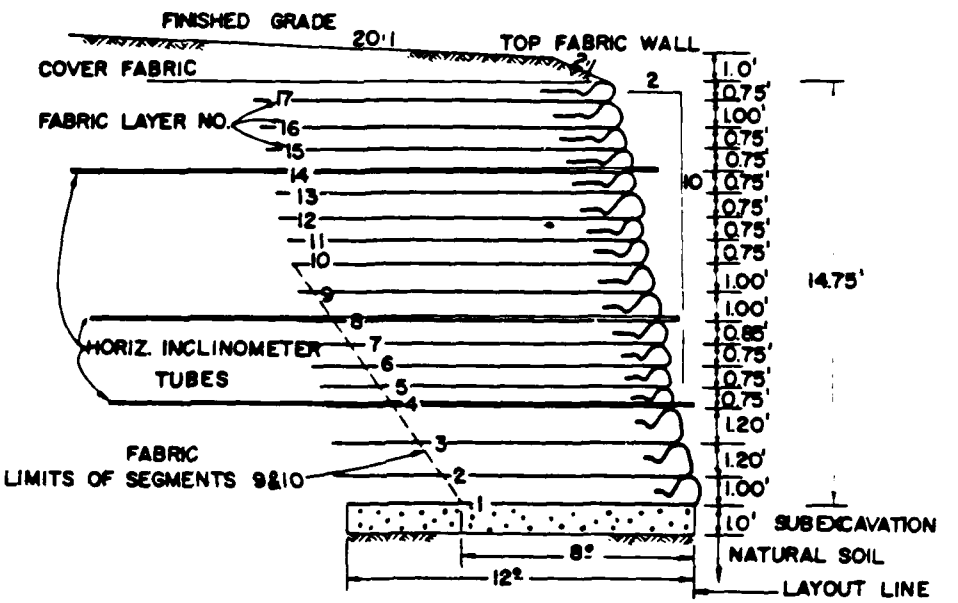

Figure 7-4. Glenwood canyon geotextile wall section, Colorado (Bell et al (1983))

face and the surface above the wall were taken to indicate settlement and creep of the geotextiles. Movements within the backfill soil mass were also monitored.

The construction technique explained in section 7-5 is very similar to the one used in the Glenwood Canyon wall. Experience shows that lifts of up to 15 inches could be used with their temporary form system (Bell et al. (1983)). Also, a continuous monitoring of the wall face inclination is recommended. That way, the specified batter can be attained at the end of construction.

New lift faces were sprayed within 5 days with a low viscosity water-cement mixture to protect the geotextile from UV radiation. The final facing utilized gunnite. This facing was applied by an experienced crew and has withstood differential settlements of about 12 inches over 300 feet in only 3 months with little cracking of the surface. About 65 yd^3 of gunnite were required for the approximately 4700 ft^2 of the wall face.

The wall was supposed to exhibit significant strains in some geotextile layers. In some segments, failure by tertiary creep was considered a real possibility. None of the above, however have occurred. Bell et al. (1983) suggest several possible reasons for this "better than expected" behavior:

1. The instrumentation did not accurately indicate the strains in the geotextiles.

2. The assumed backfill parameters used in design are incorrect.

3. The theory does not accurately model the true mechanisms.

4. The laboratory geotextile tests used do not adequately indicate the in-soil behavior of the geotextiles.

Barrett (1985) reports that a 17 feet surcharge fill was placed on top of the two weakest segments of the wall. No measurable deformation, internally or externally, about the wall has developed. Further, no creep related movement has been observed in any of the 10 test wall segments. Consolidation settlement, however, exceeded two feet at the west end of the wall. Currently, research is continuing in the form of careful exhumation of various layers, which are then subjected to grab and burst testing. The primary motive for this testing is to predict the design life for geotextile walls.

7-3. ANALYSIS

The internal stability problem of reinforced earth structure, where a material possessing high compressive strength (soil) interacts with a material possessing high tensile strength (reinforcement), is quite unique and, therefore, deserves special attention. The discussion in this section is limited to analysis dealing with the internal stability of the geotextile reinforced

wall. Analysis concerned with other aspects of the wall performance is briefly presented in paragraph 7-4-4.

7-3-1. REVIEW

A comprehensive approach to geotextile reinforced earth problem is one founded in the finite-element method (e.g., Andrawes et al. (1982), Rowe (1984)). This approach can be modified to deal with reinforced walls; however, its application to design of walls may not be practical due to its present complexity.

Currently, there are numerous limit equilibrium methods developed to deal primarily with stability of geotextile reinforced slopes (e.g., Christie and El-Hadi (1977), Fowler (1982), Ingold (1982), Jewell (1982), Murray (1982)). Essentially, in each method the failure mechanism is assumed and attempts to satisfy some of the limit-equilibrium requirements are made. These and methods alike can be modified to deal with the internal stability of reinforced walls; however, in many cases, their application may be rather involved because of the required numerical analysis.

The common analytical approaches originate from analysis of steel strip reinforced walls as presented by Lee et al. (1973, 1975). Figure 7-5 shows schematically a section through the wall. The force t_j acting on a segment of the wall face, provided there are many equally spaced geotextile sheets, is

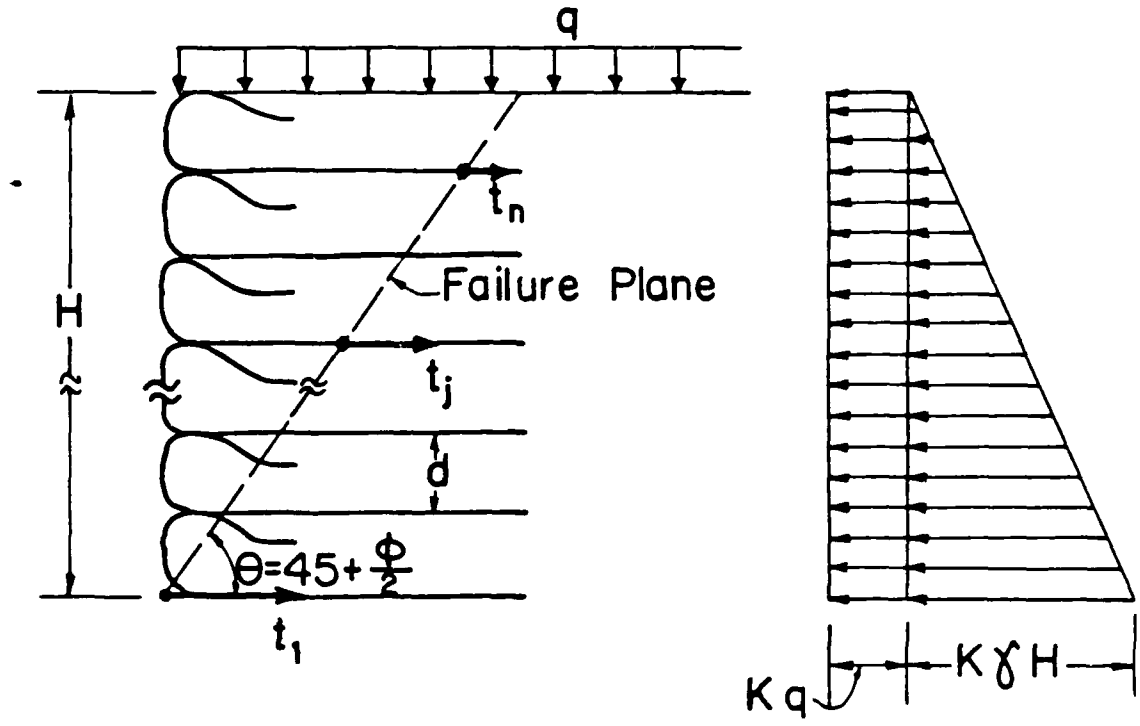

Figure 7-5. Section through the geotextile-retained earth wall and assumed lateral earth pressure distribution

$$t_j = K_a[q + \gamma(n + 1 - j)d]d \qquad (7\text{-}1)$$

where d is the geotextiles spacing; γ is the soil unit weight; q is a uniform surcharge load; n is the total number of geotextile sheets; and j is the number of a specific geotextile, $K_a = \tan^2(45-\phi/2)$ = Rankine's lateral earth pressure coefficient and ϕ is the soil angle of friction.

Although t_j is calculated at the wall face, it is assumed to act horizontally at the failure surface defined by $\theta = 45°+\phi/2$ and to be carried by the geotextile sheet (fig. 7-5). Further, it is implicitly assumed that Rankine analysis is valid despite horizontal shear stresses transferred to the soil due to its interaction with the geotextiles. Using equation 7-1 together with knowledge of the slip plane location, one can determine the required embedment length of a geotextile so as to resist pullout; i.e., develop resistance equal to t_j (e.g., Bell et al. (1975, 1977), Murray (1980, 1981)). Based on a discussion by Lee et al. (1975), however, Bell et al. (1975, 1977, 1983) used the at-rest lateral earth pressure, instead of K_a. For design of the geotextiles' embedment length, it was assumed that the reinforced soil mass fails along $\theta = 45°+\phi/2$.

Figure 7-6 represents a typical load-elongation curve of a geotextile (woven and nonwoven). Notice that as compared to steel, the reinforcing geotextile is extensible and must undergo large elongation in order to produce a significant contribution.

Subsequently, the reinforced soil must also deform largely, thus making the assumption of at-rest pressures rather questionable. It is interesting to note that there is experimental evidence indicating that using at-rest pressures may be overly conservative when extensible geotextile reinforced walls are concerned. For example, Al-Hussaini (1977), Al-Hussaini and Perry (1978) conducted a field test using extensible fabric strips as reinforcement. They concluded that Rankine lateral earth pressures are generally higher than those measured. Stilly (1974), Bell et al. (1975, 1977) conducted tests on small scale prototypes and found that failures predicted by using K_a are rather conservative. Based on field tests, Bell et al. (1983) suggest that the at-rest approach may greatly overestimate stresses in geotextiles. Considering their wall performance (see also Barrett (1985)), it appears that even the K_a approach is conservative.

It should be pointed out that by using a sliding wedge, Murray (1981) showed that if (1) all geotextiles extend to the same vertical plane, and (2) the pullout resistance of each geotextile sheet develops over the segment bracket by the slip plane and this vertical plane, the critical inclination of the failure plane deviates somewhat from $(45 + \phi/2)$. This deviation, however, is a consequence of a quadratic increase in geotextiles' pullout resistance with depth rather than linear increase which is inherent in the Rankine approach.

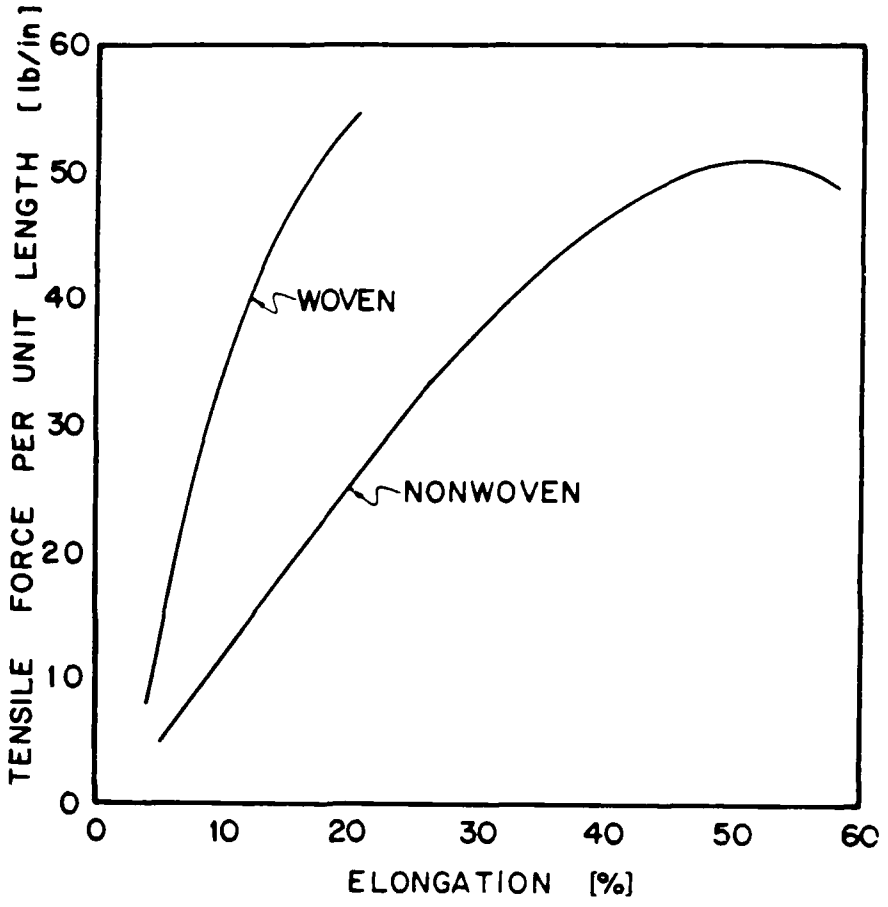

Figure 7-6. Typical force-elongation relationship of extensible woven and nonwoven geotextiles

Although the basic shape of his wall does not conform with the configuration shown in figure 7-5, it is interesting to note Broms' (1978) approach. Basically, Broms suggests to follow Terzaghi and Peck's empirical relation for laterally supported sheet-piles in sand. In this case, the lateral earth pressure is $0.65\ K_a(1.5\ q + \gamma H)$; i.e., it is constant regardless of depth. The end result of this approach is a wall comprised of geotextile sheets increasing in length as their elevation reaches the top.

7-3-2. THE MODIFIED APPROACH

The modified approach is based on a variational limiting equilibrium analysis following the procedure suggested by Baker and Garber (1977, 1978). The results of this analysis procedure satisfy all global equilibria requirements and for some practical cases, a closed-form solution can be developed. Consequently, a thorough insight of a problem behavior can be gained in a consistent manner. Furthermore, the results can be presented in practical design charts.

Details of the mathematical modification are presented by Leshchinsky (1984). The following is an outline of these details enabling further modifications so as to deal with the actual problem.

The problem is presented schematically in figure 7-7. The backfill is characterized by its unit weight γ, its friction angle ϕ and its apparent cohesion c. Each geotextile sheet

possesses a tensile resistance of t_j where j is the sheet number. In developing a design methodology it will be shown that (1) the allowable value of t may exceed only a fraction of the actual geotextile's tensile strength, (2) because of practical considerations, all geotextiles extend to the same vertical plane x = (H cot i + ℓ + ℓ_e) (fig. 7-7), (3) the geotextile restraining is along ℓ_e, i.e., the pullout resistance portion developing between the slip surface and x = (H cot i + ℓ) is neglected, and (4) the determination of the required t_j value is coupled with the geotextile pullout resistance. Based on the above one can assume that t_j is a function of the overburden pressure, obtaining the following linear relationship

$$t_j = t_1 \frac{\gamma(H-y_j) + q}{\gamma H + q} \qquad (7\text{-}2)$$

where q is a uniform surcharge load acting over ℓ_e; y_j is the elevation of geotextile j, and t_1 is the pullout resistance of the geotextile at y_1=0. It is convenient to rewrite equation 7-2 in the following non-dimensional form

$$T_j = T_1 \frac{1 - Y_j + Q}{1 + Q} \qquad (7\text{-}3)$$

where

$$Q = \frac{q}{\gamma H}$$

$$Y_j = \frac{y_j}{H}$$

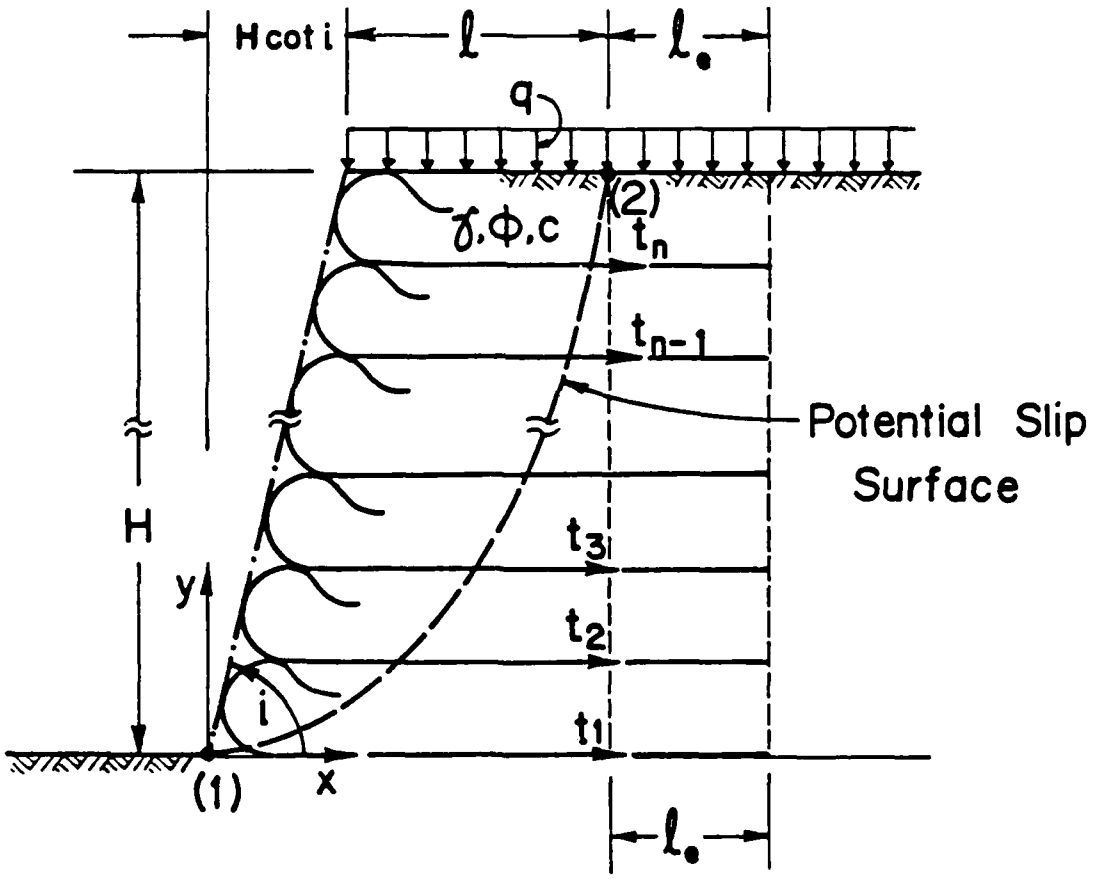

Figure 7-7. Basic definitions and conventions

$$T_j = \frac{n\, t_j}{\gamma H^2}$$

and n is the number of geotextile sheets.

It assumed that the retained soil obeys the linear Mohr-Coulomb's failure criterion

$$\tau = c + \sigma \tan\phi = c + \sigma\psi \qquad (7\text{-}4a)$$

where σ and τ are the stresses normal and tangent to the potential slip surface shown in figure 7-7, respectively; and $\psi = \tan\phi$. Once again, it is convenient to use a non-dimensional relationship

$$\bar{\tau} = N + S\psi \qquad (7\text{-}4b)$$

where

$$\bar{\tau} = \frac{\tau}{\gamma H}$$

$$S = \frac{\sigma}{\gamma H}$$

$$N = \frac{c}{\gamma H}$$

To formulate the problem in accordance with the limiting equilibrium approach, the concept of mobilized failure resistance is used. Hence, the mobilized strength of each component resisting failure in the composite structure is

$$\bar{\tau}_m = \frac{N + S\psi}{F_s} = N_m + S\psi_m \qquad (7\text{-}5a)$$

$$T_{m_j} = \frac{T_j}{F_s} \qquad (7\text{-}5b)$$

where F_s is the shear strength reduction factor, termed the factor of safety and signifying the average margin of safety; and the subscript m symbolizes a mobilized strength component. Notice that F_s is applied equally to all shear resistance components. It should be noted, however, that since T_j is dictated by the pull-out resistance which in turn is a function of ϕ (see the design procedure), F_s is actually applied only to c and ϕ (eq. 7-5), as commonly done in conventional non-composite earth structures.

The objective now is to determine the minimum value of F_s for the problem presented in figure 7-7. To attain this objective, the failure mechanism as well as S must be known. Using the variational procedure, it can be shown (e.g., Baker and Garber (1978), Leshchinsky (1984)) that there are two possible failure modes: rotational or translational. The slip surface geometry corresponding to the first mode is log-spiral and to the second mode is plane. The failure mechanism that is likely to develop, however, is the one rendering the lowest factor of safety. To completely define the failure mechanisms for the actual problem, one can assume that when the soil mass is at the verge of collapse, all geotextile sheets remain horizontal at their intersection with the slip surface. Such an assumption is commonly employed in the simplified tieback analyses. However, since geotextiles have no significant lateral stiffness and t_j is activated by soil differential movement, it is assumed that, when failure of the

composite structure occurs, the membranes at the slip surface will be inclined so as to contribute the most resistance, i.e., be most effective. It can be verified (Leshchinsky (1984)) that for rotational failure the geotextile is orthogonal to the radius of the log-spiral at their intersection. In the case of translational failure, the geotextile is inclined at ϕ_m to the failure plane where $\phi_m = \tan^{-1}[(\tan\phi)/F_s]$. These two failure mechanisms are presented in figure 7-8. It is interesting to note that these collapse mechanisms are identical to the admissible mechanisms used in the upper bound theorem of plasticity (e.g., Chen (1975)) where a rigid body is considered and the geotextile's tensile force is opposing the velocity. This equivalency has been shown by Leshchinsky et al. (1985) providing a physical interpretation for the variational extremization procedure.

To develop design charts, a closed-form solution for each failure mode was assembled. The following is just a brief presentation of these solutions.

7-3-2-1. ROTATIONAL MODE OF FAILURE

The mechanism for this mode of failure is shown in figure 7-8a. The log-spiral failure surface is

$$R = Ae^{-\psi_m \beta} \tag{7-6}$$

where R is a non-dimensional representation of a potential slip surface defined relative to a polar coordinate system having its

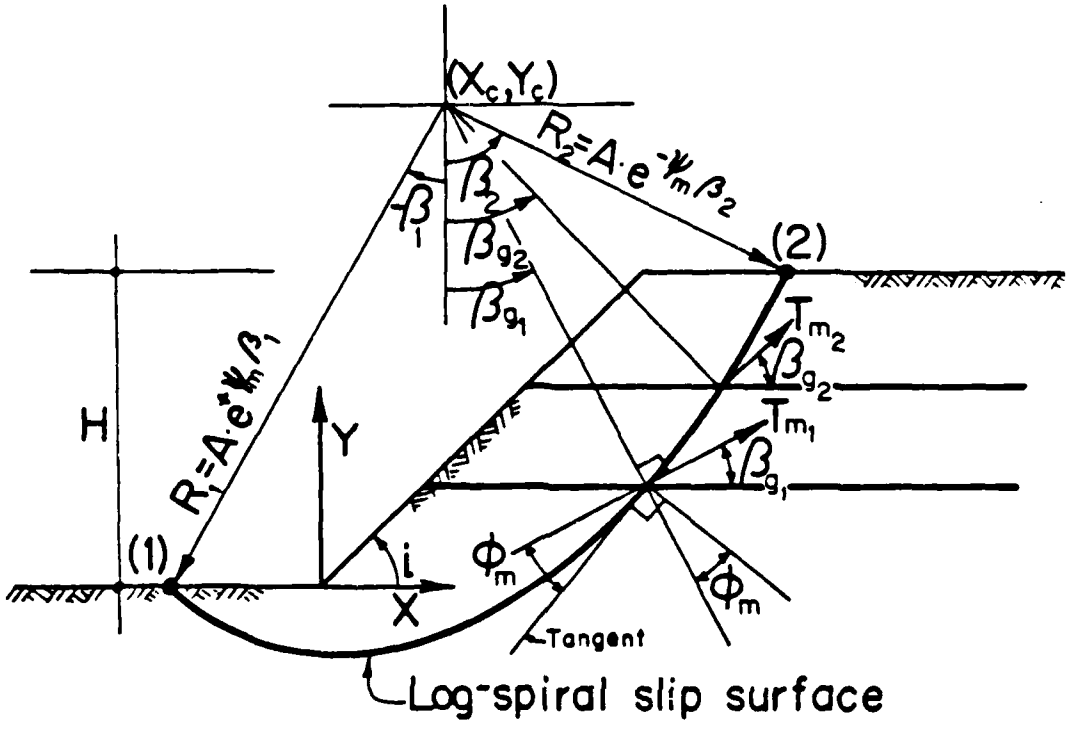

(a) Rotational

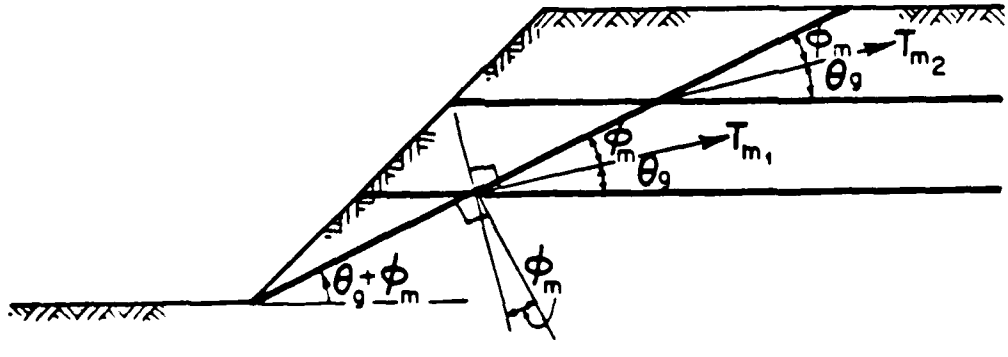

(b) Translational

Figure 7-8. Failure mechanisms

origin at an unknown point $X_c = x_c/H$ and $Y_c = y_c/H$ (fig. 7-8a); A is an unknown constant; and β is the independent variable in the polar coordinate system (equivalent to $X = x/H$).

To obtain a statically determinate problem, the normal stress $S(\beta)$ over the slip surface R (eq. 7-6) is needed. This stress should render the minimum value of the safety factor F_s for the rotational mechanism and, simultaneously, satisfy the global limiting equilibrium equations. It can be verified (e.g., Baker and Garber (1977), Baker (1981), Leshchinsky (1984)) that by using an extremization technique based on variational principles, the following non-dimensional normal stress distribution is obtained

$$S = \frac{A}{1+9\psi_m^2}(\cos\beta + 3\psi_m \sin\beta)e^{-\psi_m\beta} - N_m \frac{1-e^{2\psi_m\beta}}{\psi_m} + Be^{2\psi_m\beta} \qquad (7\text{-}7)$$

where B is an unknown constant.

Following the procedure introduced by Baker (1981), one can assemble the explicit limiting equilibrium equations for the sliding mass written about a coordinate system with an origin translated to (X_c, Y_c) -- see figure 7-8a. Utilizing equations 7-3 and 7-5b these equilibrium equations are

$$h = 0 \qquad (7\text{-}8a)$$

$$v = 0 \qquad (7\text{-}8b)$$

$$M = m_1 + N_m m_2 = 0 \qquad (7\text{-}8c)$$

where

$$h = AN_m\left\{e^{-\psi_m\beta}\sin\beta - 2\left(\sin\beta\cosh(\psi_m\beta) - \frac{\cos\beta\sinh(\psi_m\beta)}{\psi_m}\right)\right\}\Bigg|_{\beta_1}^{\beta_2}$$

$$+ AB\{(\cos\beta - \psi_m\sin\beta)e^{\psi_m\beta}\}\Big|_{\beta_1}^{\beta_2}$$

$$+ \frac{A^2}{2(1+9\psi_m^2)}\left\{[(1+3\psi_m^2) + (1-3\psi_m^2)\cos^2\beta + 2\psi_m\sin 2\beta]e^{-2\psi_m\beta}\right\}\Bigg|_{\beta_1}^{\beta_2}$$

$$+ \frac{T_{m_1}}{n}\sum_{j=1}^{n}\frac{1 - Y_j + Q}{1 + Q}\cos\beta_{g_j} \qquad (7\text{-}8d)$$

$$v = AN_m\left\{\frac{2}{\psi_m}\sin\beta\sinh(\psi_m\beta) + e^{\psi_m\beta}\cos\beta\right\}\Big|_{\beta_1}^{\beta_2} + AB\{(\sin\beta+\psi_m\cos\beta)e^{\psi_m\beta}\}\Big|_{\beta_1}^{\beta_2}$$

$$+ \frac{A^2\psi_m}{1+9\psi_m^2}\{[3-2\cos^2\beta-3\psi_m\sin 2\beta]e^{-2\psi_m\beta}\}\Big|_{\beta_1}^{\beta_2} + AY_c e^{-\psi_m\beta}\sin\beta\Big|_{\beta_1}^{\beta_2}$$

$$-X_c - Ae^{-\psi_m\beta_2}\sin\beta_2 + \frac{\cot(i)}{2} + Q[\cot(i) - X_c - Ae^{-\psi_m\beta_2}\sin\beta_2]$$

$$+ \frac{T_{m_1}}{n}\sum_{j=1}^{n}\frac{1 - Y_j + Q}{1 - Q}\sin\beta_{g_j} \qquad (7\text{-}8e)$$

$$m_1 = 2A\{\frac{\cos^3\beta}{3} + \frac{\psi_m}{1+9\psi_m^2}[\sin\beta - 3\psi_m\cos\beta]\}e^{-3\psi_m\beta}\Big|_{\beta_1}^{\beta_2}$$

$$+ Y_c e^{-2\psi_m\beta}\sin^2\beta\Big|_{\beta_1}^{\beta_2} + \left(\frac{X_c}{A}\right)^2 - e^{-2\psi_m\beta_2}\sin^2\beta_2 - \frac{\cot(i)}{3A^2}\left(3X_c - \cot(i)\right)$$

$$+ \frac{1}{A^2}Q[X_c + Ae^{-\psi_m\beta_2}\sin\beta_2 - \cot(i)][X_c - Ae^{-\psi_m\beta_2}\sin\beta_2 - \cot(i)]$$

$$+ \frac{2T_{m_1}}{nA}\sum_{j=1}^{n}\frac{1 - Y_j + Q}{1 + Q}e^{-\psi_m\beta_{g_j}} \qquad (7\text{-}8f)$$

$$m_2 = \left\{\frac{1 - e^{-2\psi_m\beta}}{\psi_m}\right\}\Big|_{\beta_1}^{\beta_2} \qquad (7\text{-}8g)$$

and where h, v and M are the horizontal, vertical and moment equilibrium equations, respectively; n is the number of geotextile sheets; and the angles defining the intersection of the slip surface with (1) the wall surface are β_1 and β_2, and (2) geotextile j is β_{g_j}.

For given i, $Q = q/\gamma H$, ψ_m, T_{m_1} and n geotextiles' elevations Y_{g_j} (j=1,2,...n), the following unknowns exist in equations 7-8a through 7-8c: N_m, A, B, X_c, Y_c, β_1, β_2 and β_{g_j} (j=1,2,...n). Thus, there are (7+n) unknowns. Additional two equations are available by virtue of the geometrical boundary conditions at

point (1) and (2) -- see figure 7-8a; i.e., the elevation of the slip surface coincides with the structure known surface: $Y(\beta_1) = 0$ and $Y(\beta_2) = 1$. It is useful to represent these two boundary conditions using the parametric equations relating the polar coordinate system to the original coordinate system (i.e., $X = X_c + R \sin\beta$ and $Y = Y_c - R \cos\beta$). After minor manipulation these equations are

$$A = \frac{-1}{e^{-\psi_m \beta} \cos\beta}\Bigg|_{\beta_1}^{\beta_2} \tag{7-9a}$$

$$Y_c = A e^{-\psi_m \beta_1} \cos\beta_1 \tag{7-9b}$$

For n geotextile sheets there are n coordinate parametric equations relating Y_{g_j} to β_{g_j}

$$Y_{g_j} = Y_c - A e^{-\psi_m \beta_{g_j}} \cos\beta_{g_j} \tag{7-10}$$

The purpose of this analysis is to assess the internal stability of a geotextile-retained soil wall. Furthermore, in the solution procedure the required N_m is sought for the given i, Q, ψ_m, T_{m_1} and Y_{g_j} (j=1,2,...n). One can state a-priori, therefore, that the slip surface (1) must exit through the toe, and (2) must not intersect the foundation material. Utilizing the geometry of the problem (fig. 7-8a), the above restrictions can be formulated in terms of the polar coordinates

$$X_c = \begin{cases} -Ae^{-\psi_m \beta_1} \sin\beta_1 & \text{if } \theta \geq 0 \quad (7\text{-}11a) \\ Ae^{+\psi_m \phi_m} \sin\phi_m & \text{if } \theta < 0 \quad (7\text{-}11b) \end{cases}$$

where

$$\theta = \beta_1 + \phi_m \quad (7\text{-}11c)$$

It should be noted that the expression for θ (eq. 7-11c) is actually the inclination of the log-spiral's tangent at β_1, measured relative to the X-axis.

An additional equation, necessary to match the number of unknowns, can be obtained from extremization of $R(\beta)$ and $S(\beta)$ at the boundary β_2. This is known in the calculus of variation as a transversality condition. It can be verified (e.g., Volk (1984)) that for the given problem, the following must exist at β_2

$$S(\beta_2)[\psi_m \cos\beta_2 + \sin\beta_2] + N_m \cos\beta_2 - Q \sin\beta_2 = 0 \quad (7\text{-}12)$$

There are now (7+n) available non-linear equations and, therefore, for given i, Q, ψ_m, T_{m_1} and Y_{g_j} (j=1,2,...n), one can determine the required non-dimensional cohesion N_m. The computation scheme used to solve these equations is presented in figure 7-9. This procedure was first presented by Baker (1981).

The computation scheme is general with respect to the shear strength parameters of the retained soil. In the design

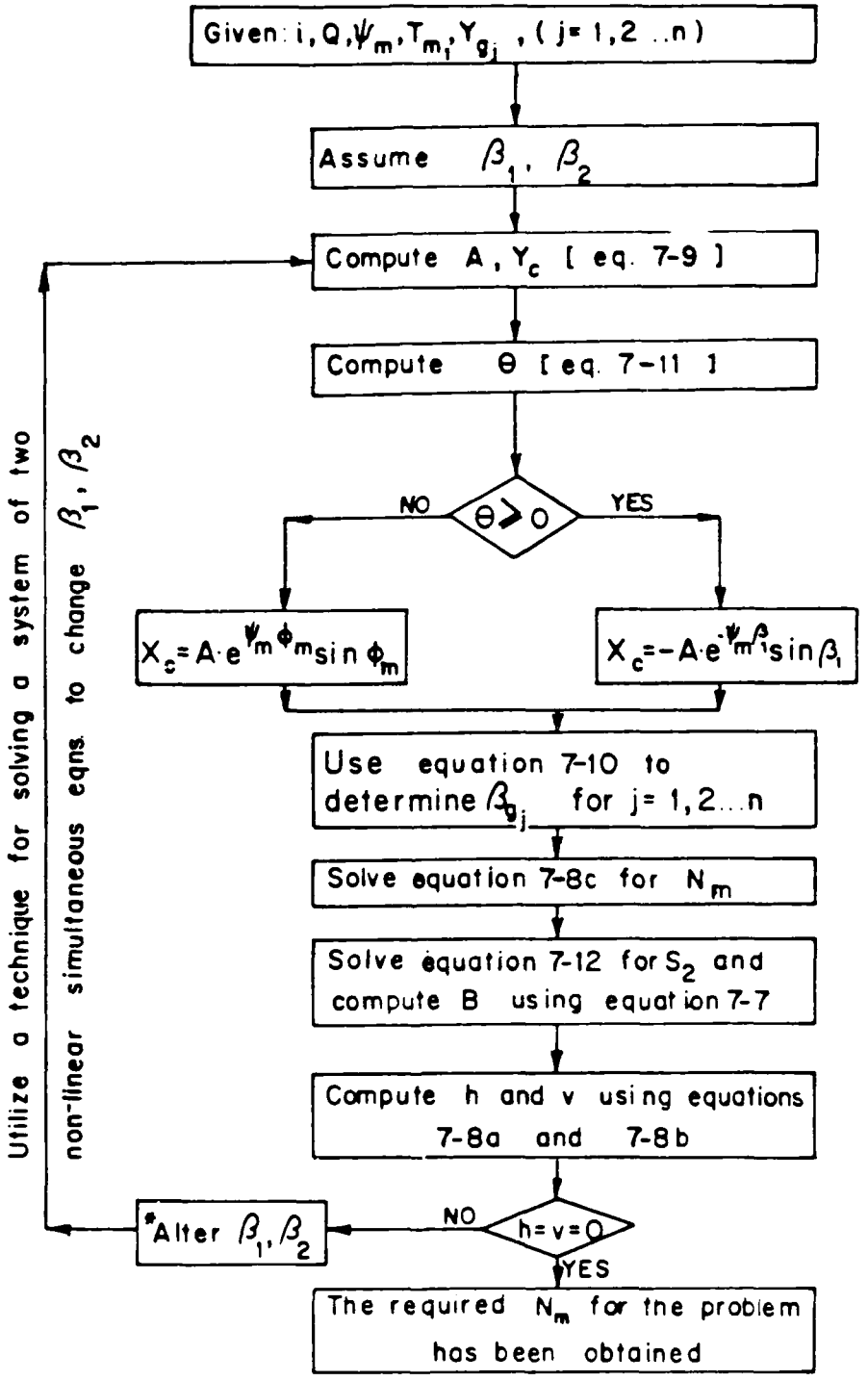

Figure 7-9. The computation scheme for the rotational failure mode

procedure presented later on, however, cohesionless backfill is specified, i.e., N_m=0. Subsequently, to utilize the computation scheme as presented, one has to use a trial and error approach seeking the required T_{m_1} for given i, Q, ψ_m and Y_{g_j} (j=1,2,...n) so that the required N_m equals zero.

7-3-2-2. TRANSLATIONAL MODE OF FAILURE

The mechanism for this mode of failure is presented in figure 7-8b. The planar failure surface is

$$Y = [\tan(\theta_g + \phi_m)]X \qquad (7\text{-}13)$$

where Y = y/H and X = x/H and θ_g is an unknown constant.

The normal stress distribution cannot be uniquely specified in this mode of failure (Leshchinsky (1984)). Therefore, developing a solution procedure similar to the rotational mode is not possible. It can be shown, however, that the force equilibrium equation, written in T_m direction (fig. 7-8b), is independent of S(X). Consequently, for given i, Q, ψ_m, T_{m_1} and Y_{g_j}, the required cohesion N_m can be written as a function of the unknown θ_g

$$N_m = \frac{1}{2}\frac{\sin\theta_g \sin(i-\theta_g-\phi_m)}{\sin i \cos\phi_m} - \frac{\sin(\theta_g+\phi_m)}{\cos\phi_m}\left\{\frac{T_{m_1}}{n}\sum_{j=1}^{n}\frac{1-Y_{g_j}+Q}{1+Q}\right.$$

$$\left. - Q[\cot(\theta_g-\phi_m) - \cot i]\sin\theta_g\right\} \qquad (7\text{-}14)$$

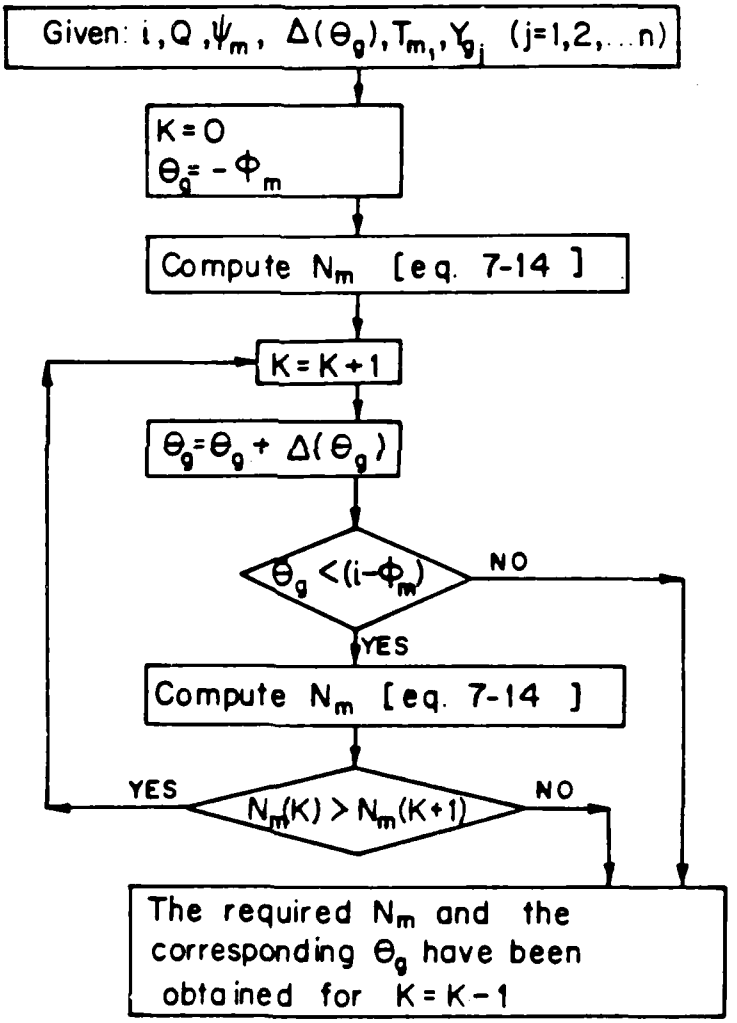

Figure 7-10. The computation scheme for the translational mode

The required N_m can be obtained now through maximization of N_m with respect to θ_g. Such a procedure is identical to Culmann analysis for unreinforced problems. It should be noted that once θ_g and the corresponding N_m are determined, one can select any stress distribution that will satisfy the other two equilibrium equations without violating Coulomb's failure condition in terms of the theoretical tensile strength of the soil.

The computation scheme for the determination of N_m is presented in figure 7-10. Notice that a numerical procedure is being used to maximize N_m with respect to θ_g. Similar to the rotational case for cohesionless soil, one can use the scheme in figure 7-10 by employing a trial and error approach, seeking the required T_{m_1} for given i, Q, ψ_m and Y_{g_j} (j=1,2,...n) so that max(N_m) equals zero.

7-3-2-3. TYPICAL RESULTS

In the recommended design procedure only cohesionless soil is prescribed as a backfill material. The attention here, therefore, is restricted to this type of soil (i.e., N_m=0). In each analyzed case, the required T_{m_1} for given ϕ_m and N_m=0 was computed twice: for rotational and translational modes of failure. The presented results, however, are only for the prevailing critical mode, i.e., the mode for which the required T_{m_1} is maximum. It should be pointed out that the transition, in terms of the required

T_{m_1} and slip surface for a given case, is smooth as one failure mode becomes more critical than the other.

The results indicate that for vertical walls the critical slip surface is always planar (e.g., fig. 7-11). As the wall face inclination flattens, however, the log-spiral surface becomes the critical one (e.g., fig. 7-12). Figures 7-11 and 7-12 demonstrate the following trends:

1) As ϕ increases (i.e., $\lambda_{T\phi}$ decreases) the critical surface becomes shallower.
2) As t_1 increases (i.e., $\lambda_{T\phi}$ increases) the critical surface becomes deeper.
3) As Q increases, a shallower slip surface is rendered.
4) As the geotextile's restraining force distribution increases for constant T_{m_1} (i.e., the larger the area over which Q is acting) the slip surface becomes deeper. It should be noted that the anchoring force is assumed to develop only beyond the slip surface. Consequently, if Q acts above the geotextile's restraining zone, the anchoring forces increase as expressed by equation 7-3.

Figures 7-12 and 7-14 illustrate the complete failure mechanisms. The vectors representing T_{m_j} are plotted parallel to their line of action. Notice that when Q acts above the

(a) No surcharge load

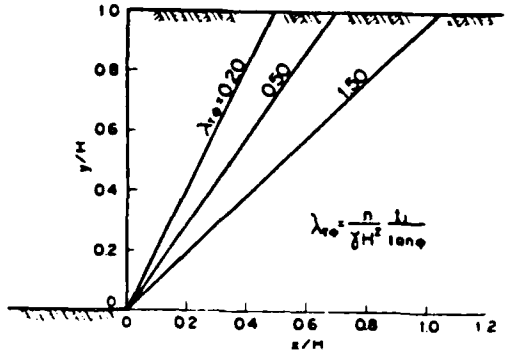

(b) Surcharge load acts over large area

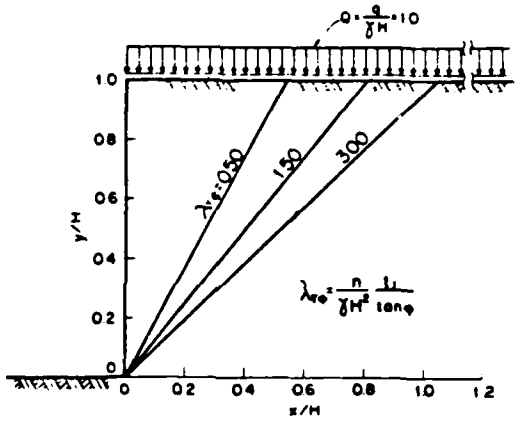

(c) Surcharge load acts only on top of the sliding mass

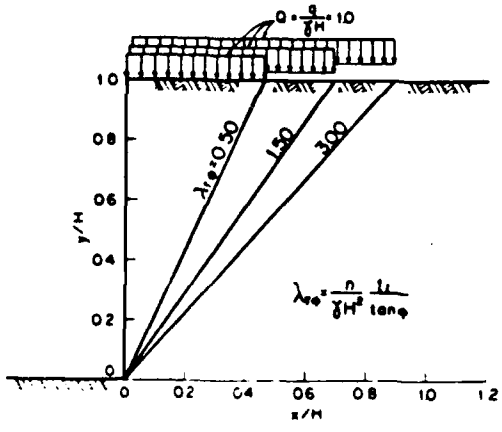

Figure 7-11. The effect of $\lambda_{T\phi}$ on the potential slip surface (vertical wall)

(a) No surcharge load

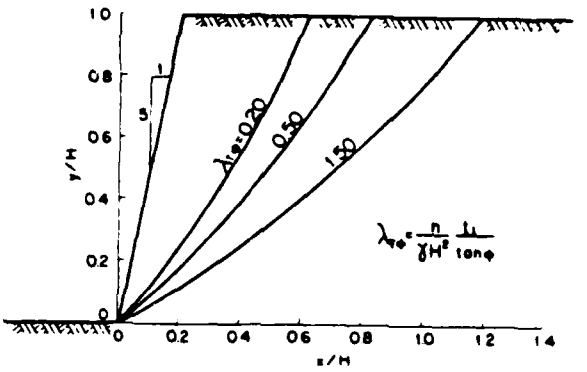

(b) Surcharge load acts over large area

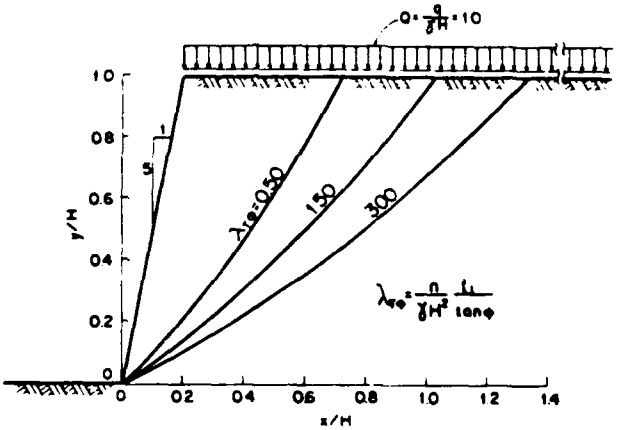

(c) Surcharge load acts only on top of the sliding mass

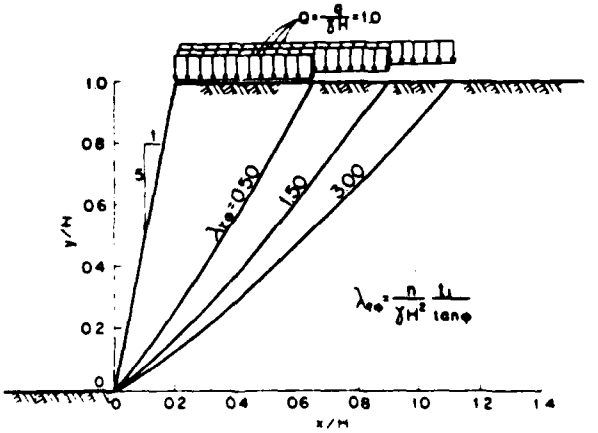

Figure 7-12. The effect of $\lambda_{T\phi}$ on the potential slip surface (inclined wall)

(a) No surcharge load

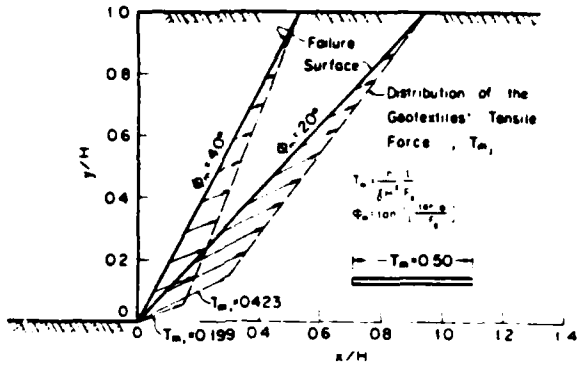

(b) Surcharge load acts over large area

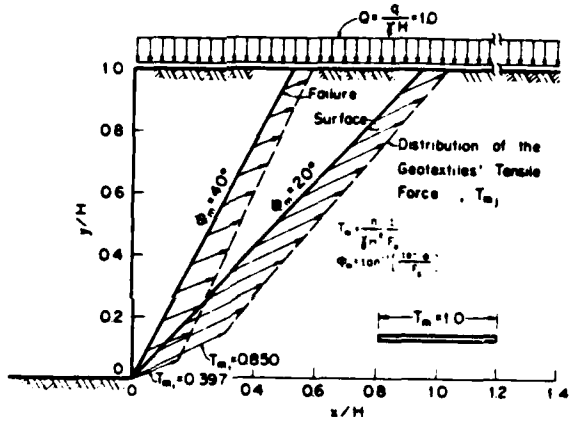

(c) Surcharge load acts only on top of the sliding mass

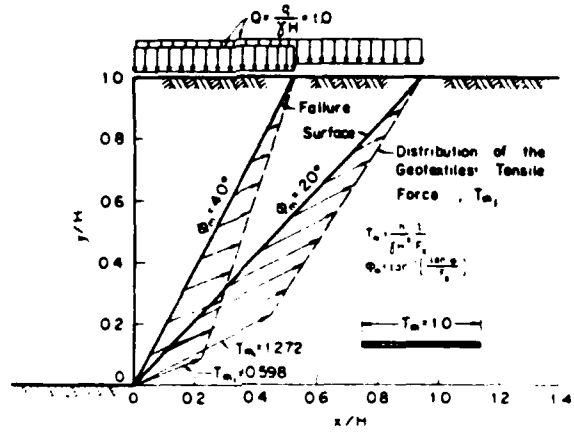

Figure 7-13. Distribution of geotextiles' tensile force (vertical wall)

(a) No surcharge load

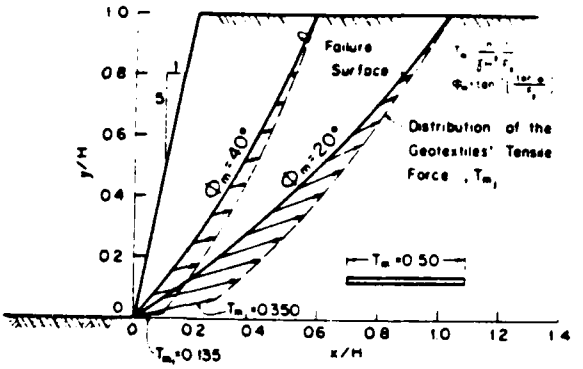

(b) Surcharge load acts over large area

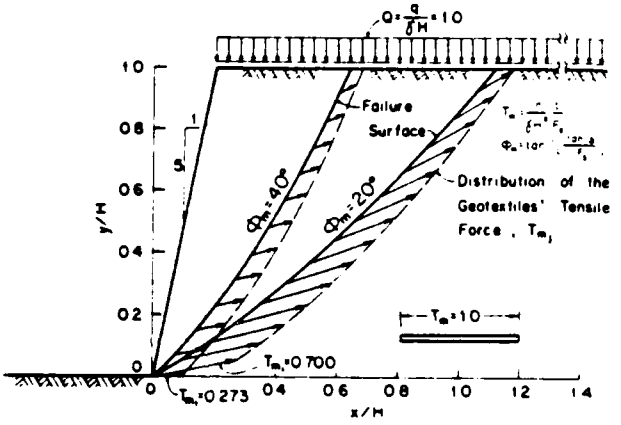

(c) Surcharge load acts only on top of the sliding mass

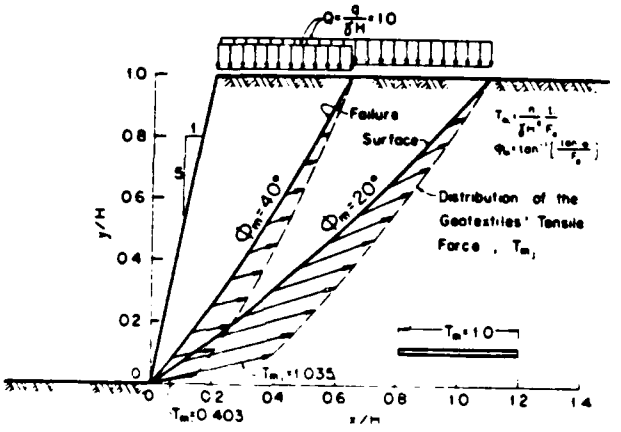

Figure 7-14. Distribution of geotextiles' tensile force (inclined wall)

geotextiles' restraining zone, a trapezoidal distribution of T_{m_j} is attained and consequently, a lower value of T_{m_1} is needed.

Figures 7-15 and 7-16 show typical distributions of stress normal to critical slip surfaces. As stated before, there is no unique solution for S(X) when planar failure is considered. The normal stress distributions illustrated for the translational case, however, were obtained via a numerical approximation using the rotational solution scheme, utilizing the fact that the transition between the two failure modes is smooth.

It has been observed that an increase in T_{m_1} results in an increase in the magnitude of compressive stress over the slip surface. Consequently, the soil's shear resistance increases and higher stability is attained.

It is interesting to assess the effect the assumed inclination of T_{m_j} has on the analysis results. One can repeat the procedure presented in paragraphs 7-3-2-1 and 7-3-2-2 for the case where geotextile sheets (and hence T_{m_j}) are assumed to be horizontal at the slip surface. Appendix 7-B contains a set of charts developed based on this assumption. Paragraph 7-4-3 deals with design and contains a similar set but this time for the mechanisms shown in figure 7-8. Comparison of the two sets reveals that the largest discrepancy occurs when vertical wall and $\phi_m = 15°$ are considered. The required T_{m_1} then for the horizontal case and Q=0 is only about 18% more than the required T_{m_1} for the

(a) No surcharge load

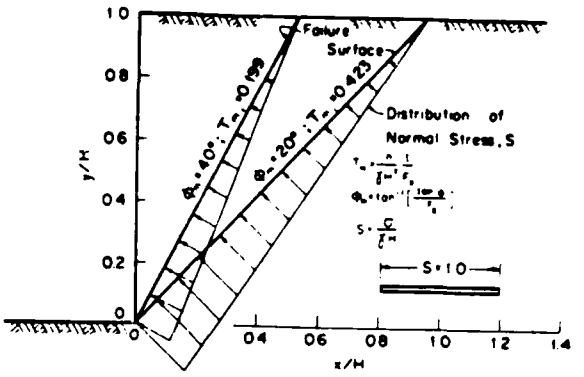

(b) Surcharge load acts over large area

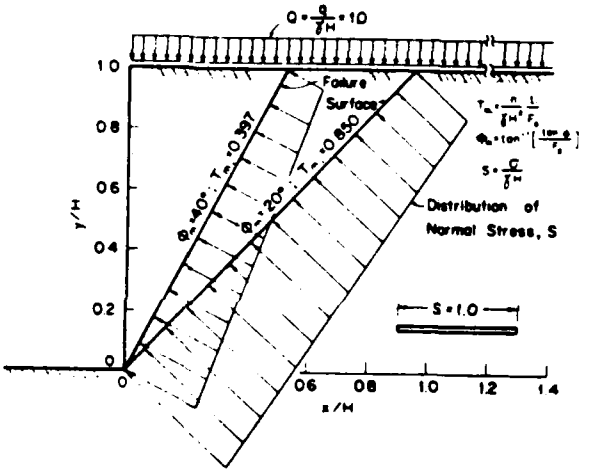

(c) Surcharge load acts only on top of the sliding mass

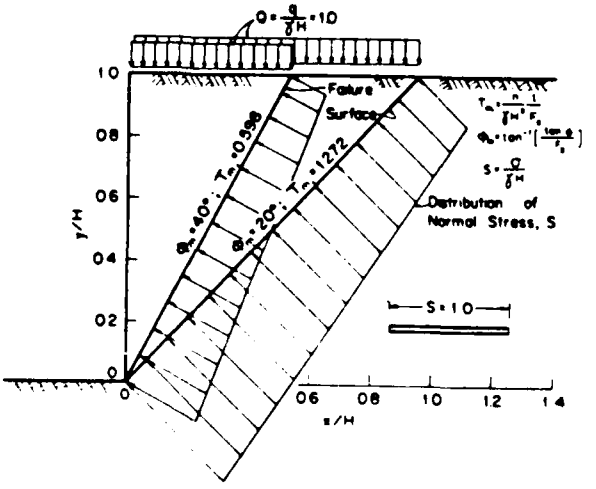

Figure 7-15. Approximated distribution of stress normal to the slip surface (vertical wall)

(a) No surcharge load

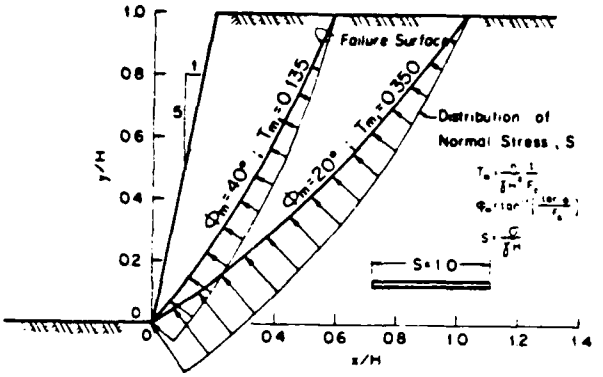

(b) Surcharge load acts over large area

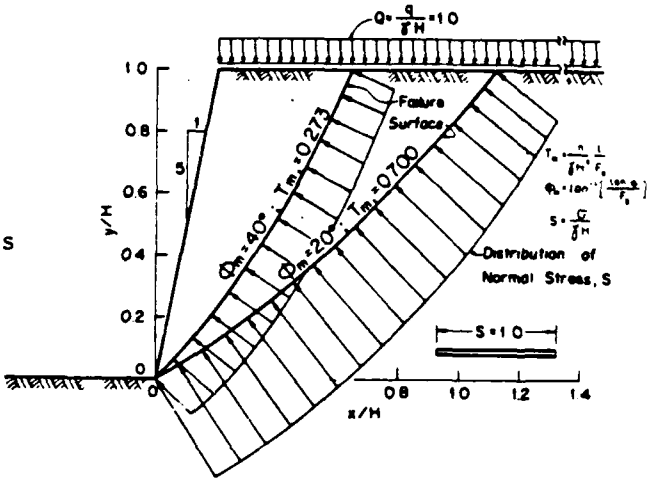

(c) Surcharge load acts only on top of the sliding mass

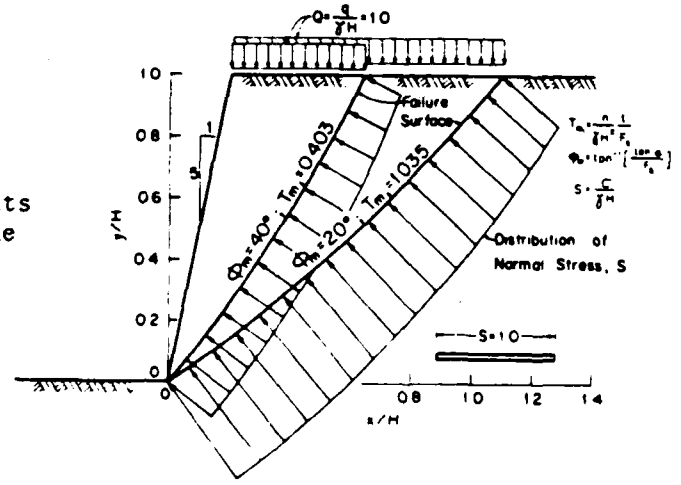

Figure 7-16. Distribution of stress normal to the slip surface (inclined wall)

mechanism adopted here. For Q=1.0 this difference remains approximately the same. When ϕ_m values larger than 15° are considered, this difference is rapidly decreasing. It can be verified that the corresponding difference in the composite structure factor of safety (F_s) is at most 11 to 12%. One should bear in mind, however, that the above comparison is valid only for cohesionless soils.

Finally, comparing predictions rendered by the modified Rankine approach (para. 7-3-1, eq. 7-1) with predictions based on the charts in appendix 7-B for vertical walls subjected to uniform loading indicates identical figures, although the analytical approaches are fundamentally different. This implies that the adopted mechanism produces somewhat non-conservative results as compared to Rankine's extended approach. Despite this apparent non-conservative deviation it was decided to use the mechanisms shown in figure 7-8 because (1) it has been shown experimentally that Rankine's predictions are rather conservative (e.g., Bell et al. (1975, 1977), Al-Hussaini and Perry (1978)), (2) the difference in F_s predictions is very small (typically only a few percents), and (3) when the composite system is at the verge of failure (note: the margin of safety is defined relative to this state), one would expect the geotextiles to contribute their maximum slide resistance thus rendering the mechanisms shown in figure 7-8. It should be noted that unlike steel, geotextiles

possess no lateral stiffness thus making the selected mechanisms possible (i.e., the geotextile sheets can bend at the slip surface). Further parametric studies of the variational solution applied to different stability problems of geotextile-reinforced earth are presented by Leshchinsky and Volk (1985) and Leshchinsky and Reinschmidt (1985).

7.4 DESIGN PROCEDURE

7-4-1. GENERAL CONSIDERATIONS

The conceptual configuration of a geotextile-retained soil wall is illustrated in figure 7-17. Notice that all geotextile sheets, except, perhaps, for the lowest one, extend to the same vertical plane. Although this configuration of the composite wall requires, apparently, an excessive embedment length of geotextiles at the lower elevations, this shape is recommended at present because of the followings:

1. The structure externally remembles the conventional steel strips reinforced wall for which extensive experience has been gained. Hence, adopting and applying the well established design approach, concerned with various potential external failure mechanisms, is straightforward.
2. Due to complex interaction, there are some uncertainties in estimating the geotextiles' pullout resistance

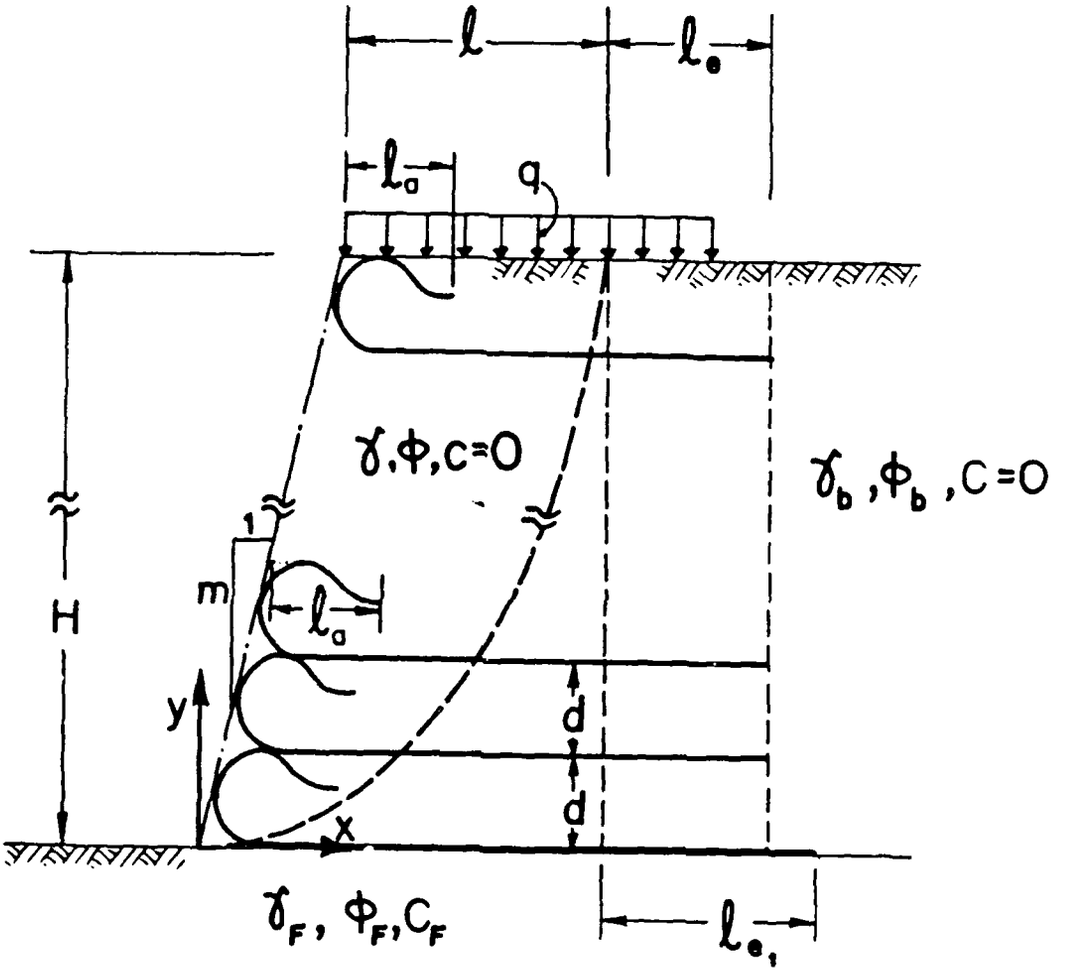

Figure 7-17. General configuration of the geotextile-retained soil wall

contributed by their embedded portion next to the idealized potential slip surface. This resistance, in turn, produces an internally stable structure. Extending the geotextile sheets beyond ℓ, neglecting any resistance effect generated along portions underneath the sliding mass, adds confidence in design.

3. Construction is facilitated due to simpler specifications.

Notice in figure 7-17 that the wall face may be inclined. This can be due to structural reasons (e.g., internal stability), ease of construction or architectural purposes (e.g., see fig. 7-18b). Also, notice that all geotextiles are equally spaced so that construction is simplified.

Geotextiles exposed to UV light degrade quite rapidly. At the end of construction, therefore, protective coating should be applied to the exposed face of the wall. Steward et al. (1977) recommend application of 0.25 gal./yd^2 of CSS-1 emulsified asphalt. Bell et al. (1983) sprayed a low viscosity water-cement mixture. This cement mixture bonded well and provided satisfactory protection, even for smooth geotextiles. To protect the face of the wall from possible vandalism, a layer of about 3 inches of gunnite can be applied (e.g., Bell et al. (1983), Douglas (1982)). This can be done by projecting concrete over a reinforcing mesh (e.g., mesh manufactured from No. 12 wires,

spaced 2 inches in each direction, supported by No. 3 rebars inserted between geotextile layers to a depth of 3 feet -- Douglas (1982)).

When aesthetics is important, a low cost solution may be the one used in Matchell Creek Project of Glenwood Springs, Colorado. For this 16 feet high wall, a facing system comprised of used railroad ties was used -- figure 7-18a (Barrett (1985)). Figure 7-18b represents a handsome but expensive solution. Notice that the walls shown in figure 7-18 are UV and vandalism protected. Their facing is part of a simple construction procedure, i.e., each facing module is placed before each layer lift, thus acting also as a form.

Note that no weepholes are specified although after UV and vandal protection measures the wall face may be impermeable. To ensure the fast removal of seeping water in a permanent structure, however, it is recommended to replace one to two feet of the natural foundation soil (in case it is not free-draining) with a crushed-stone foundation layer (Douglas (1982)). This foundation material should provide adequate drainage from within and behind the wall. The crushed-rock should be separated from the natural soil by a heavy weight filter fabric.

Since the geotextile materials are relatively new, long term effects, such as creep, chemical and biological degradation,

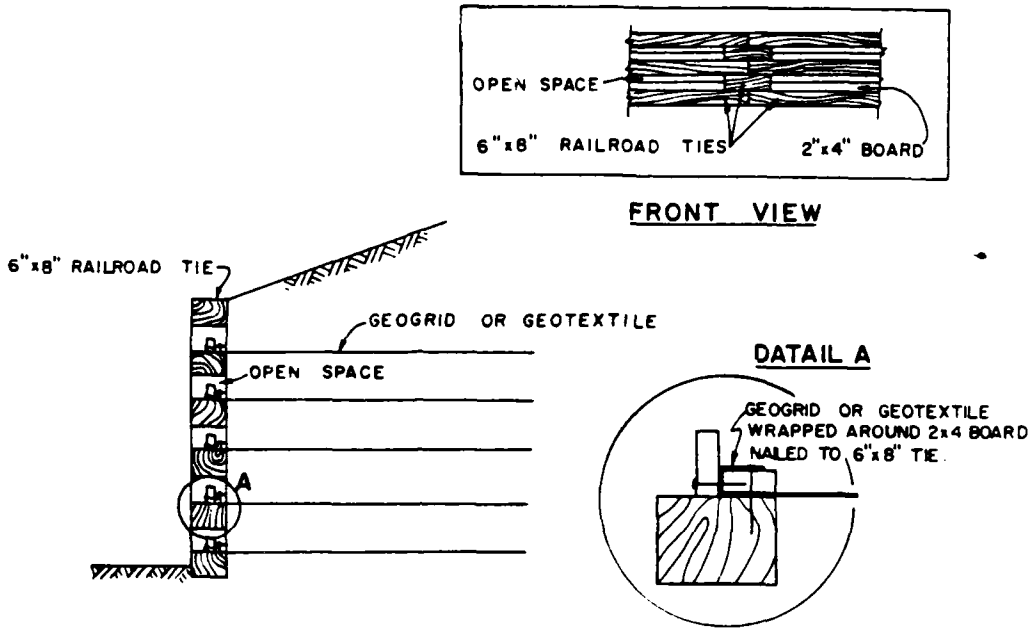

Figure 7-18a. Section of timber faced earth reinforced wall (Barrett (1985))

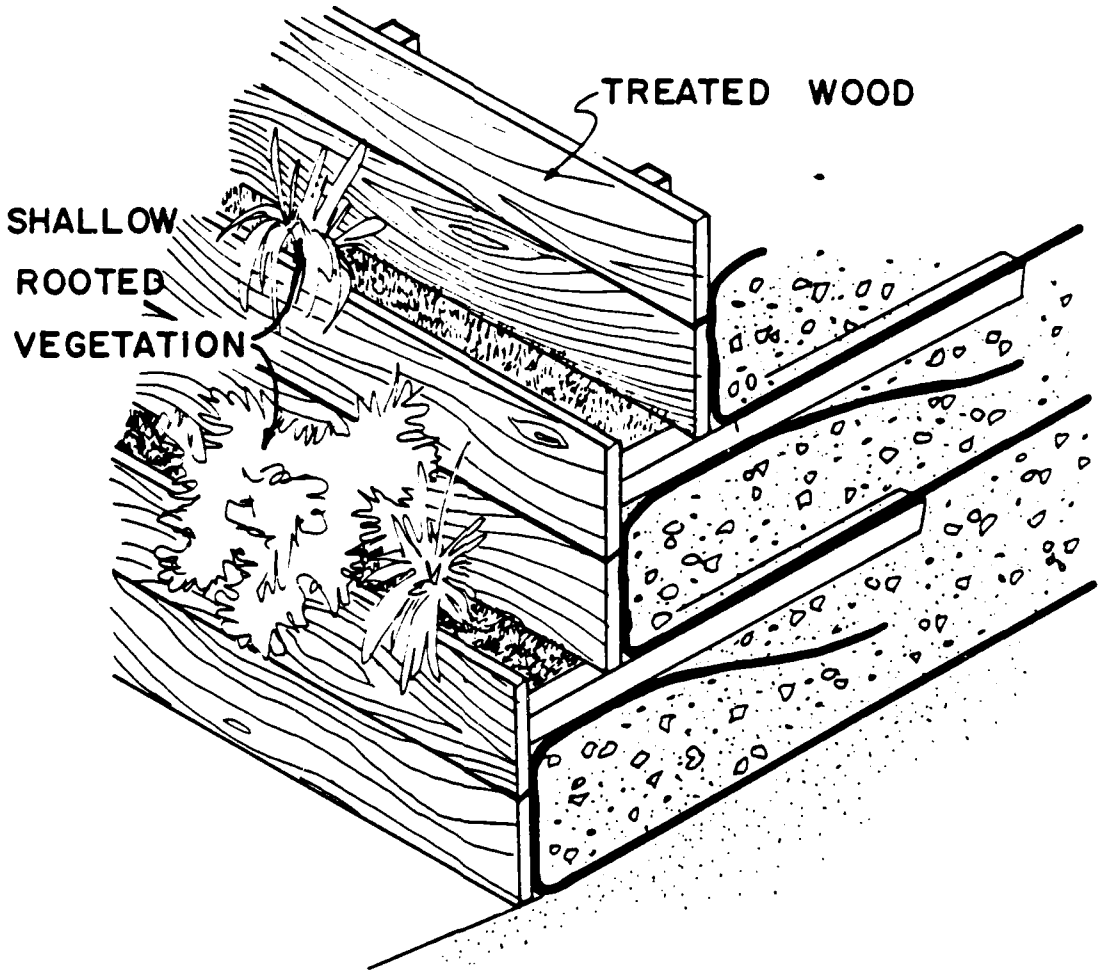

Figure 7-18b. An aesthetic arrangement of a wall face

are not known based on actual experience. Life expectancy, therefore, cannot be predicted on a non-speculative basis yet.

7-4-2. PROPERTIES OF MATERIALS

7-4-2-1. RETAINED SOIL

The soil wrapped by the geotextile sheets is termed "retained soil". This soil must be free draining and non-plastic. The ranking (most desirable to less desirable) of various retained soils for permanent walls, using the Unified Classification System, is as follows: 1. SW, 2. SP, 3. GW, 4. GP and 5. Any of the above as a borderline classification, dual designated with GM or SM. Notice that the amount of fines in the above soil is limited to 12% passing sieve #200. This restriction is mainly because of possible migration of fines, being washed by seeping water. The fines may be trapped by the geotextile sheets (or accumulate at the lower wall elevation), thus eventually creating low permeability liners. Generally, the permeability of the retained soil must be more than 10^{-3} cm/sec.

The ranking order indicates that gravels are not at the top. Although it possesses high permeability and, possibly, high strength, its utilization requires special attention. Gravel, especially if it contains angular grains, can puncture the geotextile sheets during construction. Consequently, consideration must be given to geotextile selection so as to resist possible

damage (see para. 7-4-2-3). It should be noted, however, that if a geotextile possessing high puncture resistance is available, then GP and GW should replace SP and SW, respectively, in their ranking order.

The geotextile-retained soil wall is a flexible structure, possibly deriving its composite strength from uneven deformations of the retained soil, occurring mainly during construction. Since these deformations might be of large magnitude, it is recommended to determine the retained soil internal angle of friction, ϕ, based on its ultimate strength (i.e., shearing at constant volume). Although the wall is assumed to be under plane-strain conditions, it is recommended to conduct a drained triaxial or direct shear tests to determine ϕ. The samples in these tests should be subjected to stresses similar to those anticipated in the structure. It should be emphasized that proper selection of ϕ is particularly important since it is a key factor affecting the wall's stability (see para. 7-4-3 and 7-4-4).

The retained soil unit weight should be specified based on conventional laboratory compaction tests. Because of wall performance requirements, a minimum of 95% of the maximum dry unit weight should be attained during construction. Since the retained soil will probably be (1) further densified as additional layers are placed and compacted, and (2) subjected to transitional external sources of water, such as rainfall, it is recommended to

use for design purposes the value of γ equal to the maximum density as calculated for zero air voids.

7-4-2-2. BACKFILL SOIL

The soil supported by the reinforced wall (i.e., the soil to the right of ($\ell_e+\ell$) -- see fig. 7-17) is termed "backfill soil". This soil has a direct effect on the external stability of the wall (para. 7-4-4) and, therefore, should be carefully selected.

Generally, the backfill specifications used for conventional retaining walls should be employed here as well. Such specifications are given in most geotechnical handbooks (e.g., Terzaghi and Peck (1967), p. 364). Because of limited experience with geotextile reinforced walls, however, clay, silt or any other material with low permeability should be avoided next to a permanent wall (i.e., adjacent to ($\ell+\ell_e$)). Figure 7-19 presents a possible arrangement for using such low grade backfill. Notice that a filter fabric separates the fine and the free draining backfills, thus preventing fouling of the higher quality material. Since both backfills may have an effect on the reinforced wall external stability, the properties of both materials are needed. The unit weight should be estimated similar to the retained soil; for analysis take γ equals the maximum density at zero air voids. The strength parameters should be determined using drained triaxial or direct shear tests for the permeable backfill. For the low permeability backfill, drained and undrained triaxial shear tests

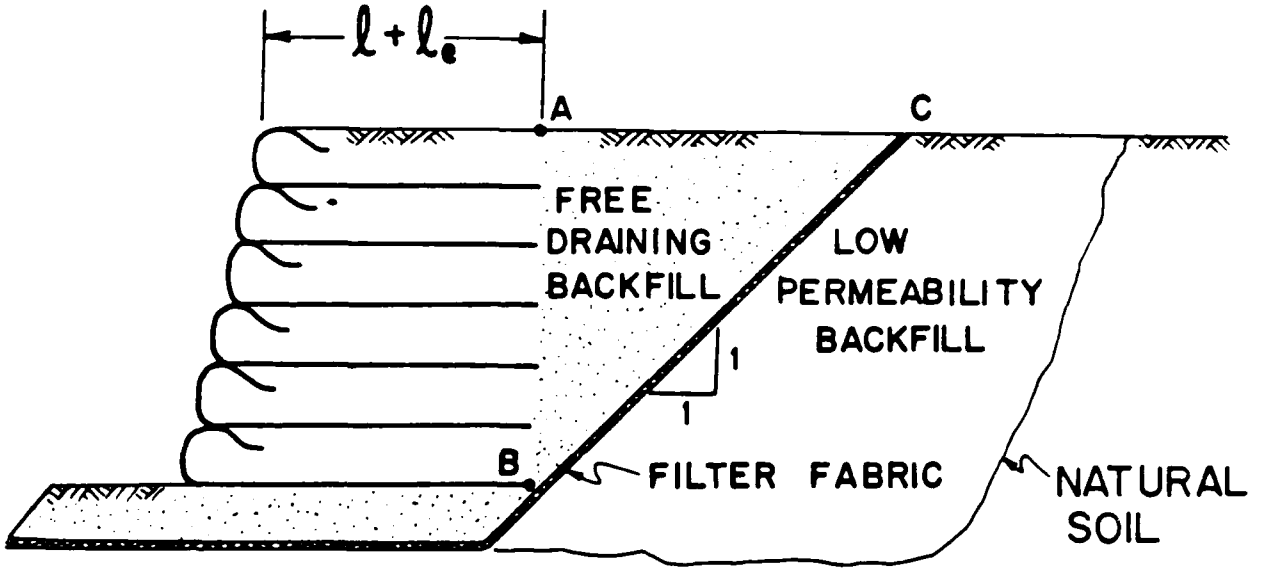

Figure 7-19. An arrangement for low permeability backfill

should be conducted so that the short- and long-term external stability of the wall could be assessed (see para. 7-4-4).

The backfill and the retained soil (line AC in fig. 7-19) must have similar gradation at their interface so as to minimize the potential for lateral migration of soil particles. If such requirement is not practical, then a filter should be designed based on the grain-size distribution of the two materials. Alternatively, a filter fabric can be used along AB.

7-4-2-3. GEOTEXTILES

Either woven or non-woven geotextiles may be used, provided they meet the required specifications.

The potential for developing a prescribed geotextile tensile resistance, t_j, must be ensured. As long as t_j, determined in the next section, is not fully mobilized, the reinforced wall must be interally stable. Most polymers, however, exhibit significant creep elongation when subjected to tensile force. This creep tendency increases rapidly with the level of tensile force. Specifying a geotextile possessing tensile strength equal to t_j, therefore, may result with intolerable wall deformations due to excessive creep. Steward et al. (1977) recommended that t_j will be selected as a fraction of the geotextile tensile strength, t_{ult}:

Geotextile Type	$\frac{\text{tensile resistance}}{\text{tensile strength}} = \frac{t_j}{t_{ult}}$
Polyester needled	0.70
Polypropylene needled	0.55
Polypropylene bonded	0.40
Polypropylene woven	0.25

It should be noted that t_{ult} has to be determined using specimen width to gage ratio of 2:1 (at least 4 inch net length), where the tensile load is applied at a constant strain rate of 10% per minute at a nominal temperature of 70°F. If the geotextile is expected to perform at higher temperature, the tensile strength test should be conducted at that temperature. The specimen must soak water for a minimum of 12 hrs and failure is not allowed near the grips. The strength should be determined in the geotextile's weakest principal direction. Also, the load-elongation curve up to failure should be determined.

Mobilization of t may require large elongation in the geotextile sheets. Consequently, large shear strains may be induced into the adjacent soil that restrain the geotextile from slipage thus enabling the development of t_j. These induced strains must be acceptable. It is recommended, therefore, to ensure that for the required tensile resistance, t_j, the corresponding geotextile sheet elongation shall not exceed 10%. This can be determined by using the load-elongation curve measured

previously. Both the creep and elongation criteria must be satisfied in selecting a geotextile based on t_j.

Research indicates that non-woven geotextiles tend to increase their strength, t_{ult}, as well as their stiffness as their confining pressure increases (e.g., McGowen et al. (1982), El-Fermaoui et al. (1982)). Because of insufficient experience, however, it is recommended to ignore this phenomenon in design.

An important component of the soil-geotextile interaction is the friction and adhesion developed at their interface. In the next paragraph it is assumed that the friction angle between the retained soil and geotextiles is $2\phi/3$. In paragraph 7-4-4 it is assumed, for external stability purposes, that the friction and adhesion between geotextiles and the foundation soil is $2\phi/3$ and $2c/3$, respectively, where ϕ and c are the foundation strength properties. The above values are commonly used in design of conventional retaining walls and experience has shown that, at least, the assumed friction value is conservatively valid for most geotextiles. In specifying a geotextile, however, one must ensure that the assumed design values for the interface are met. These values can be determined from a direct shear test using the soils involved.

If the retained soil is comprised of coarse and sharp-edged aggregate, the question whether the geotextile will survive installation arises; i.e., will it resist puncture during

construction. This survivability is heavily dependent on the construction technique and equipment. Based on experience related to highways (Christopher et al. (1984)), the following modified recommendations are given for walls with geotextile sheets spacing of up to one foot. If the aggregate average diameter is less than one-half lift thickness, use minimum puncture strength of 75 lbs. If some aggregates possess average diameter greater than one-half lift thickness, use minimum puncture strength of 110 lbs. The minimum puncture strength required for all other types of retained soil (para. 7-4-2-1) must be 40 lbs. The above strength values are for construction equipment exerting ground pressures up to 8 psi. If the exerted pressures are higher than 8 psi, the first lift should be, at least, 10 inches. Note that in this case, there will practically be only one lift equal to the geotextiles specified spacing (which is limited to a maximum of 12 inches). If coarse angular aggregate is used and the structure is anticipated to carry external loads, the thickness of the soil layer above the top geotextile sheet must be at least 18 inches, preferably of finer grade. This should protect the top sheet from possible puncture and abrasion damage during its service life. It should be noted that the above specified strength is measured by puncturing the geotextile with a 5/16 inch diameter solid steel cylinder with hemispherical tip.

Most commercially available geotextiles possess equivalent permeability which will not alter the free-draining characteristic of the wall. It is recommended, however, to specify geotextiles with equivalent permeability of, at least 10^{-2} cm/sec.

Finally, when selecting a geotextile it is worthwhile to bear in mind its cost. Barrett (1985) has indicated that the geotextile cost amounts to only 5 to 10% of the total wall's construction cost. Therefore, factors such as availability of less expensive geotextile and construction schedule must be considered in selecting a geotextile.

7-4-3. INTERNAL STABILITY

Internal stability is a result of sufficient resistance to collapse developed by the geotextile-retained soil and the geotextiles' tensile force. This type of stability can be viewed from two different prospectives. In the first one it is assumed that all shear resistance components are equally mobilized; i.e., both soil and geotextile approach their prescribed shear strength simultaneously. It is regarded as the internal stability of the composite structure and, conceptually, it is similar to the conventional slope stability approach where the cohesion and the friction are assumed to be equally mobilized. The second prospective assumes that the soil attains failure first (i.e., fully mobilized), thus activating geotextiles' tensile resistance. It implies that the structure's margin of safety against collapse

depends now on the degree of the geotextiles' tensile resistance mobilization. This type of stability is analogous to the common approach used for design of geotextile-retained soil walls.

When the composite structure is actually at the verge of failure, both of the above prospectives coincide. Adequate design, however, requires a specified margin of safety against collapse which may be different for each prospective of failure. Consequently, there is a need to assess the safety using each prospective of stability separately. It is recommended, therefore, to carry out a design trial based on each approach, using the more stringent result as the final design. This ensures that the safety, based on both criteria, is satisfied.

7-4-3-1. COMPOSITE STRUCTURE

In assessing the internal stability of the composite structure, it is assumed that the soil's friction, tan ϕ, and the geotextiles' tensile resistance, $t_j (j=1,2,...n)$, are equally mobilized. Consequently, the analysis presented in paragraph 7-3-2-2 is adequate to deal with this type of stability.

Typically, the following parameters are given: H and m (i.e., the height and face inclination of the wall, respectively); and γ and ϕ (i.e., the unit weight and internal angle of friction of the retained soil, respectively). For a prescribed factor of safety, F_s, one has to determine the required tensile resistance

of the geotextile sheets, t_j, as well as their embedment length, $\ell+\ell_e$.

To facilitate a design procedure, it is assumed that the effective restraining zone over which the geotextiles' tensile forces dissipate is ℓ_e -- see figure 7-17. The geotextiles' restraining force capacity must be, at least, equal to their required tensile resistance. Assuming these forces to be proportional to the overburden pressure one gets

$$t_j = [\gamma(H-y_j) + q]\ell_e(\mu_t + \mu_b) \qquad (7\text{-}15)$$

where y_j is the elevation of geotextile j, measured from the toe; q is a uniform surcharge load (zero if not acting over ℓ_e); and μ_t, μ_b are the friction coefficients between geotextile j and the soil above and below it, respectively. Generally, μ is a function of ϕ. It is recommended to use the following relationship

$$\mu_t = \tan(\tfrac{2}{3}\,\phi_{top}) \qquad (7\text{-}16a)$$

$$\mu_b = \tan(\tfrac{2}{3}\,\phi_{bottom}) \qquad (7\text{-}16b)$$

Since a uniform soil is retained, μ_t equals μ_b for all geotextiles j=2,3...n. This, however, may not be the case for the geotextile interfacing the foundation soil (i.e., j=1). Utilizing equations 7-2, 7-15 and 7-16, the following expressions are obtained

$$\ell_e = \frac{t_1}{2(\gamma H+q)\tan(\frac{2}{3}\,\phi)} \quad \text{for all geotextiles } j=2,3,\ldots n \qquad (7\text{-}17a)$$

$$\ell_{e_1} = \frac{t_1}{(\gamma H+q)\left[\tan\left(\frac{2}{3}\phi\right)+\tan\left(\frac{2}{3}\phi_F\right)\right]} \quad \text{for geotextile } j=1 \qquad (7\text{-}17b)$$

$$\text{If } \ell_{e_1} < \ell_e \quad \text{then take } \ell_{e_1} = \ell_e \qquad (7\text{-}17c)$$

where ϕ_F is the friction angle of the foundation material, and ℓ_{e_1} is the effective embedment length of the geotextile at the bottom -- see figure 7-17. The condition in equation 7-17c (i.e., $\ell_{e_1} < \ell_e$) can exist when $\phi_F > \phi$. It is not recommended, however, to use $\ell_{e_1} < \ell_e$. Notice that equations 7-17 do not contain any explicit factor of safety for ℓ_e (or ℓ_{e_1}). There is, however, an undeclared safety factor resulting from the added restraining capacity contributed by the neglected zone defined by the slip surface and beginning of ℓ_e.

The restraining force t_j counterbalances a force generated within the sliding mass. To ensure that t_j can indeed develop within the active mass as well as to retain the soil at the wall face, each geotextile sheet is folded back at the wall face and re-embedded over a length $(\ell_a)_j$ -- see figure 7-17. To determine $(\ell_a)_j$, the following assumptions are combined with the rationale used in stating equation 7-15:

1. The average elevation of ℓ_a is at the center in between two adjacent geotextile sheets.
2. The full intensity of t_j is carried along $(\ell_a)_j$.

3. For non-vertical walls the average overburden pressure acting along ℓ_a is proportional to $(m\ell_a/2)$ so long as it is less than H. One can see the geometrical interpretation of this assumption by looking at figure 7-17.

Based on the above, the following approximate expressions are assembled

$$(\ell_a)_j = \begin{cases} \dfrac{d}{2m}\left\{\sqrt{1 + \dfrac{8m\ell_e}{d^2}\left[(H-y_j) + \dfrac{q_e}{\gamma}\right]} - 1\right\} & \text{for } m < \infty \text{ and } \left(\dfrac{m\,\ell_a}{2}\right)_j < H \\ \ell_e \dfrac{\gamma(H - y_j) + q_e}{\gamma(H - y_j - \frac{d}{2}) + q_a} & \text{otherwise} \end{cases} \tag{7-18}$$

where q_e is a uniform surcharge load, zero if not acting above ℓ_e (same as q in equation 7-15); q_a is a uniform surcharge load, taken as zero if not acting over the entire length of $(\ell_a)_j$; m expresses the wall face inclination (see fig. 7-17); and d is the geotextile sheets spacing (see fig. 7-17).

To simplify construction, a uniform length of ℓ_a is taken. The value of ℓ_a is selected based on its maximum required length as expressed by equation 7-18. Thus ℓ_a is

$$\ell_a = \begin{cases} \dfrac{d}{2m}\left\{\sqrt{1 + \dfrac{8m\ell_e}{d^2}\left[H + \dfrac{q_e}{\gamma}\right]} - 1\right\} & \text{only for } m < \infty \text{ and } \dfrac{m\,\ell_a}{2} < H \\ 2\ell_e \dfrac{1 + \dfrac{q_e}{\gamma d}}{1 + \dfrac{2q_a}{\gamma d}} & \text{for all cases} \\ \geq 3 \text{ ft.} & \text{for all cases} \end{cases} \qquad (7\text{-}19)$$

For each problem, the longest ℓ_a should be selected. Notice that a minimal value of ℓ_a = 3 ft., adopted from Steward et al. (1977), should ease construction and, physically, will ensure adequate embedment. It is interesting to note that, in most practical cases, equation 7-19 will indicate that ℓ_a is specified by its required minimal value.

Figures 7-20a and 7-20b are design charts based on the analysis in paragraph 7-3-2-2. They represent the results only for the critical mode of collapse, i.e., either plane or log-spiral failure surface.

It is recommended to use a factor of safety of F_s = 1.5 for the composite structure. This F_s value is typical in design of slopes where long-term stability is concerned. The following are the steps necessary to utilize the charts in the design process:

1. Determine the wall's geometry; i.e., height H and face average inclination -- 1 (horizontal); m (vertical).

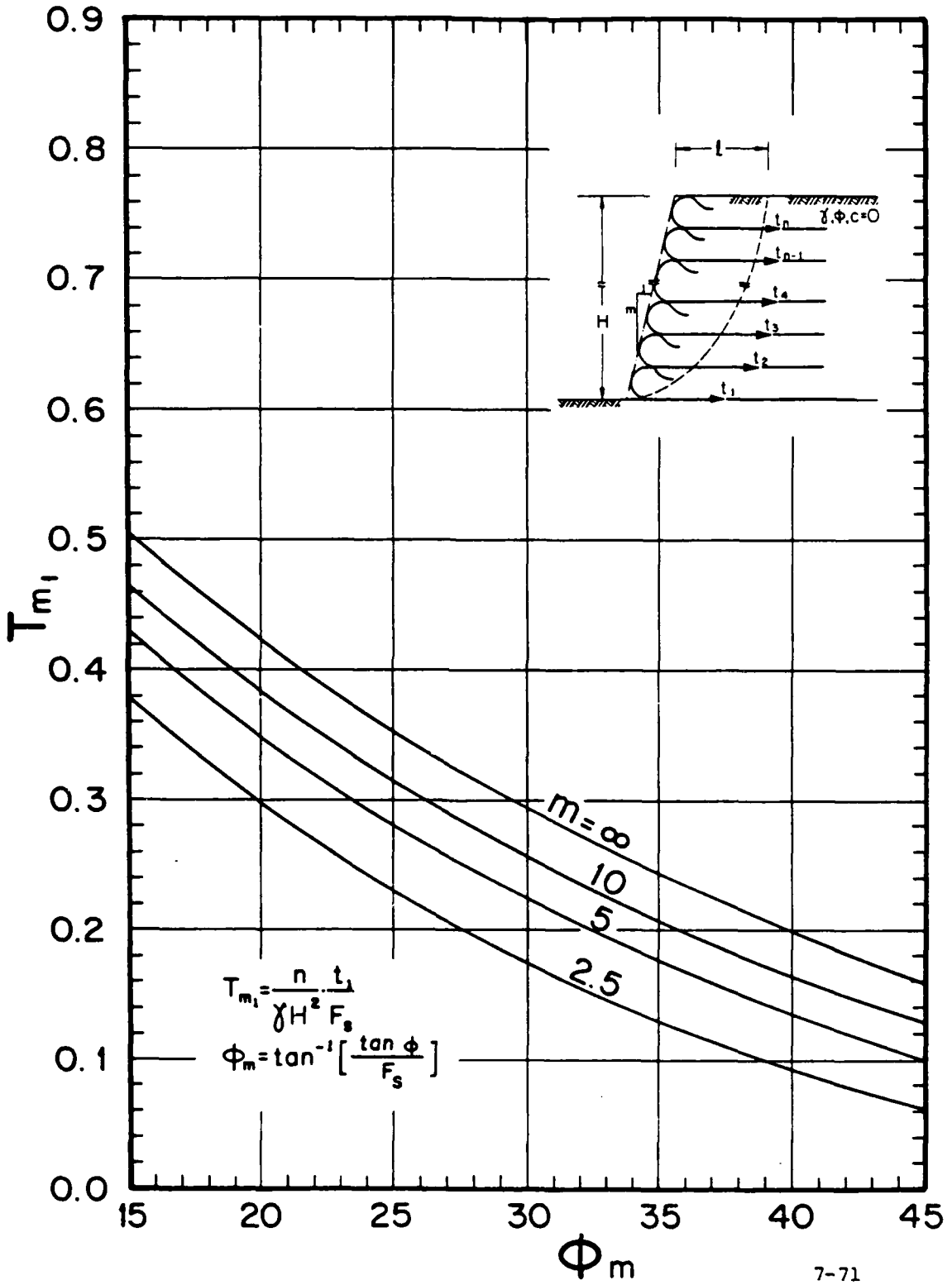

Figure 7-20a. Design chart

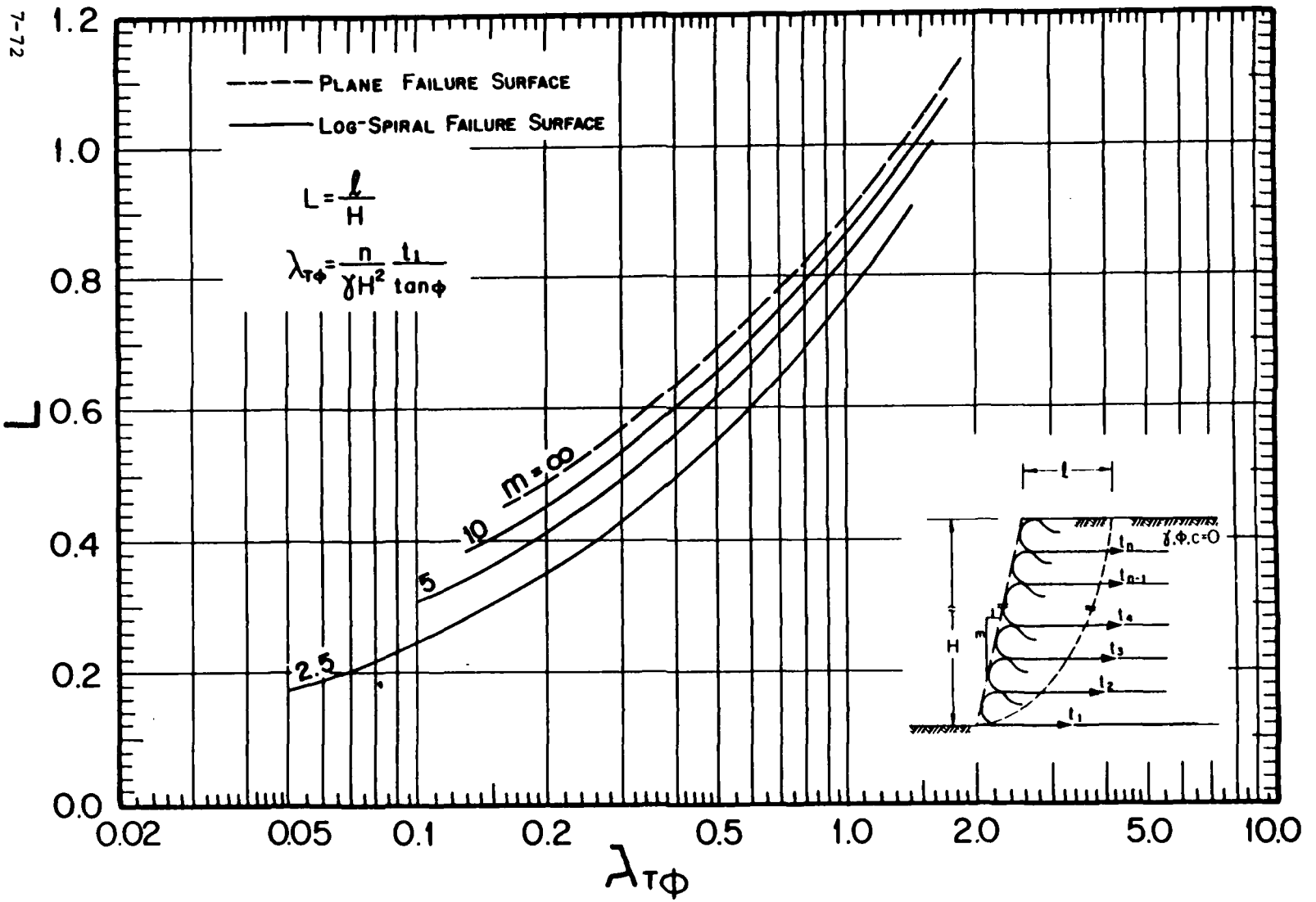

Figure 7-20b. Design chart

2. Determine the retained soil properties, i.e., unit weight γ and friction angle ϕ (see para. 7-4-2).

3. Select a value for the composite structure factor of safety, F_s. The recommended value is $F_s = 1.5$

4. Select the geotextile sheets spacing, d. To ease construction, this spacing should be limited to a maximum of d = 12 inches.

5. Compute $\phi_m = \tan^{-1}[(\tan\phi)/F_s]$.

6. For the given m and computed ϕ_m, determine T_{m_1} utilizing figure 7-20a.

7. The number of the required equally spaced goetextile sheets is n = H/d.

8. Compute the required tensile resistance of the geotextile sheet at the toe elevation $t_1 = T_{m_1} F_s \gamma H^2/n$.

9. Calculate the required tensile resistance of all other geotextile sheets using equation 7-2; i.e., $t_j = t_1(H-y_j)/H$.

10. Based on the recommendations in paragraph 7-4-2 and the required t_j, select the proper geotextiles. In case the specified geotextile tensile strength is excessively high as compared to available geotextiles, decrease the spacing d and return to step 7. If only one type of geotextile is used, skip step 9; t_1 will be used to determine this geotextile type.

11. Use equation 7-17 to compute the required length of the restraining zone so that the geotextiles' tensile resistance can actually develop; i.e., calculate ℓ_e and ℓ_{e_1}.

12. Compute $\lambda_{T\phi} = (nt_1)/(\gamma H^2 \tan\phi)$.

13. Based on m and $\lambda_{T\phi}$, determine L from figure 7-20b.

14. Compute $\ell = L \cdot H$ where ℓ defines the location at which the potential slip surface intersects the crest.

15. Based on equation 7-19, select the geotextile re-embedment length ℓ_a at the wall face -- see figure 7-17. It is recommended to use ℓ_a equal to at least 3 feet.

16. Determine the required length of each geotextile sheet j: $\ell_e + \ell + d + \ell_a + (H-y_j)/m$. For geotextile j=1 use ℓ_{e_1} rather than ℓ_e. Add one foot as tolerance permitting curvature along ℓ_a and over the wall face.

7-4-3-1-1. SURCHARGE LOADS

In this paragraph the design based on the composite structure stability is expanded to deal with two external loading cases: (a) uniform surcharge load, acting on top of the wall over a large area, and (b) strip surcharge loads, extending, at most, to ℓ.

(a) Uniform Surcharge Load: The following procedure is valid only if the load q extends, at least, to $\ell+\ell_e$; i.e., it acts

over the geotextiles' tensile force restraining zone, ℓ_e, and hence, it increases the geotextiles' tensile resistance via an increase in overburden pressure (eq. 7-2).

Although satisfaction of this condition may not be known a-priori, once a trial design is carried out one can check if q indeed acts over $\ell+\ell_e$ as was initially assumed.

Figures 7-21 through 7-25 are the design charts for this surcharge load. These charts are similar to the previous ones and their utilization is identical. The following is the design procedure, essentially repeating the steps presented in paragraph 7-4-3-1:

1. Determine the wall's geometry: H and m.
2. Determine the retained soil properties: γ and ϕ.
3. Select F_s for the composite structre. Recommended value is $F_s = 1.5$.
4. Select the geotextiles spacing d ($d \leq 12$ inches).
5. Compute $\phi_m = \tan^{-1}[(\tan\phi)/F_s]$ and $Q = q/\gamma H$.
6. Select the proper design chart based on Q. If there is no chart for the exact value of Q, use two charts for which the normalized surcharge loads bracket Q. Use these two charts to linearly interpolate the needed parameters.
7. Compute $n = H/d$.

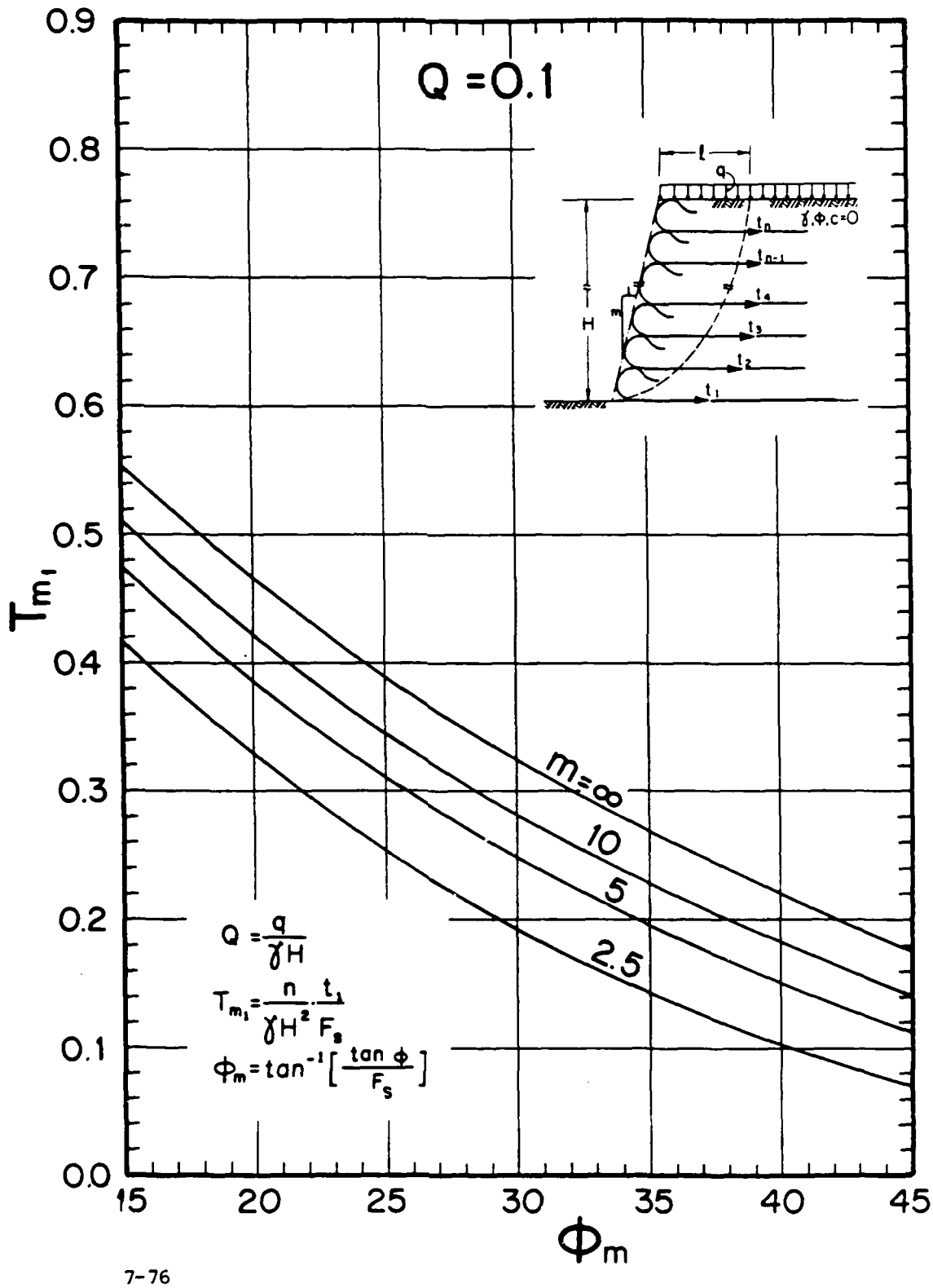

Figure 7-21a. Design chart (uniform surcharge load of Q = 0.1)

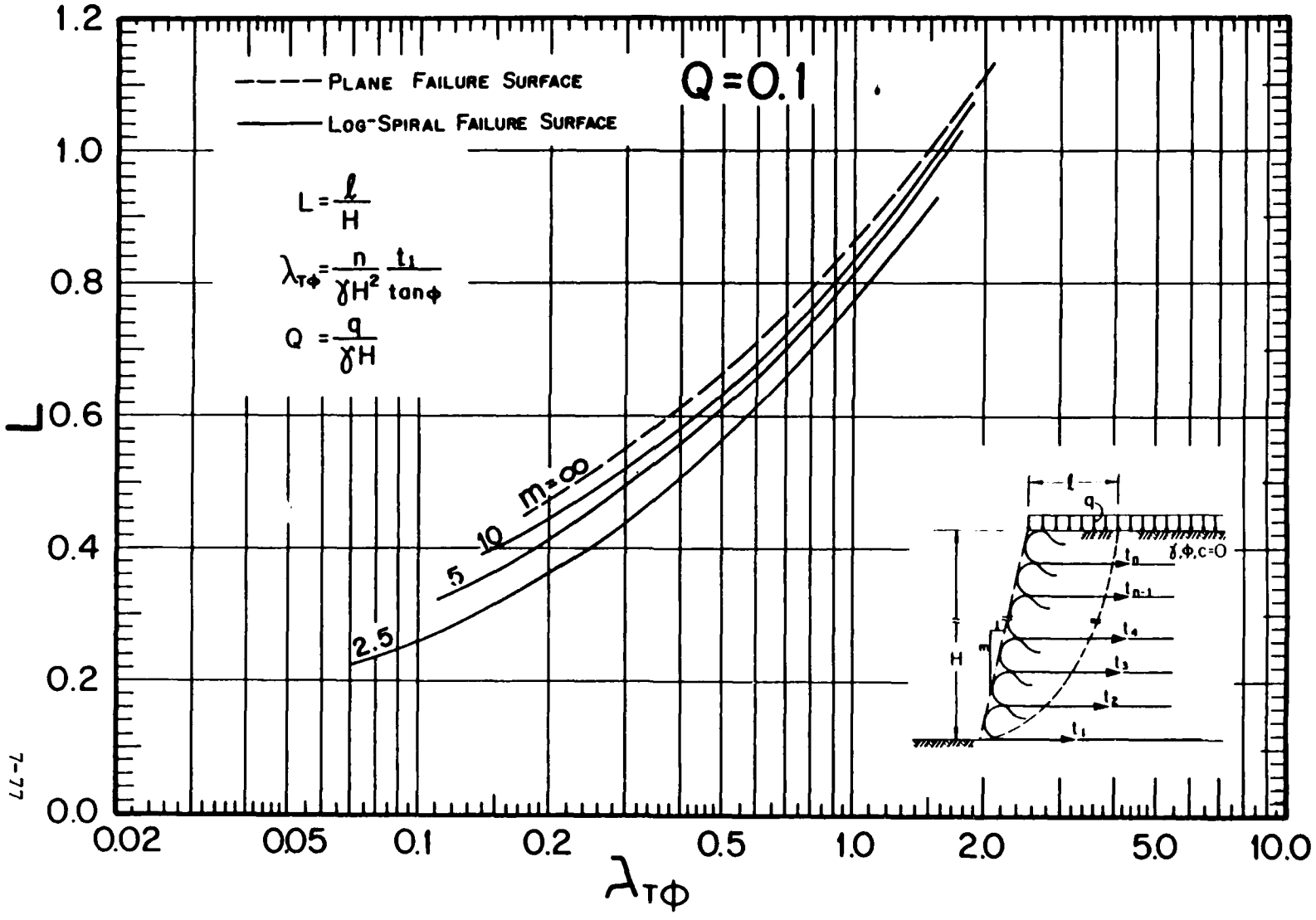

Figure 7-21b. Design chart (uniform surcharge load of Q = 0.1)

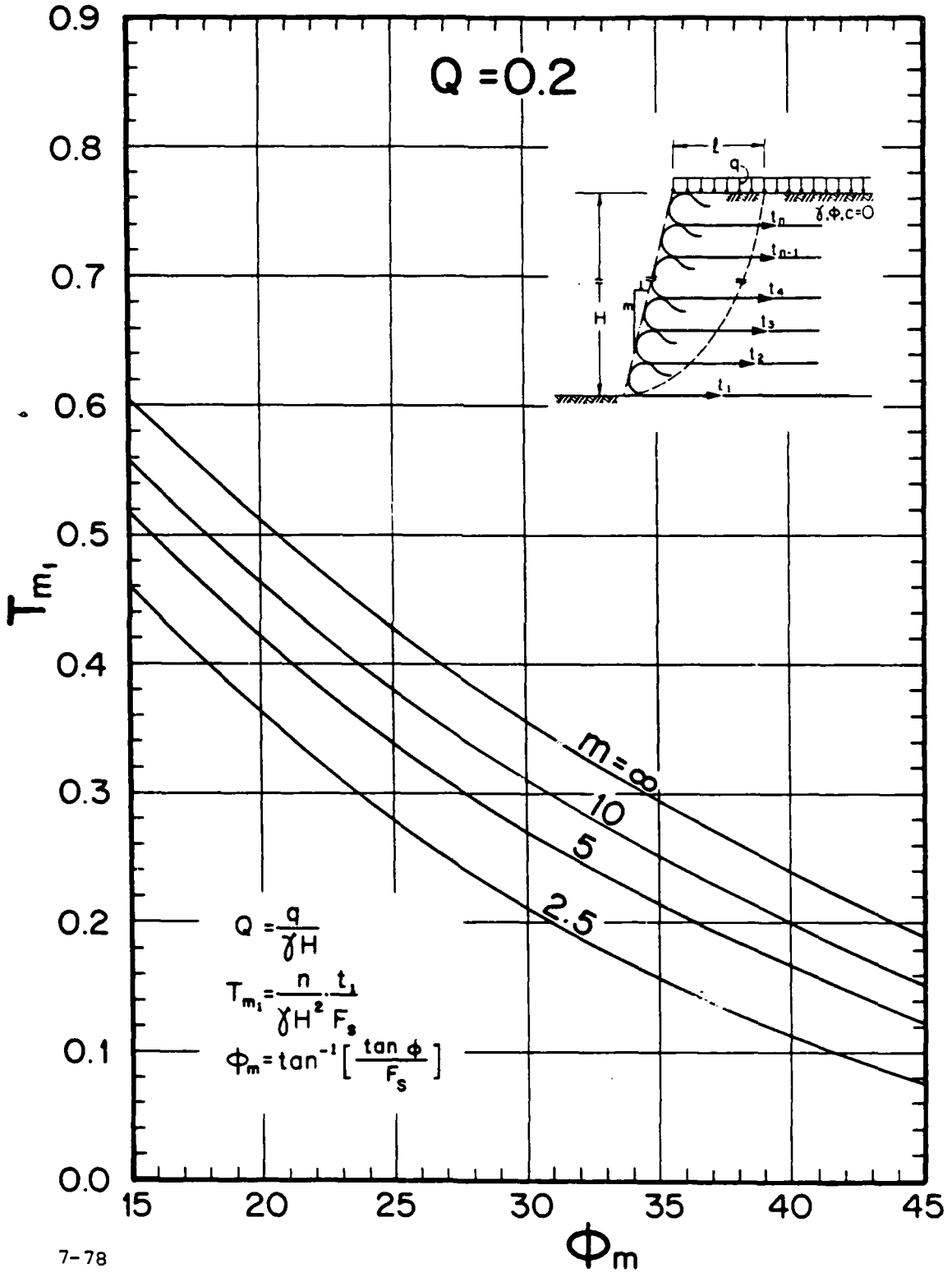

Figure 7-22a. Design chart (uniform surcharge load of Q = 0.2)

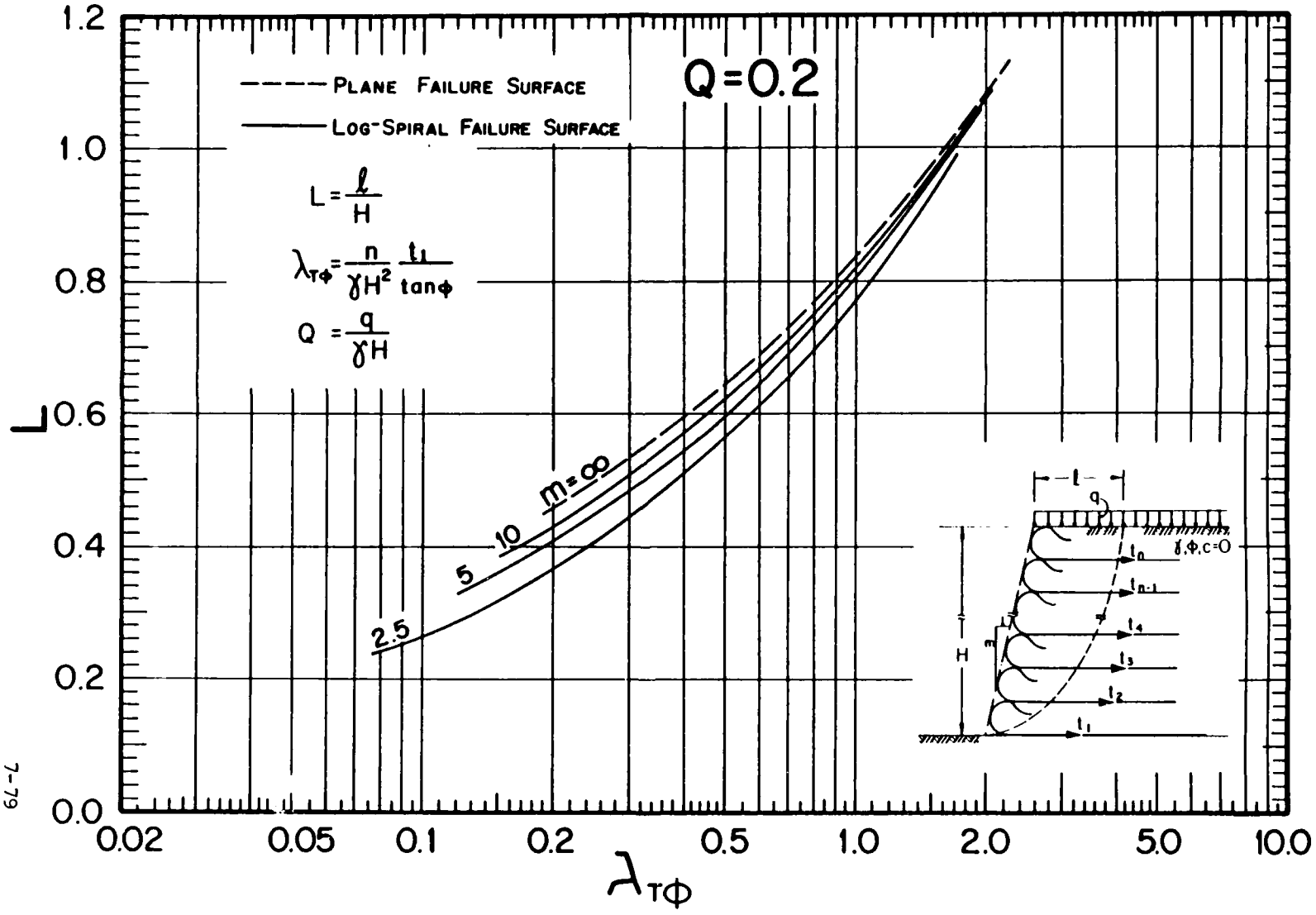

Figure 7-22b. Design chart (uniform surcharge load of Q = 0.2)

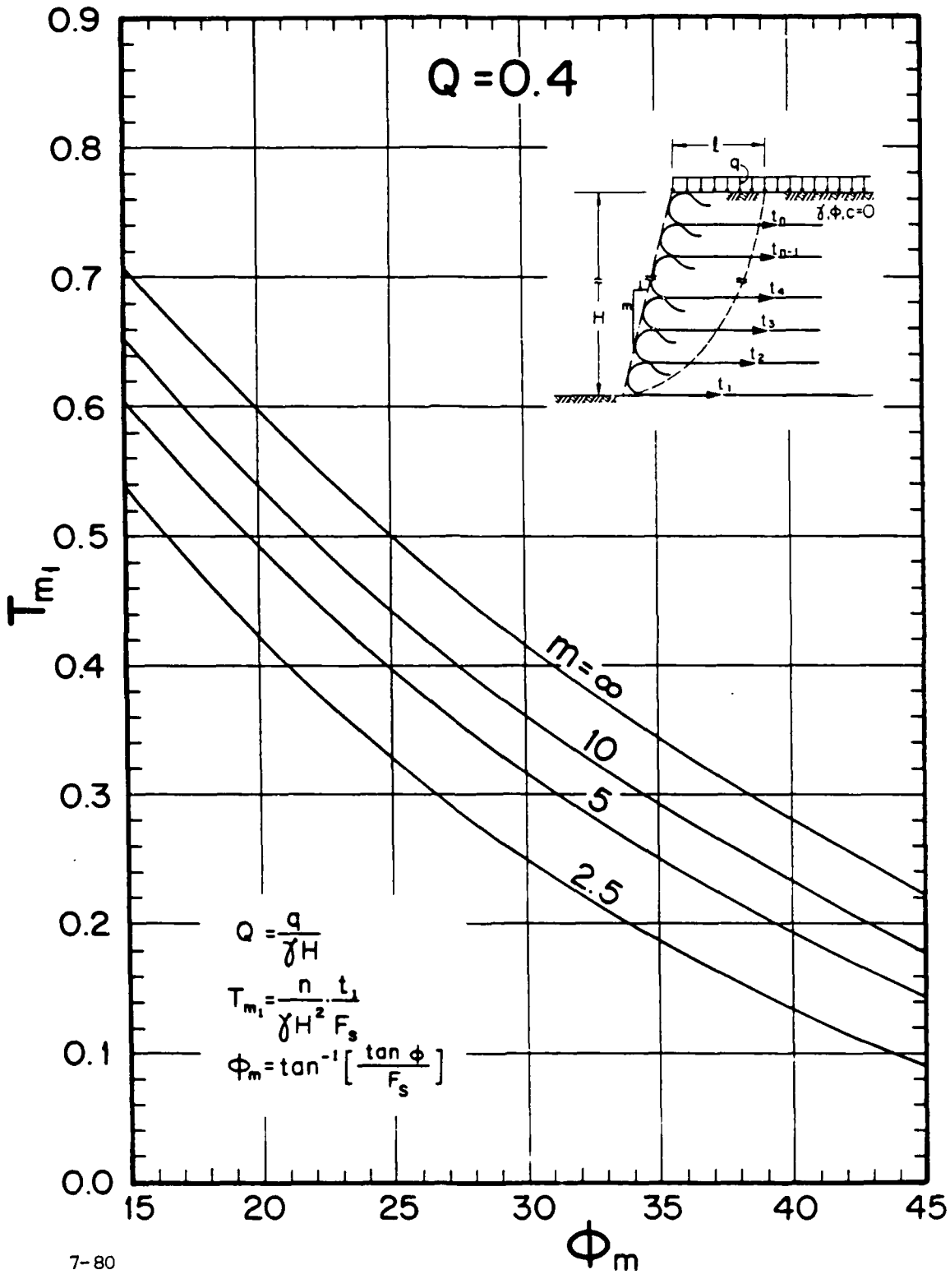

Figure 7-23a. Design chart (uniform surcharge load of Q = 0.4)

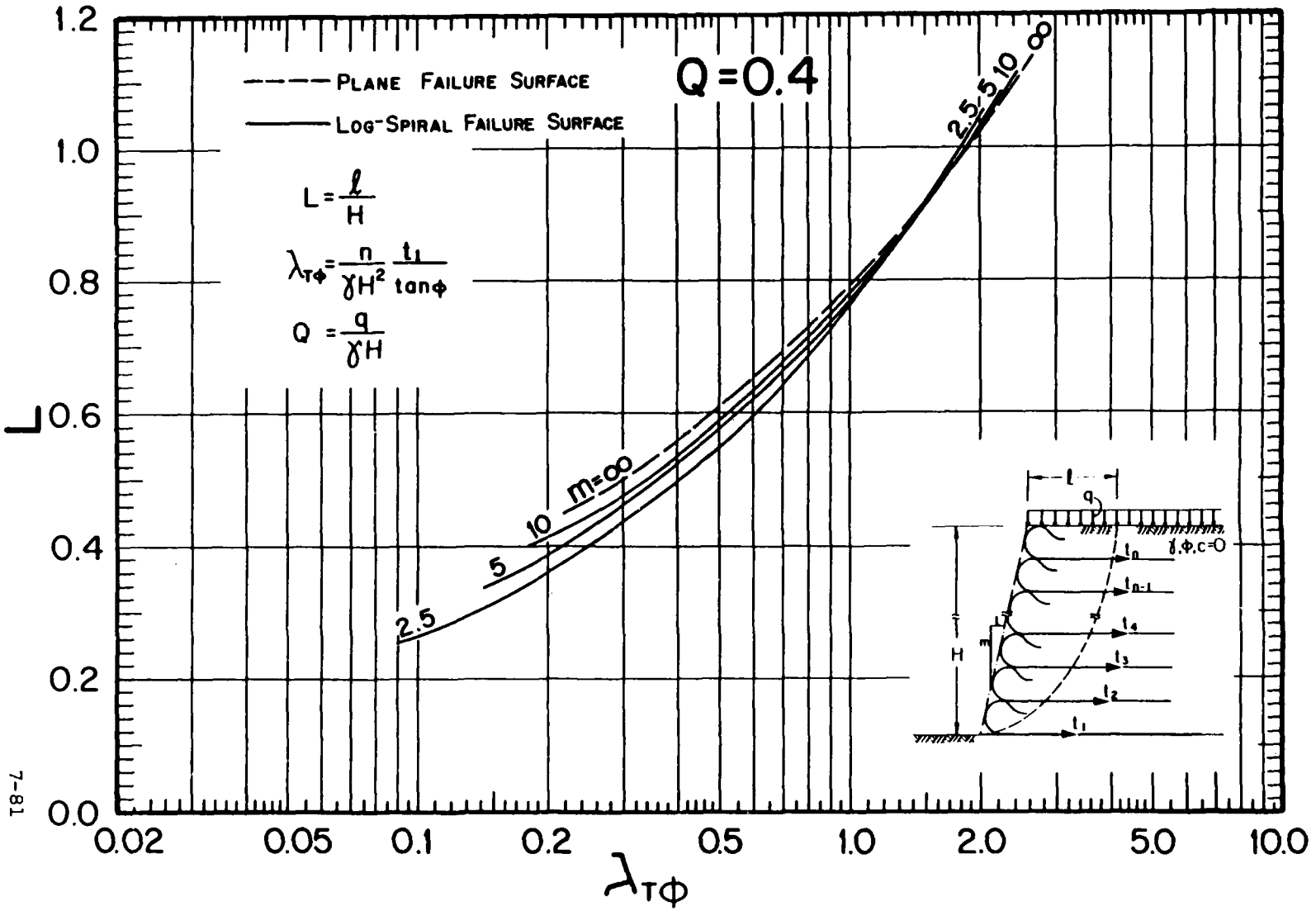

Figure 7-23b. Design chart (uniform surcharge load of Q = 0.4)

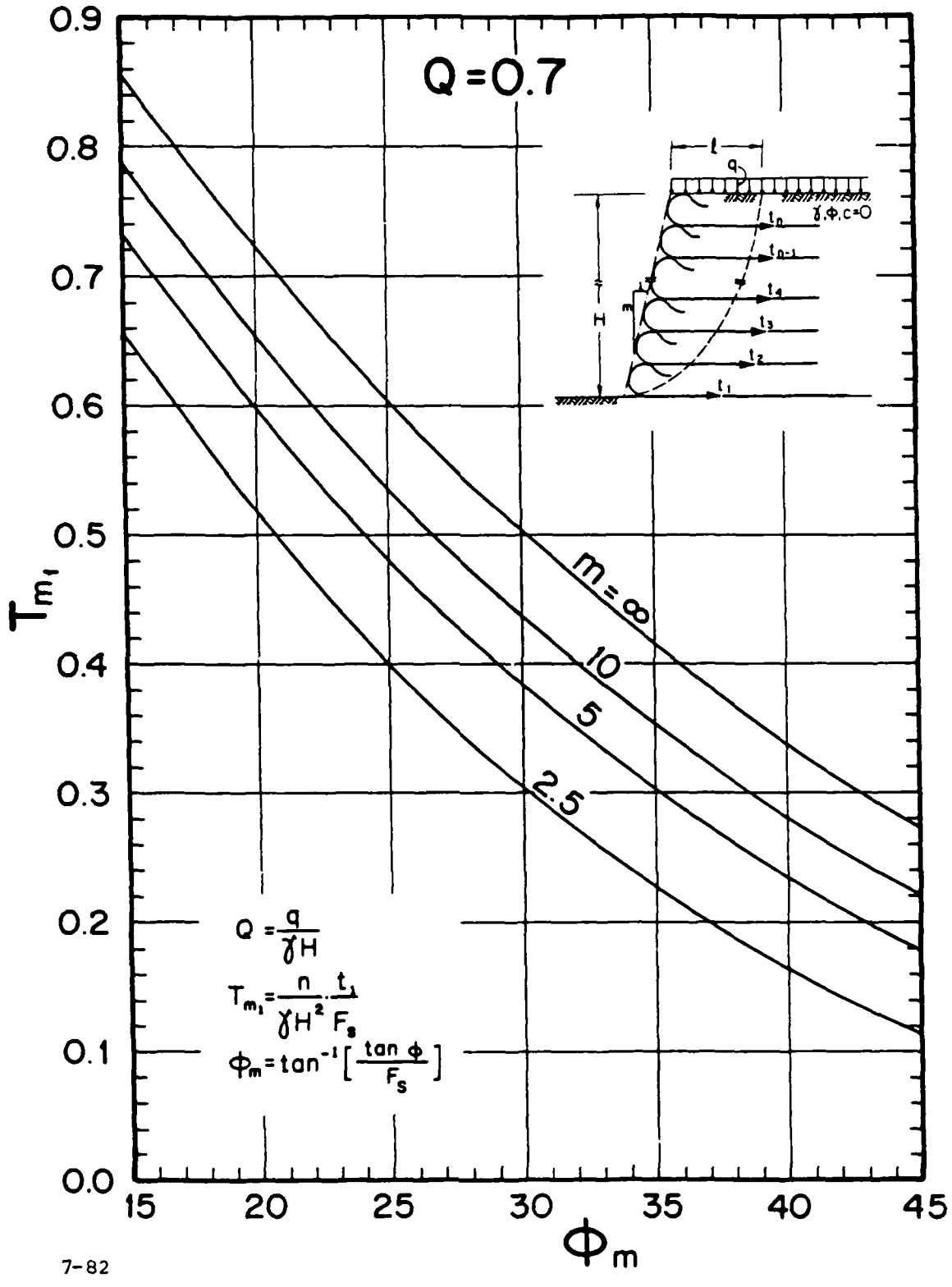

7-82

Figure 7-24a. Design chart (uniform surcharge load of Q = 0.7)

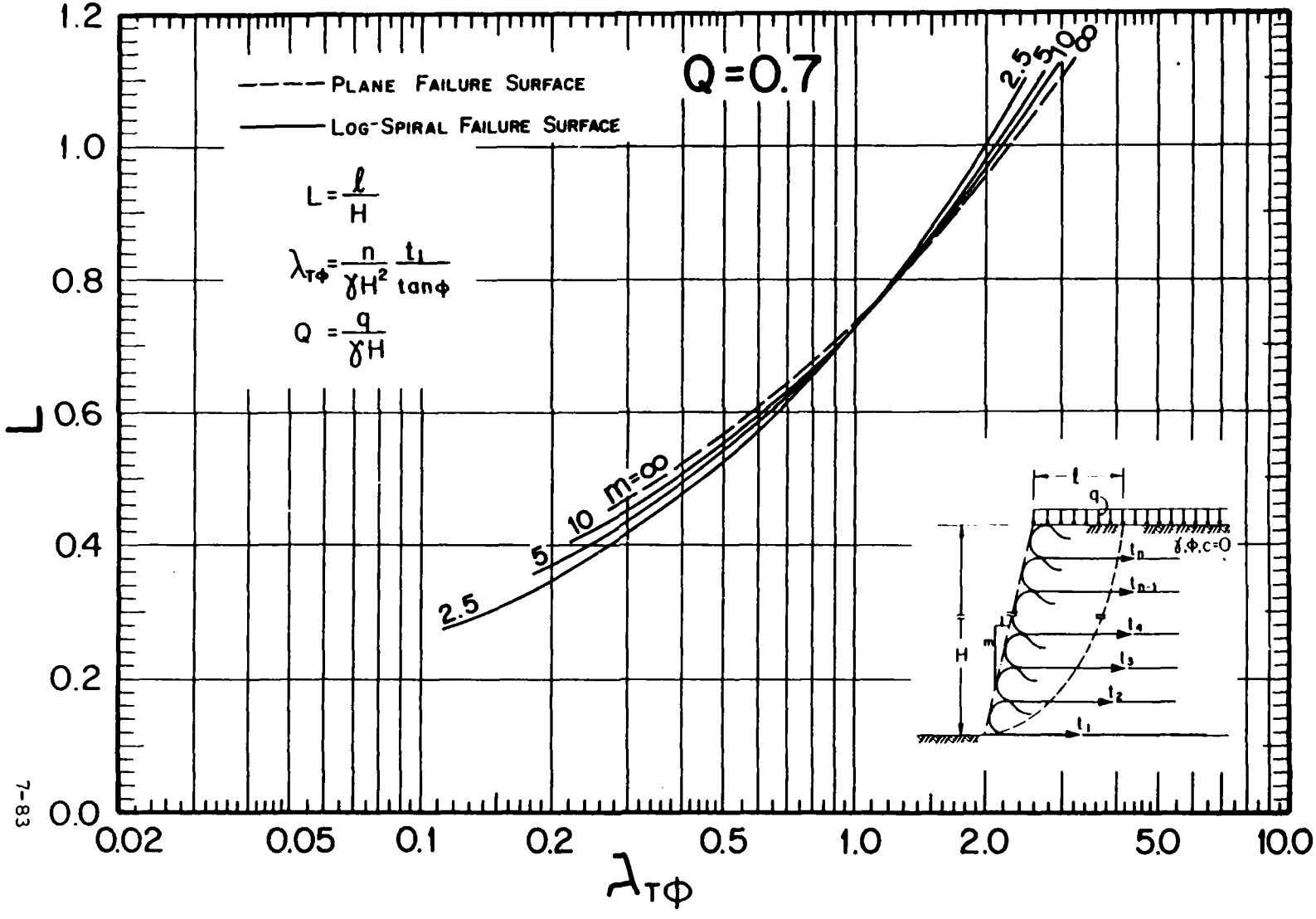

Figure 7-24b. Design chart (uniform surcharge load of Q = 0.7)

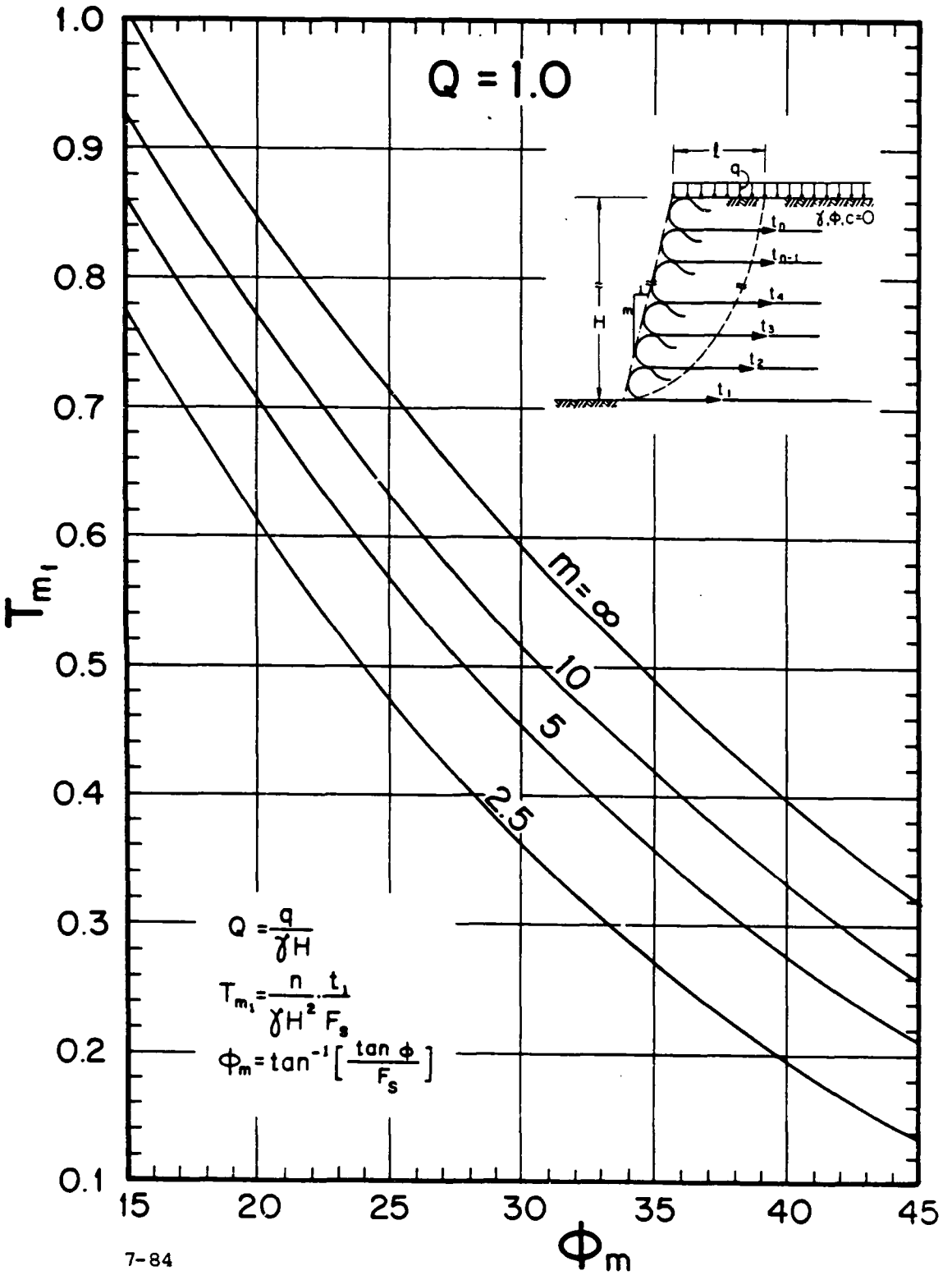

Figure 7-25a. Design chart (uniform surcharge load of Q = 1.0)

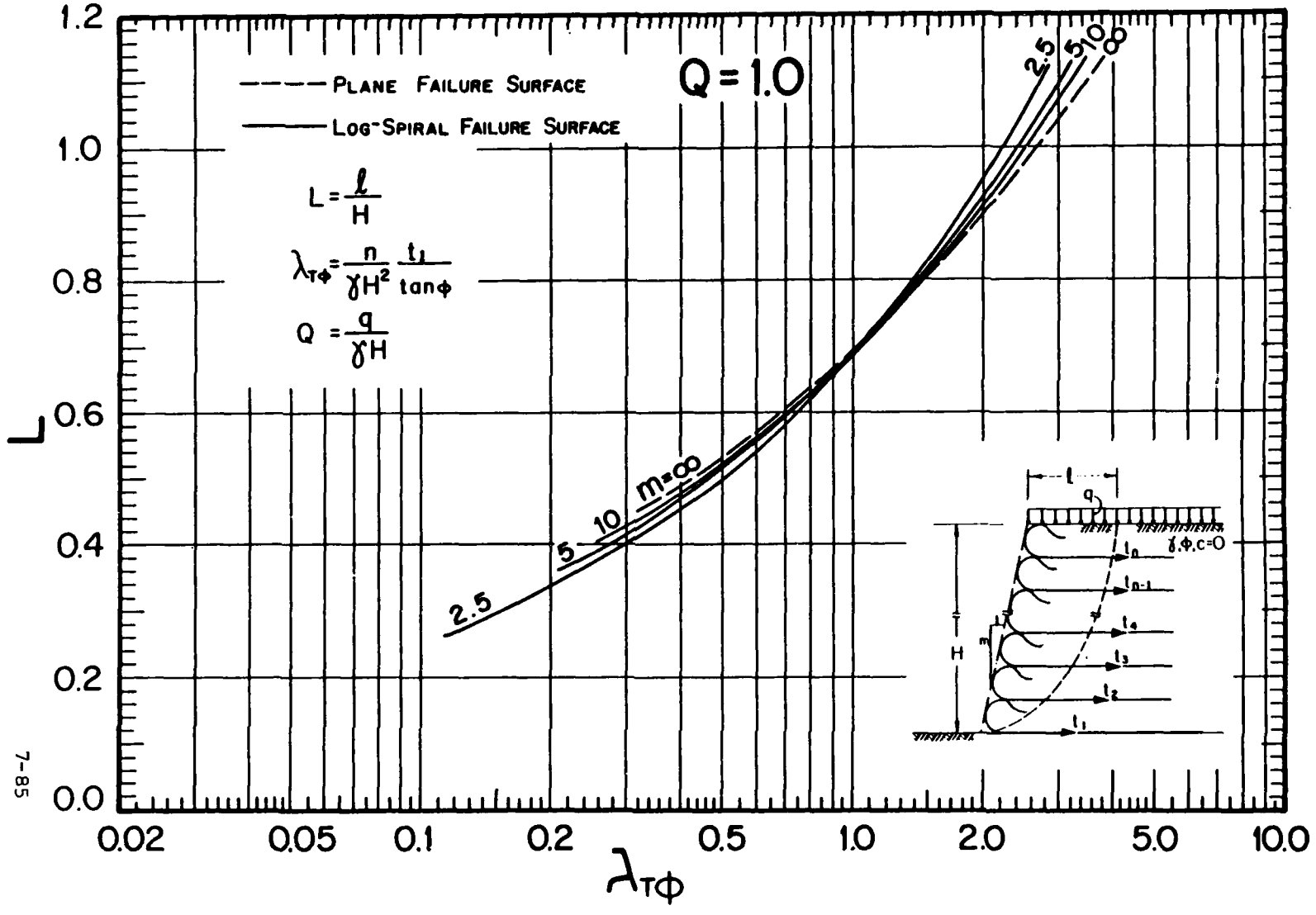

Figure 7-25b. Design chart (uniform surcharge load of Q = 1.0)

8. Compute $t_1 = T_{m_1} F_s \gamma H^2/n$.

9. Use equation 7-17 to compute ℓ_e and ℓ_{e_1}.

10. Compute $\lambda_{T\phi} = (nt_1)/(\gamma H^2 \tan\phi)$.

11. Based on m, $\lambda_{T\phi}$ and Q determine L from the proper design chart.

12. Compute $\ell = L \cdot H$.

13. Is q extending over $(\ell+\ell_e)$? If yes, the results comply with the basic premise of the analysis and therefore one should proceed with the design. If not, then the analysis is inappropriate and one should skip to the next type of surcharge loading.

14. Select ℓ_a as recommended by equation 7-19 ($\ell_a \geq 3$ feet).

15. Calculate the required tensile resistance of each geotextile sheet $t_j = t_1[\gamma(H-y_j)+q]/(\gamma H+q)$. This step is necessary only if geotextiles possessing different strength properties are going to be used in the reinforced structure.

16. Select geotextiles based on t_j and the recommendations in paragraph 7-4-2. If the specified strength is excessively high, decrease the spacing and return to step 7.

17. For each geotextile sheet determine the required length = $\ell_e+\ell+d+\ell_a+(H-y_j)/m$. For the geotextile at the

toe elevation use ℓ_{e_1} instead of ℓ_e. Add one foot to the required length as tolerance.

(b) Strip Surcharge Load: The solution presented in paragraph 7-3-2-2 can be modified to deal with various cases of strip surcharge loading. There are, however, infinite such cases. Developing design charts, even for a few loading configurations, is impractical. To overcome this problem, a generalized approximated methodology, which renders conservative results compared to accurate formulation, is introduced.

Figure 7-26a illustrates a general case of strip surcharge loading. Notice that only the loads acting up to ℓ are considered. Figure 7-26b shows the assumed equivalent problem; i.e., the wall is subjected to a uniform load q acting over ℓ. This load is taken as the maximum of all actual strip loads; i.e.,

$$q = \max(q_j) \qquad \text{for } j = 1,2,\ldots k \tag{7-20}$$

where q_j is the magnitude of strip surcharge load number j, acting over a segment of ℓ (see fig. 7-26a).

For this equivalent loading, design charts, similar to the previous ones, were developed. Checking some typical cases, one may realize that this load equivalency is reasonably conservative. Furthermore, using the charts it can be verified that the added safety implies that a load bearing capacity type of failure, where the slip surface exits above the toe, is unlikely to occur.

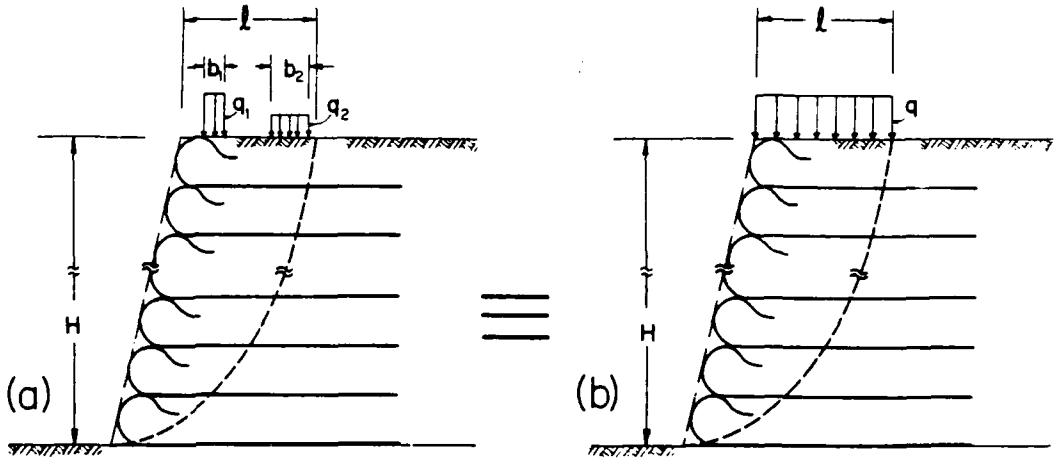

Figure 7-26. The equivalency used for strip surcharge load

Figures 7-27 through 7-31 are the design charts for the equivalent problem. The following are the design steps needed to utilize these charts:

1. Determine the wall's geometry: H and m.
2. Determine the retained soil properties: γ and ϕ.
3. Select F_s for the composite structure. Recommended value is $F_s = 1.5$
4. Select the geotextiles spacing d ($d \leq 12$ inches).
5. Assume a value for ℓ; e.g., take $\ell = 0.5$ H.
6. Among all strip footings acting over ℓ, select the one that exerts the maximum q. Take this q as the equivalent load (eq. 7-20).
7. Compute $\phi_m = \tan^{-1}[(\tan\phi)/F_s]$ and $Q = q/\gamma H$.
8. Select the proper design chart based on Q. If there is no chart for the exact value of Q, use two charts for which the normalized strip loads bracket Q. Use these two charts to linearly interpolate the needed parameters.
9. For m, ϕ_m and Q determine T_{m_1}.
10. Compute $\lambda_{T\phi} = (nt_1)/(\gamma H^2 \tan\ ) = T_{m_1}/\tan\phi_m$.
11. Based on m, $\lambda_{T\phi}$ and Q determine L from the proper design chart.
12. Compute $\ell = L \cdot H$.

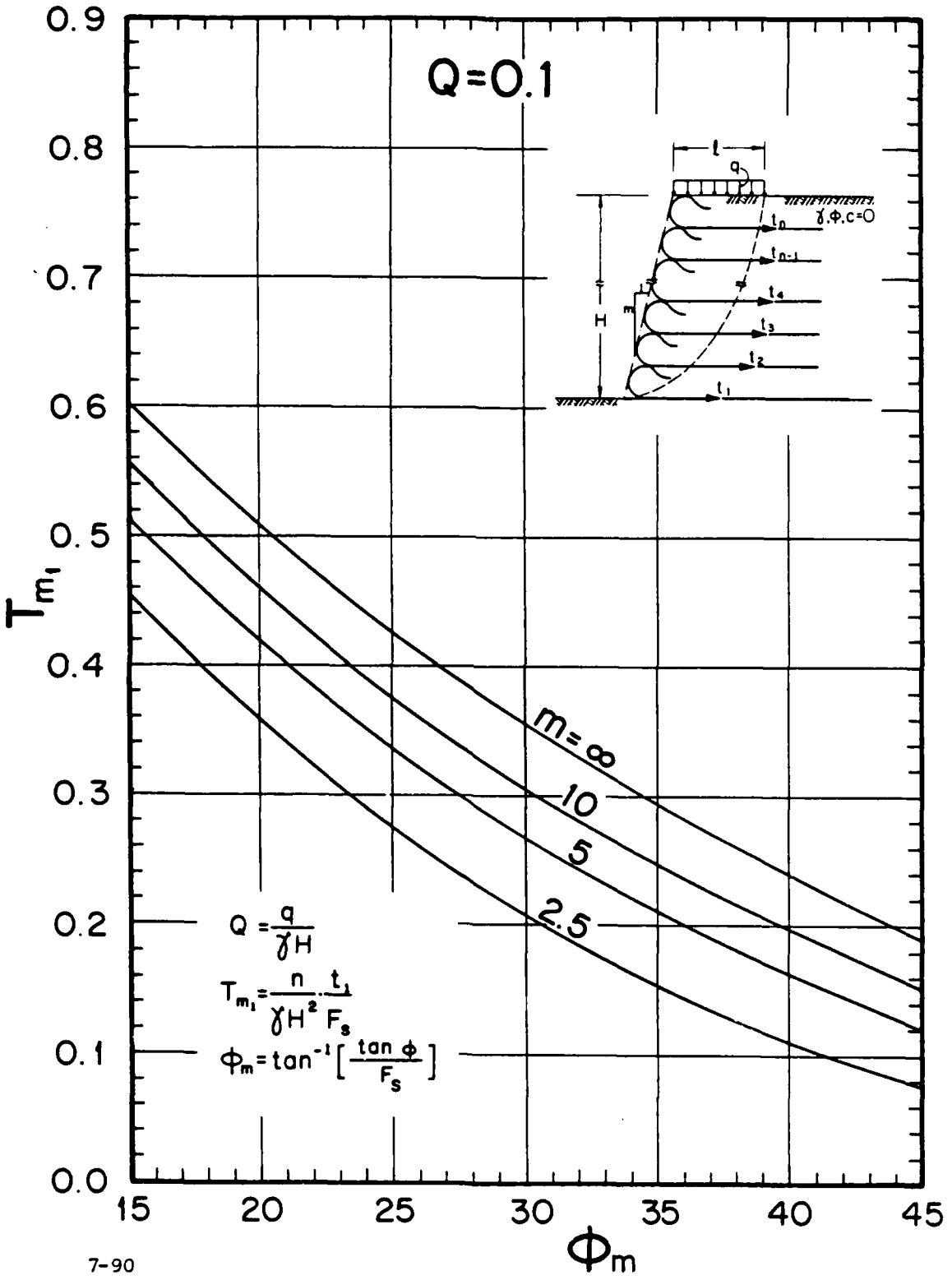

7-90

Figure 7-27a. Design chart (strip surcharge load of Q = 0.1)

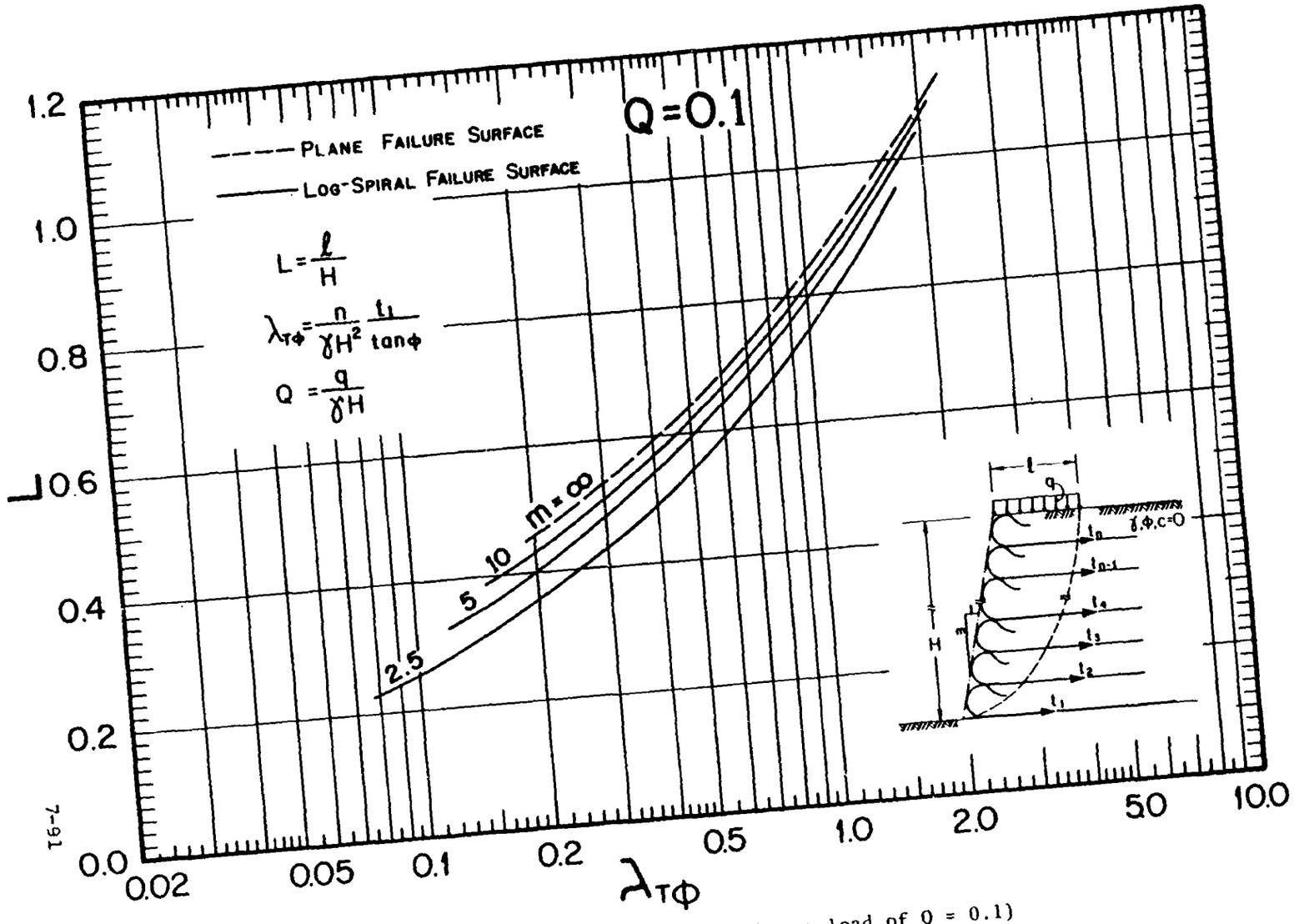

Figure 7-27b. Design chart (strip surcharge load of Q = 0.1)

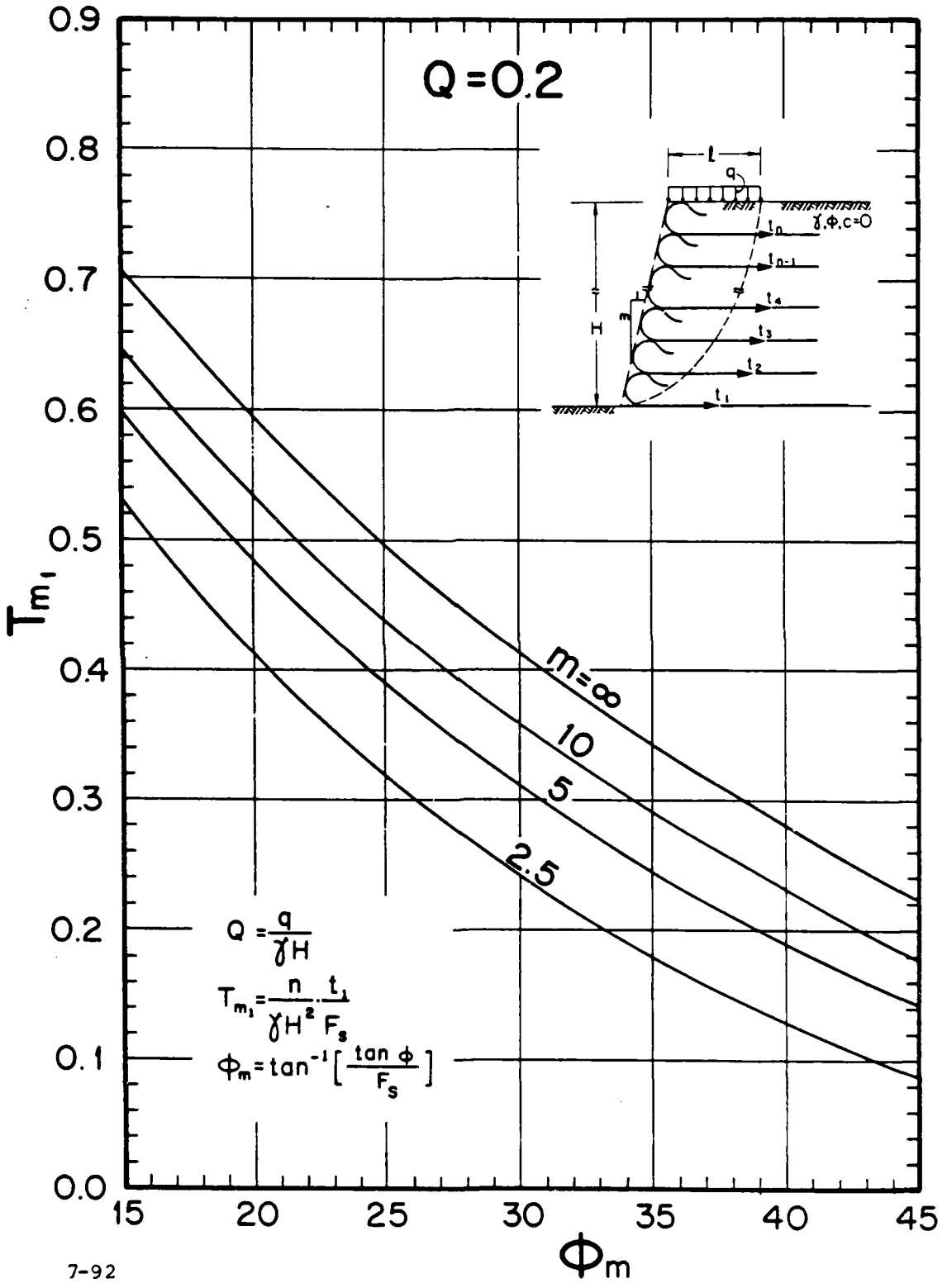

Figure 7-28a. Design chart (strip surcharge load of Q = 0.2)

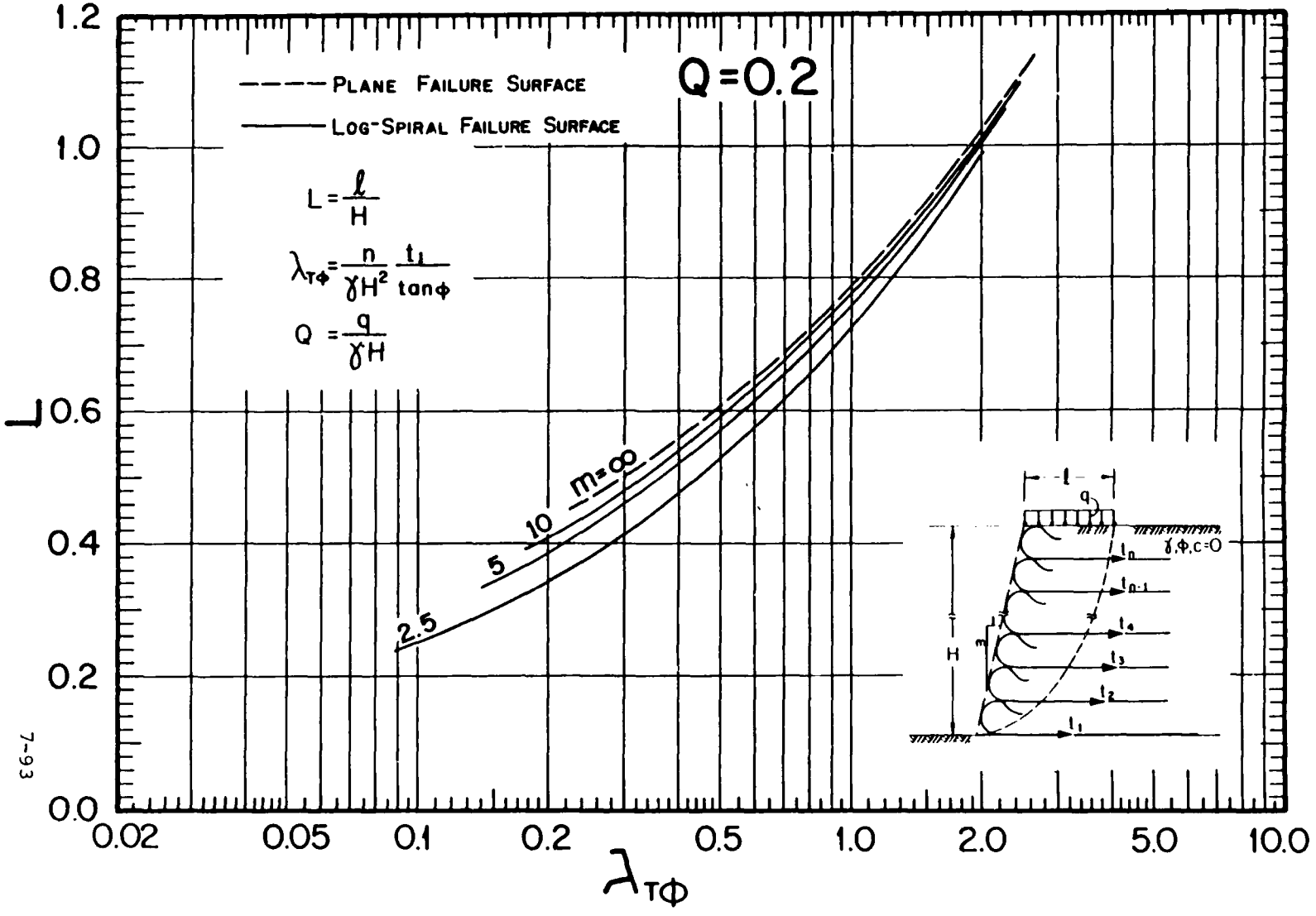

7-93

Figure 7-28b. Design chart (strip surcharge load of Q = 0.2)

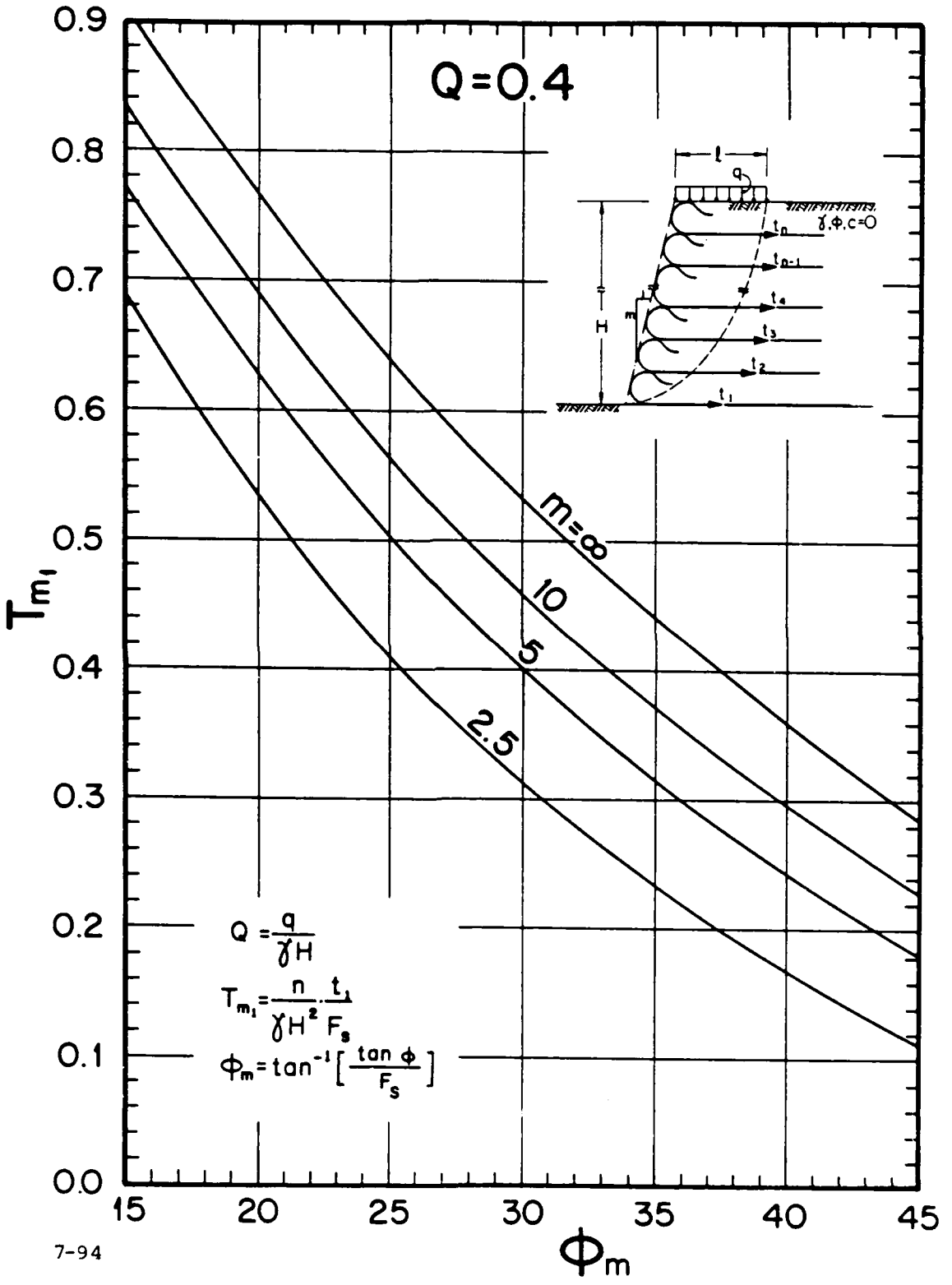

Figure 7-29a. Design chart (strip surcharge load of Q = 0.4)

AD-A191 510 DESIGN MANUAL FOR GEOTEXTILE-RETAINED EARTH WALLS(U) 2/2
DELAWARE UNIV NEWARK DEPT OF CIVIL ENGINEERING
D LESHCHINSKY SEP 85 CE-85-51

UNCLASSIFIED F/G 8/10 NL

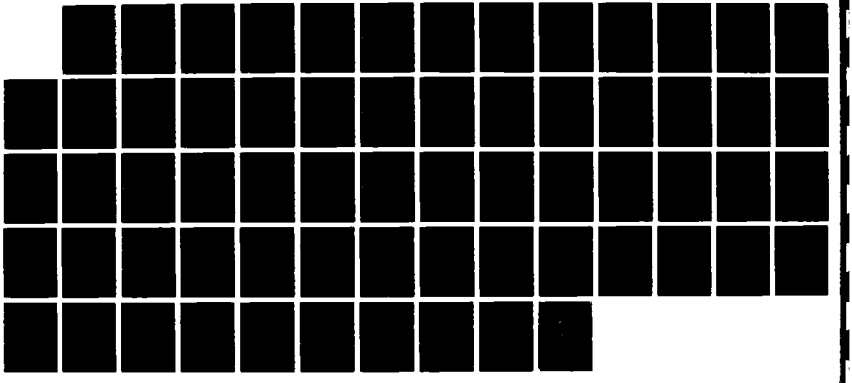

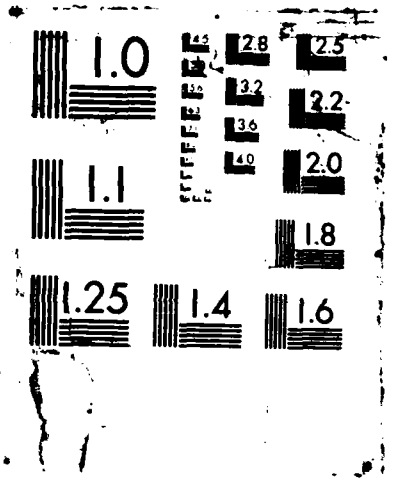
1.0
1.1
1.25
1.4
1.6
1.8
2.0
2.2
2.5
2.8
3.2
3.6
4.0

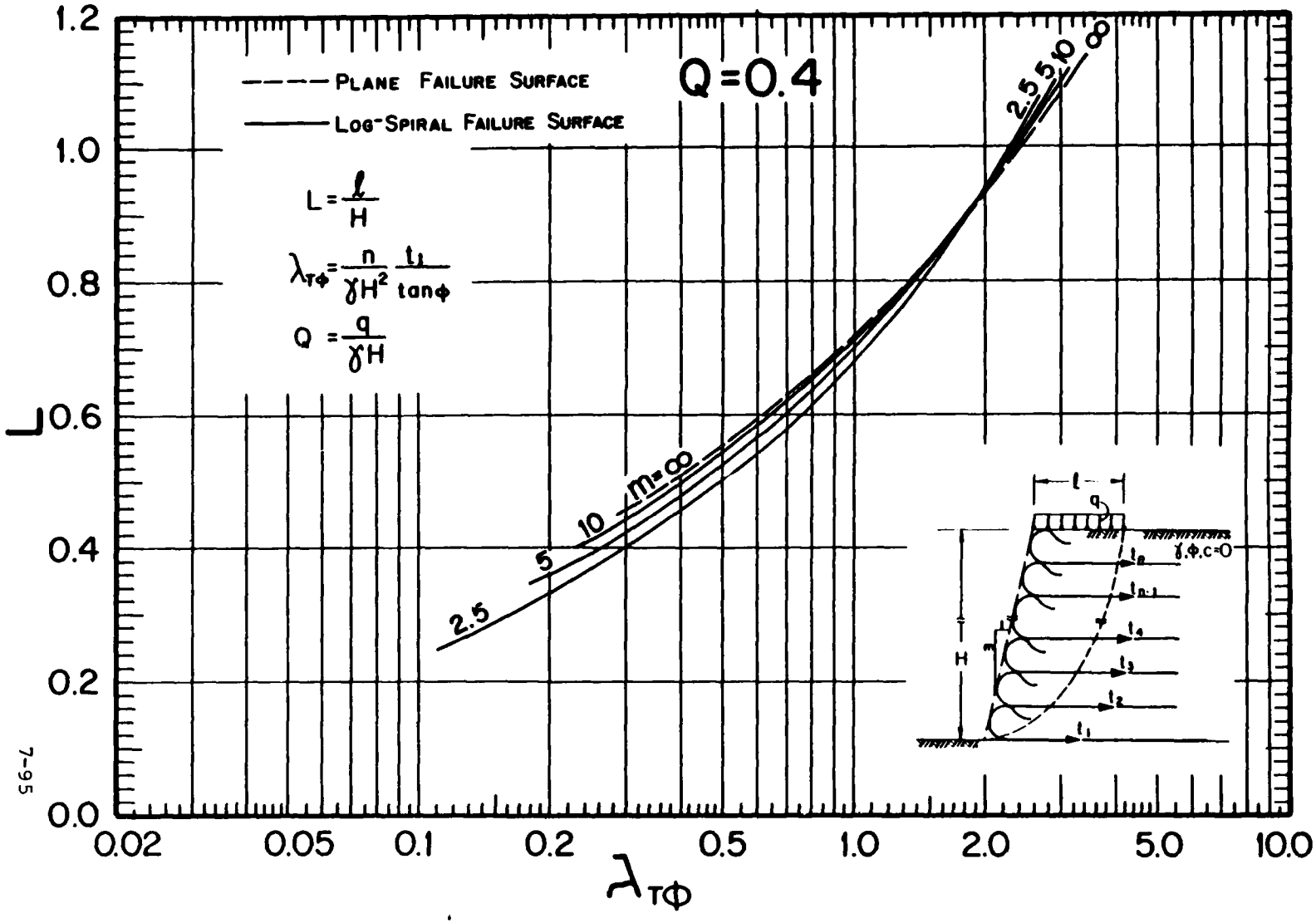

Figure 7-29b. Design chart (strip surcharge load of Q = 0.4)

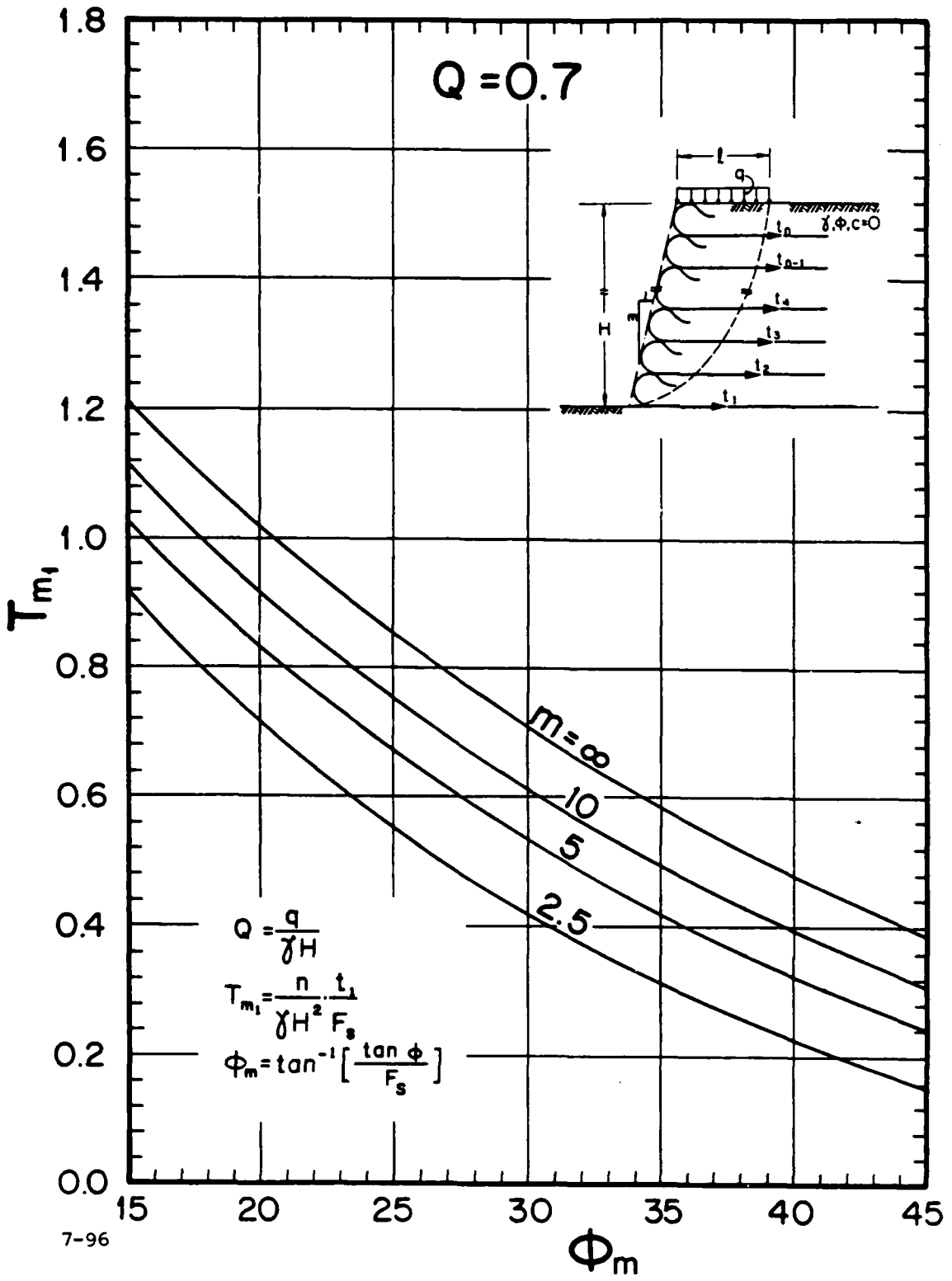

7-96

Figure 7-30a. Design chart (strip surcharge load of Q = 0.7)

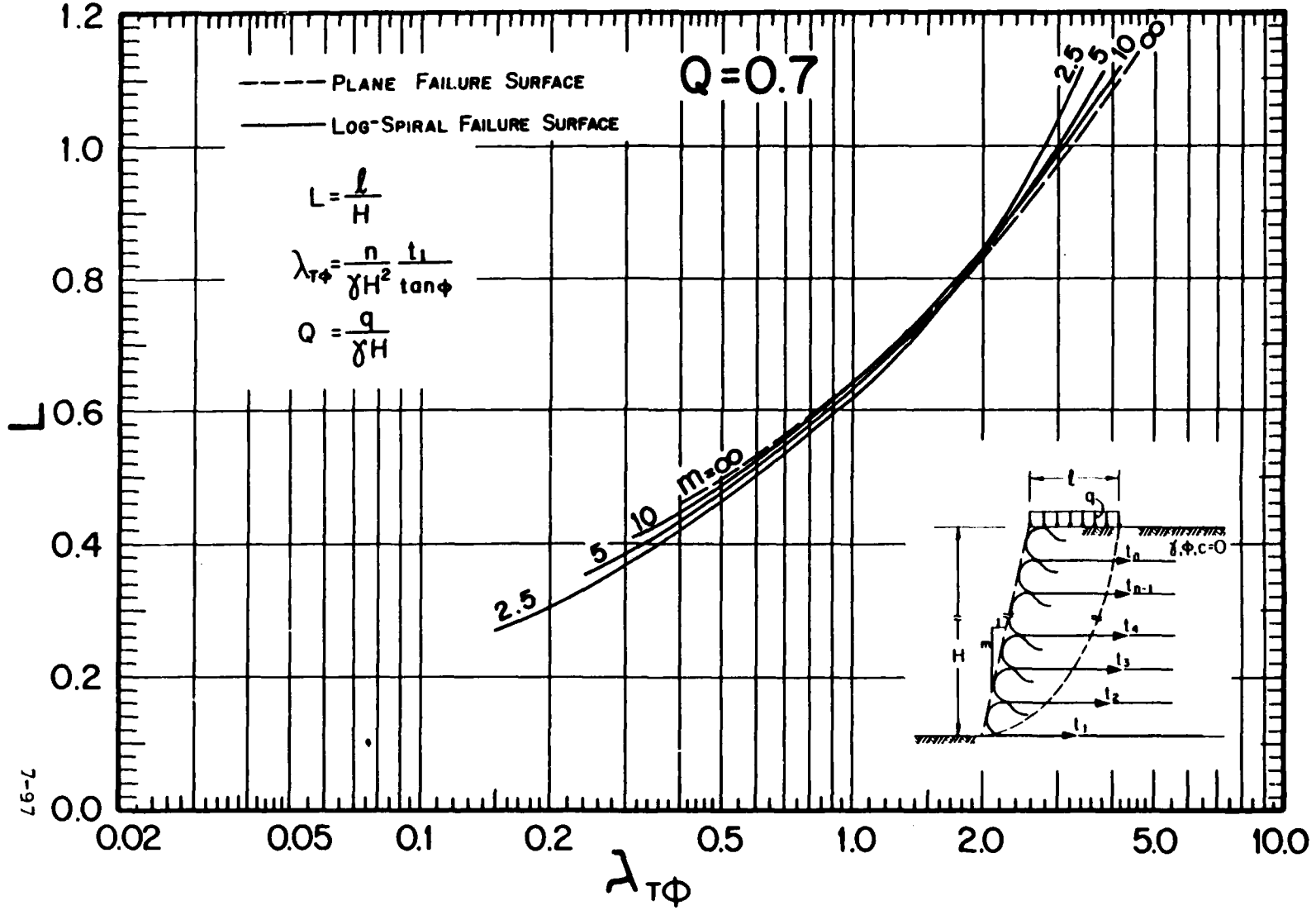

Figure 7-30b. Design chart (strip surcharge load of Q = 0.7)

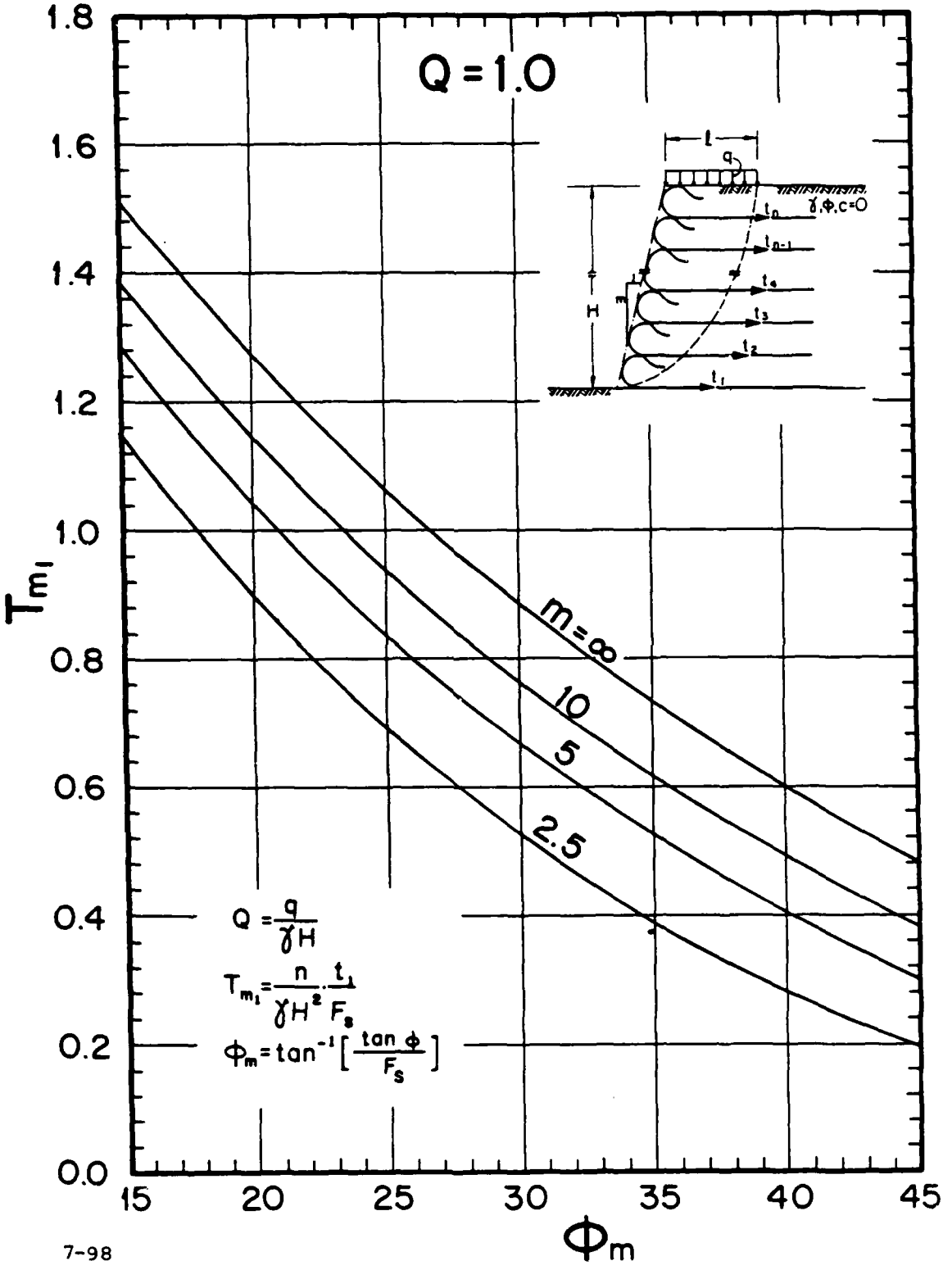

Figure 7-31a. Design chart (strip surcharge load of Q = 1.0)

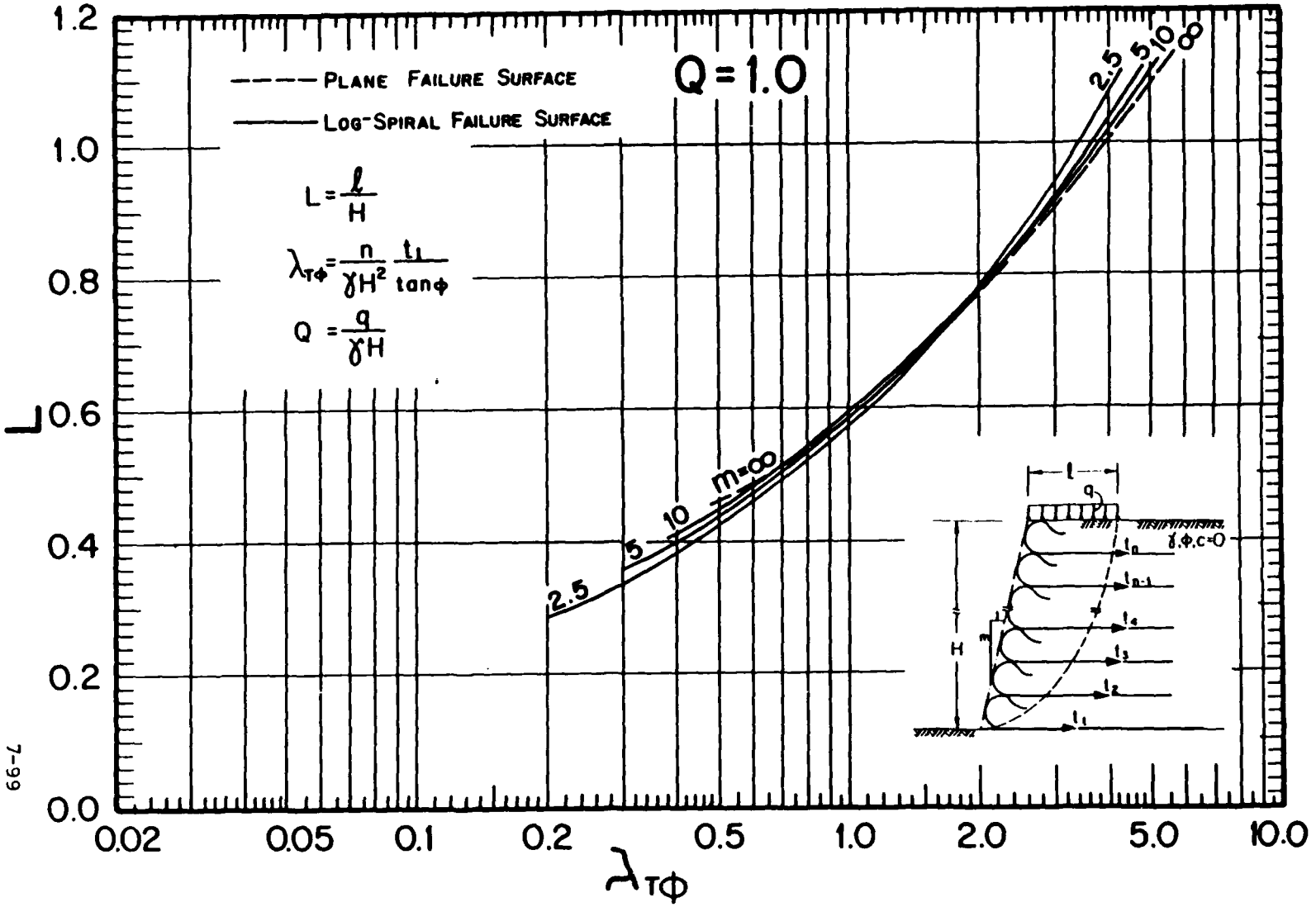

7-99

Figure 7-31b. Design chart (strip surcharge load of Q = 1.0)

13. Check if the selected maximum q indeed acts over ℓ. If yes, proceed. If not, assume this ℓ to be valid and go back to step 6.

14. Compute $n = H/d$.

15. Compute $t_1 = T_{m_1} F_s \gamma H^2/n$.

16. Use equation 7-17 to compute ℓ_e and ℓ_{e_1}. Take q equals zero in this equation.

17. Select ℓ_a based on equation 7-19 ($\ell_a \geq 3$ feet).

18. Determine the required length for each geotextile sheet: $\ell_e+\ell+d+\ell_a+(H-y_j)/m$. For the geotextile at the toe elevation use ℓ_{e_1} instead of ℓ_e. Add one foot to the required length as tolerance.

19. Select a geotextile based on t_1 and the recommendations in paragraph 7-4-2. In this particular type of loading, it is recommended to use one type of geotextile for the entire structure.

7-4-3-2. *GEOTEXTILE TENSILE RESISTANCE*

As was stated before, the internal stability can be viewed from another prospective. One can assume that the soil is fully mobilized (i.e., $\phi_m=\phi$) and that the margin of safety then is solely contributed by the geotextile tensile resistance. This margin of safety is defined as

$$F_g = \frac{t_j}{t_{m_j}} \qquad (7\text{-}21)$$

where F_g is the factor of safety with respect to a geotextile tensile resistance; $t_{m_j} = T_{m_j} \gamma H^2/n$ = the tensile resistance of geotextile j yielding a composite structure which is at the verge of failure (i.e., F_s=1.0); and t_j is the required tensile resistance of geotextile j so that F_g is attained. Conceptually, this definition of safety coincides with the conventional approach to reinforced walls.

It is recommended to use F_g = 2.0. It can be verified that this F_g value combined with the suggested design procedure will render structures possessing safety factors greater than one when their stability is analyzed using other design methods such as those introduced by Steward et al. (1977) and Murray (1980).

The assumptions made regarding the geotextiles restraining over ℓ_e (see fig. 7-17) are used. To design a wall, possessing a specified F_g value, the design charts, presented in the previous sections, are utilized. The composite factor of safety, however, must be taken as F_s = 1.0 when using the charts. The following are the steps necessary to utilize the charts, assuming that a preliminary design, based on F_s, has been carried out:

1. Select a value for F_g. The recommended value is 2.0.
2. Take F_s = 1.0; hence, $\phi_m = \phi$.
3. Use figure 7-20a to determine T_{m_1} for m and ϕ_m.
4. Compute the required tensile resistance of the geotextile sheet at the toe elevation $t_1 = F_g T_{m_1} \gamma H^2/n$.

5. Calculate the required tensile resistance of all other geotextile sheets using equation 7-2; i.e., $t_j = t_1(H-y_j)/H$.

6. Compare t_j for all n sheets with those obtained based on a prescribed F_s in the previous section. If t_j here is smaller, take the previous t_j for design and skip to the next step. If t_j here is larger than the previously required, select the proper geotextiles based on the recommendations in paragraph 7-4-2. In case the specified geotextile tensile strength is excessively high, increase the number of geotextile sheets n and return to step 4.

7. Regardless of the conclusion in step 6, in steps 7 and 8 use t_1 as computed in step 4. Use equation 7-17 to compute the required length of the restraining zone ℓ_e and ℓ_{e_1}.

8. Compute $\lambda_{T\phi} = (nt_1)/(F_g\gamma H^2 \tan\phi)$. Notice that t_1/F_g is used here, whereas before only t_1 was used.

9. Use figure 7-20b to determine L and m and $\lambda_{T\phi}$.

10. Compute $\ell = L \cdot H$.

11. Is $(\ell+\ell_e)$ smaller than the value obtained based on a prescribed F_s? If yes, then the embedment length is dictated by the procedure based on the safety factor for the composite structure, F_s. If no, proceed.

12. Select ℓ_a based on equation 7-19 ($\ell_a \geq 3$ feet).

12. Determine the required length of each geotextile sheet j: $\ell_e+\ell+d+\ell_a+(H-y_j)/m$. Add one foot as tolerance. Use ℓ_{e_1} instead of ℓ_e for geotextile #1 (at the elevation of the toe).

7-4-3-2-2. SURCHARGE LOADS

It is assumed that a preliminary design, based on F_s, has been carried out as instructed in paragraph 7-4-3-1-1. Hence, the user is familiar with the load definitions.

(a) Uniform Surcharge Load: Figures 7-21 through 7-25 are the design charts adequate to handle this type of surcharge load. The following are the steps necessary to use these charts:

1. Select a value for F_g. The recommended value is 2.0.
2. Take $F_s = 1.0$; hence, $\phi_m = \phi$.
3. Compute $Q = q/\gamma H$.
4. Select the adequate design chart based on Q.
5. Use this chart to determine T_{m_1} for m and ϕ_m.
6. Compute the required tensile resistance of the geotextile sheet at the toe elevation $t_1 = F_g T_{m_1} \gamma H^2/n$.
7. Calculate the required tensile resistance of all other geotextile sheets using equation 7-2, i.e., $t_j = t_1[\gamma(H-y_j)+q]/(\gamma H+q)$.

8. Compare t_j for all sheets with those obtained based on a prescribed F_s in paragraph 7-4-3-1-1. For design select the maximum of the two values. Select the adequate geotextile based on the recommendations in paragraph 7-4-2. In case the specified geotextile tensile strength is excessively high, increase the number of geotextile sheets n and return to step 6.

9. Regardless of step 8 comparison conclusion, in steps 9 and 10 use t_1 as computed in step 6. Use equation 7-17 to compute the required length of the restraining zone ℓ_e and ℓ_{e_1}.

10. Compute $\lambda_{T\phi} = (nt_1)/(F_g \gamma H^2 \tan\phi)$.

11. Use the adequate design chart to determine L for m, $\lambda_{T\phi}$ and Q.

12. Compute $\ell = L \cdot H$.

13. Is q extending over $(\ell+\ell_e)$? If yes, the results comply with the basic premise of the analysis and therefore one should proceed. Otherwise, the analysis is inappropriate and one should skip to the next type of surcharge loading.

14. Is $(\ell+\ell_e)$ smaller than the value obtained in paragraph 7-4-3-1-1? If yes, then the embedment length is dictated by the procedure based on the safety factor for the composite structure, F_s. If no, proceed.

15. Select ℓ_a based on equation 7-19 ($\ell_a \geq 3$ feet).

16. Determine the required length of each geotextile sheet j: $\ell_e+\ell+d+\ell_a+(H-y_j)/m$. Add one foot as tolerance. Use ℓ_{e_1} instead of ℓ_e for geotextile #1.

(b) Strip Surcharge Load: The methodology of determining an equivalent load q is explained in paragraph 7-4-3-1-1. Figures 7-27 through 7-31 are the design charts for the equivalent surcharge load. The following are the steps necessary to use these charts.

1. Select a value for F_g. The recommended value is 2.0.
2. Take $F_s = 1.0$; hence, $\phi_m = \phi$.
3. Assume a value for ℓ; e.g., take the result obtained in the preliminary design.
4. Among all strip footings acting over ℓ, select the one that exerts the maximum q. Take this q as the equivalent load (eq. 7-20).
5. Compute $Q = q/\gamma H$.
6. Select the adequate design chart based on Q.
7. Use this chart to determine T_{m_1} for m and ϕ_m.
8. Compute $t_1 = F_g T_m \gamma H^2/n$.
9. Compute $\lambda_{T\phi} = (nt_1^1)/F_g \gamma H^2 \tan\phi)$.
10. Use the adequate design chart to determine L for m, $\lambda_{T\phi}$ and Q.
11. Compute $\ell = L \cdot H$.

12. Check if the selected maximum q indeed acts over ℓ. If yes, proceed. If not, assume this ℓ to be valid and go back to step 4.

13. Compare t_1 with those obtained based on a prescribed F_s in paragraph 7-4-3-1-1. For design select the maximum of the two values. Select the adequate geotextile based on the recommendations in paragraph 7-4-2. It is recommended to use one type of geotextile for this particular case of loading. In case the specified geotextile tensile strength is excessively high, increase the number of geotextile sheets n and return to step 8.

14. Regardless of step 13 comparison conclusion, in this step use t_1 as computed in step 8. Use equation 7-17 to compute ℓ_e and ℓ_{e_1}. Take q equal to zero in this equation.

15. Is $(\ell+\ell_e)$ smaller than the value obtained in paragraph 7-4-3-1-1? If yes, then the embedment length is dictated by the procedure based on F_s. If no, proceed.

16. Select ℓ_a based on equation 7-19 ($\ell_a \geq 3$ feet).

17. Determine the required length of each geotextile sheet j: $\ell_e+\ell+d+\ell_a+(H-y_j)/m$. Add one foot as tolerance. Use ℓ_{e_1} instead of ℓ_e for geotextile #1.

7-4-3-3. EXAMPLES

The following are design examples, based solely on internal stability considerations. In all cases, the specified factor of safety for the composite structure is $F_s = 1.5$ and for the geotextile tensile resistance is $F_g = 2.0$.

Example I: Given a wall data: height H = 10 ft., face inclination 1:∞ (m = ∞, i.e., vertical wall) and surcharge load q = 0. The retained soil data: total unit weight $\gamma = 120$ lb/ft^3 and friction angle $\phi = 35°$. The foundation possesses $\phi_F = 20°$.

Design based on $F_s = 1.5$: Following the procedure presented in paragraph 7-4-3-1, one can choose a spacing of d = 1 ft. Computing ϕ_m gives $\phi_m = \tan^{-1}[(\tan 35°)/1.5] = 25°$. For m = ∞ and $\phi_m = 25°$, it follows from figure 7-20a that $T_{m_1} = 0.35$. For a spacing of d = 1 ft., the number of required geotextile sheets is n = H/d = 10/1 = 10 sheets. Hence, the required tensile resistance of the geotextile sheet at the toe elevation is $t_1 = T_{m_1} F_s \gamma H^2/n = 0.35 \cdot 1.5 \cdot 120 \cdot (10)^2/10 = 630$ lb. per foot width. Using the equation $t_j = t_1(H-y_j)/H$, where y_j is zero at the toe and H at the crest, one can calculate the tensile resistance of all other geotextile sheet:

Geotextile #	1	2	3	4	5	6	7	8	9	10
Elevation y_j [ft]	0	1	2	3	4	5	6	7	8	9
t_j [lb/ft]	630	567	504	441	378	315	252	189	126	63

Now, a geotextile can be selected based on the recommendations in paragraph 7-4-2. It should be noted that if only one type of geotextile is going to be used, t_1 should be the key value for selecting this type. If, however, geotextiles with decreasing strength properties are preferred, take the maximum t_j for each cluster of homogeneous geotextiles as the key value.

The required length of the restraining zone, so that t_j can realize without pullout, should be calculated based on equation 7-17, i.e.,

$$\ell_e = \frac{630}{2(120 \cdot 10 + 0)\tan(\frac{2}{3} \cdot 35°)} = 0.61 \text{ ft} \cong 8"$$

$$\ell_{e_1} = \frac{630}{(120 \cdot 10 + 0)[\tan(\frac{2}{3} \cdot 35°) + \tan(\frac{2}{3} \cdot 20°)]} = 0.78 \text{ ft} \cong 10"$$

For all practical purposes a uniform value of ℓ_e equals one foot can be selected.

Now, calculate $\lambda_{T\phi} = (10 \cdot 630)/(120 \cdot 10^2 \tan 35°) = 0.75$. For $m = \infty$ and $\lambda_{T\phi} = 0.75$ read $L = 0.8$ from figure 7-20b. Hence, the potential slip surface is located at a distance of $\ell = 0.8 \cdot 10 = 8$ ft. Using equation 7-19 one obtains $\ell_a = 3$ ft. Allowing one additional foot as tolerance, the length of all geotextile sheets should be equal to $[\ell_e + \ell + d + \ell_a + (H - y_j)/m] + 1 = (1 + 8 + 1 + 3) + 1 = 14$ ft.

Design based on $F_g = 2.0$: Here, the procedure presented in paragraph 7-4-3-2 is followed. Taking $F_s = 1.0$, ϕ_m then equals ϕ.

Using figure 7-20a for $\phi_m = 35°$ and $m = \infty$, the corresponding T_{m_1} is 0.241. Hence, $t_1 = F_g t_{m_1} \gamma H^2/n = 2.0 \cdot 0.241 \cdot 120 \cdot (10)^2/10 =$ 580 lb per foot width. Using equation 7-2, the required tensile resistance of all other geotextiles is:

Geotextile #	1	2	3	4	5	6	7	8	9	10
Elevation y_j [ft]	0	1	2	3	4	5	6	7	8	9
t_j [lb/ft]	580	522	464	406	348	290	232	174	115	58

Comparing t_j's based on $F_g = 2.0$ and $F_s = 1.5$ implies that the key value of t_j is dictated by the composite structure stability (i.e., by $F_s = 1.5$). Hence, the previous results are taken for design.

Based on equation 7-17 the following is obtained

$$\ell_e = \frac{580}{2(120 \cdot 10 + 0)\tan(\frac{2}{3} \cdot 35°)} = 0.56 \text{ ft} \cong 7"$$

$$\ell_{e_1} = \frac{580}{(120 \cdot 10 + 0)[\tan(\frac{2}{3} \cdot 35°) + \tan(\frac{2}{3} \cdot 20°)]} = 0.72 \text{ ft} \cong 9"$$

Once again, take $\ell_{e_1} = \ell_e = 1$ ft. Compute $\lambda_{T\phi} = (10 \cdot 580)/(2.0 \cdot 120 \cdot 10^2 \cdot \tan 35°) = 0.35$. For $m = \infty$ and $\lambda_{T\phi} = 0.35$ read L = 0.6 from figure 7-20b. Consequently, $\ell = 0.6 \cdot 10 = 6$ ft and $(\ell + \ell_e) = 7$ ft. This embedment length is less than the one resulted for the prescribed $F_s = 1.5$ (i.e., less than 9 ft.). In this particular problem the predominant factor is the design based on the safety for the composite structure. It determines

both the required tensile resistance (t_1 = 630 lb/ft) and the embedment length ($\ell+\ell_e$ = 9 ft). This resulted structure will have F_s equals 1.5 but F_g somewhat greater than 2.0.

Example II; Given the same data as in Example I. This time, however, the wall is subjected to a uniform surcharge load of $q = 840$ lb/ft^2 acting over 12 ft. from the wall's top.

Design based on $F_s = 1.5$: Following the procedure presented in paragraph 7-4-3-1-1, the non-dimensional Q is computed as $Q = q/\gamma H = 840/(120 \cdot 10) = 0.7$. From the previous example d = 1 ft., n = 10 and $\phi_m = 25°$. Using figure 7-24a for $m = \infty$ and $\phi_m = 25°$ one obtains $T_{m_1} = 0.603$. Hence, the required tensile resistance of the geotextile sheet at the toe elevation is $t_1 = T_{m_1} F_s \gamma H^2/n = 0.603 \cdot 1.5 \cdot 120 \cdot (10^2)/10 = 1085$ lb per foot width.

The required length of the restraining zone is

$$\ell_e = \frac{1085}{2 \cdot (120 \cdot 10 + 840) \tan(\frac{2}{3} \cdot 35°)} = 0.62 \text{ ft.} \cong 8"$$

$$\ell_{e_1} = \frac{1085}{(120 \cdot 10 + 840)[\tan(\frac{2}{3} \cdot 35°) + \tan(\frac{2}{3} \cdot 20°)]} = 0.80 \text{ ft.} \cong 10"$$

Calculate $\lambda_{T\phi} = (10 \cdot 1085)/(120 \cdot 10^2 \cdot \tan 35°) = 1.29$. For $m = \infty$, $Q = 0.7$ and $\lambda_{T\phi} = 1.29$ read L = 0.81 from figure 7-24b. The distance ℓ, therefore, is $0.81 \cdot 10 = 8.1$ ft. Since $(\ell+\ell_e) \cong$ 9 ft. and q extends to 12 ft., the analysis used here is adequate. Once again, based on equation 7-19 $\ell_a = 3$ ft. Taking $\ell_{e_1} = \ell_e = 0.9$ ft.

and 1 additional foot as tolerance, the required length of each sheet is $\ell_e+\ell+d+\ell_a+(H-y_j)/m-1 = 0.9+8\cdot1+1+3+0+1 = 14$ ft. The required tensile resistance of each geotextile sheet is calculated based on $t_j = t_1[\gamma(H-y_j)+q]/(\gamma H+q)$.

Geotextile #	1	2	3	4	5	6	7	8	9	10
Elevation y_j [ft]	0	1	2	3	4	5	6	7	8	9
t_j [lb/ft]	1085	1021	957	894	830	766	702	638	574	511

In essence, the same structure as in Example I was rendered. The required geotextile tensile resistance, however, has increased from 630 to 1085 lb/ft. Notice that the geotextiles at the top are subjected to much higher forces as compared to the previous case.

Design based on $F_g = 2.0$: The procedure presented in paragraph 7-4-3-2-2 is followed. For $F_s = 1.0$, $\phi_m = 35°$, $m = \infty$ and $Q = 0.7$ use figure 7-24a to get $T_{m_1} = 0.42$. Hence, $t_1 = 2.0\cdot0.42\cdot120\cdot(10)^2/10 = 1008$ lb/ft. The required tensile strength of all other geotextiles is

Geotextile #	1	2	3	4	5	6	7	8	9	10
Elevation y_j [ft]	0	1	2	3	4	5	6	7	8	9
t_j [lb/ft]	1008	945	889	830	771	712	652	593	534	474

Comparing the values of t_j's with those obtained for F_s = 1.5 indicates that the prevailing values are those previously obtained.

The required restraining zone is

$$\ell_e = \frac{1008}{2\cdot(120\cdot10+840)\tan(\frac{2}{3}\cdot35°)} = 0.57 \text{ ft.} \cong 7"$$

$$\ell_{e_1} = \frac{1008}{(120\cdot10+840)[\tan(\frac{2}{3}\cdot35°)+\tan(\frac{2}{3}\cdot20°)]} = 0.74 \text{ ft.} \cong 9"$$

Take the same value as before, i.e., $\ell_e = \ell_{e_1} = 0.9$ ft. Compute $\lambda_{T\phi} = (10\cdot1008)/(2.0\cdot120\cdot10^2\tan 35°) = 0.6$. For $m = \infty$, $\lambda_{T\phi}$ = 0.6 and Q = 0.7 read L = 0.605 from figure 7-24b. Consequently, $\ell = 0.605\cdot10 = 6.1$ ft. and $(\ell+\ell_e) = 7$ ft. Since q extends to 12 ft. the analysis used here is adequate. This embedment length, however, is less than the one resulted for the prescribed F_s(~9 ft.). Once again, the predominant factor in designing this wall is the safety of the composite structure.

Example III: Given the same basic data as in Example I. The wall is subjected to strip surcharge loading as shown in figure 7-32.

Design based on F_s = 1.5: Based on the procedure presented in paragraph 7-4-3-1-1, assume $\ell = 0.5\cdot H = 5$ ft. Maximum value of q_j is over this ℓ is $q = 840$ lb/ft^2. As in Example II, d = 1 ft, n = 10, $\phi_m = 25°$ and Q = 0.7. The adequate design charts

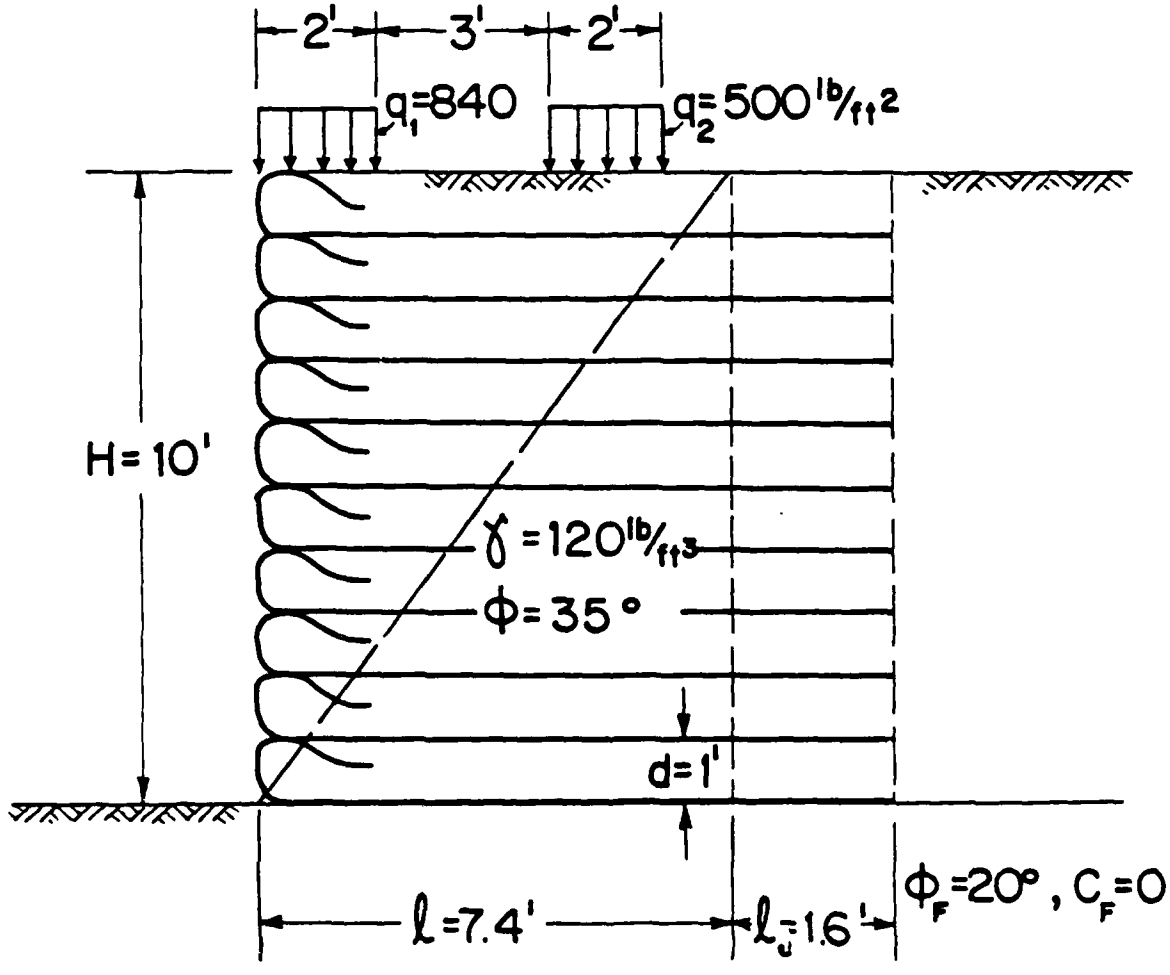

Figure 7-32. Illustration of the problem shown in Example III

are figures 7-30a and 7-30b. Utilizing figure 7-30a for $m = \infty$ and $\phi_m = 25°$ the resulted T_{m_1} is 0.7 and hence $t_1 = 0.7 \cdot 1.5 \cdot 120 \cdot (10^2)/10 = 1260$ lb per foot width. Taking $\lambda_{T\phi} = T_{m_1}/\tan\phi_m = 0.7/\tan 25 = 1.50$ and using figure 7-30b it follows that $L \tilde{=} 0.74$; hence $\ell = 0.74 \cdot 10 = 7.4$ ft. Looking at figure 7-32 one sees that the selected q is indeed the maximum load acting over this ℓ.

Using equation 7-17, ℓ_e and ℓ_{e_1} can be calculated (ignoring the restraining effect that a surcharge acting beyond ℓ may have):

$$\ell_e = \frac{1260}{2 \cdot (120 \cdot 10 + 0) \tan(\frac{2}{3} \cdot 35°)} = 1.22 \text{ ft.}$$

$$\ell_{e_1} = \frac{1260}{(120 \cdot 10 + 0)[\tan(\frac{2}{3} \cdot 35°) + \tan(\frac{2}{3} \cdot 20°)]} = 1.57 \text{ ft.}$$

For design take $\ell_e = \ell_{e_1} = 1.6$ ft., $\ell_a = 3$ ft. and add 1 ft. as tolerance. Consequently, the required length of each geotextile sheet is $\ell_e + \ell + d + \ell_a + (H - y_j)/m + 1 = 14$ ft. The required tensile resistance distribution can be computed using $t_j = t_1(H - y_j)/H$:

Geotextile #	1	2	3	4	5	6	7	8	9	10
Elevation y_j [ft]	0	1	2	3	4	5	6	7	8	9
t_j [lb/ft]	1260	1134	1008	882	756	630	504	378	252	126

Now a geotextile may be selected based on paragraph 7-4-2. It is recommended to use t_1 (and not t_j) in the selection process. Notice that t_j distribution here is triangular whereas in Example II it was trapezoidal.

Design based on $F_g = 2.0$: The procedure presented in paragraph 7-4-3-2-2 is followed. Assuming $\ell = 7.4$ ft., the maximum surcharge is $q = 840$ lb/ft^2. For $F_s = 1.0$, $\phi_m = 35°$, $m = \infty$ and $Q = q/\gamma H = 0.7$ use figure 7-30a to determine $T_{m_1} = 0.58$ and hence, $t_1 = 1044$ lb per foot width. Comparing this t_1 with the one obtained for $F_s = 1.5$ indicates that the governing design value is the previous one (i.e., $t_1 = 1260$ lb/ft).

Computing $\lambda_{T\phi} = (10 \cdot 1044)/(2 \cdot 120 \cdot 10^2 \tan 35) = 0.62$ and using figure 7-30b, one gets $L = 0.54$ or $\ell = 0.54 \cdot 10 = 5.4$ ft. The selected maximum q indeed acts over this ℓ.

It can be vertified by calculating ℓ_e here that $(\ell+\ell_e)$ for $F_s = 1.5$ is more stringent than the one obtained here. Therefore, the design based on F_s completely prevails.

7-4-4. EXTERNAL STABILITY

The composite wall interacts with its foundation soil and is subjected to lateral earth pressures induced by the soil retained behind the reinforced portion. The effects of these factors were not considered in the internal stability design. Consequently, an internally stable reinforced wall may have unacceptable external stability. Typically, the reinforced wall

is taken as a monolithic block having to be stable under the following conditions:

1. Overturning about the wall's toe.
2. Sliding of the wall along its base or above it.
3. Overall slope stability.
4. Bearing capacity failure of the wall's base.
5. Excessive settlement of the foundation material.

The following is just a brief description of methods assessing the external stability. They are based on the common practice used for conventional retaining walls. Additional information is available in most foundation engineering handbooks (e.g., Winterkorn and Fang (1975)).

7-4-4-1. OVERTURNING

Figure 7-33 is a freebody diagram of the composite wall (taken as a rigid body) assumed to be at the verge of its rotation about the hinge (toe) O. Notice that the following assumptions are incorporated in the forces shown:

1. Rankine's lateral earth pressures are acting on the rigid block.
2. Passive resistance pressure that may develop in front of the wall is ignored.
3. Any surcharge load acting over $(\ell+\ell_e)$ is ignored.
4. The surcharge load q acting to the right of $(\ell+\ell_e)$ is uniform.

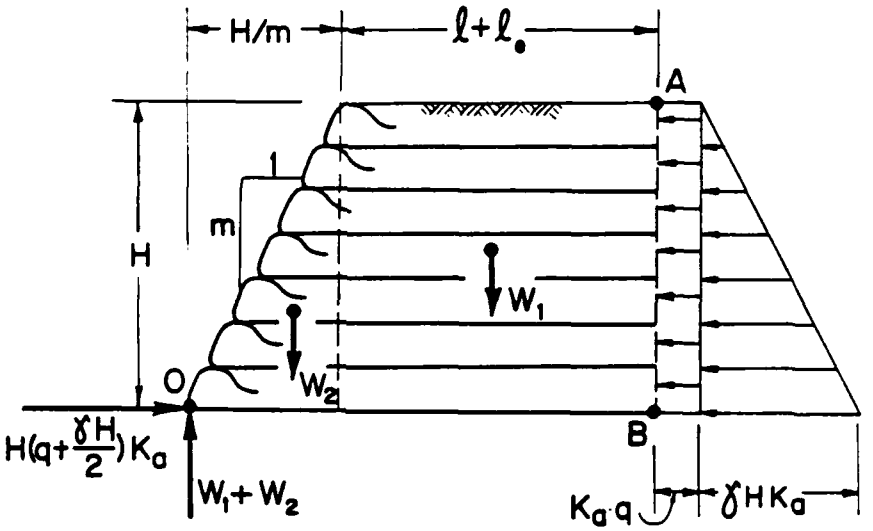

Figure 7-33. Freebody diagram of the wall at the verge of overturning

The safety factor against rotation is defined as

$$(F_s)_{ot} = \frac{\sum M_R}{\sum M_E} \tag{7-22}$$

where $\sum M_E$ is the sum of all moments tending to overturn the reinforced wall, and $\sum M_R$ is the sum of moments resisting this overturning tendency.

For the case shown in figure 7-33, the following general expressions can be assembled

$$\sum M_R = W_1\left(\frac{\ell+\ell_e}{2} + \frac{H}{m}\right) + W_2\left(\frac{2}{3}\frac{H}{m}\right) \tag{7-23a}$$

$$\sum M_E = K_a \frac{H^2}{2}\left(\frac{\gamma H}{3} + q\right) \tag{7-23b}$$

where $K_a = \tan^2(45 - \frac{\phi_b}{2})$ = Rankine's lateral earth pressure coefficient and ϕ_b the friction angle of the backfill; $W_1 = \gamma H(\ell+\ell_e)$; $W_2 = \gamma H^2/(2m)$; and γ is the unit weight assumed to have the same value for the backfill and the soil wrapped by the geotextiles.

Substituting equations 7-23a and 7-23b into equation 7-22 will result with the margin of safety against overturning. The recommended minimal values for $(F_s)_{ot}$ are 1.5 if the foundation material is granular and 2.0 if cohesive. If these recommended values do not exist for the wall designed in paragraph 7-4-3, $(\ell+\ell_e)$ must be increased so that this requirement is attained.

As an example, one can calculate the following for Example III, presented in paragraph 7-4-3-3 (see fig. 7-32): $K_a = \tan^2(45-35/2) = 0.27$ (assuming that $\phi_b = 35°$), $W_1 = 120 \cdot 10 \cdot 9 = 10800$ lb/ft, and $W_2 = 0$. Subsequently, $\sum M_R = 48600$ lb·ft/ft, $\sum M_E = 5400$ lb·ft/ft, and the resulted safety factor is $(F_s)_{ot} = 9$. It can be verified that if a uniform surcharge of $q = 840$ lb/ft^2 is applied (as is the case in Example II, paragraph 7-4-3-3) the factor of safety will drop to 2.9.

It should be noted that in case there is a point, line or strip surcharge load acting to the right of $(\ell+\ell_e)$, one will need to calculate the lateral earth pressure along the interface AB in figure 7-33 using techniques presented in most foundation handbooks (e.g., Winterkorn et al. (1975)). The resulting moments from these pressures must be properly introduced into equation 7-23b.

If the construction arrangement shown in figure 7-19 is preferred, the estimation of the lateral earth pressure along AB, needed here and in paragraphs 7-4-4-2 and 7-4-4-4 requires special attention. One must determine this lateral pressure based on assumed two possible failure modes. The first mode is for failure occurring within the superior backfill (i.e., within wedge ABC in figure 7-19). Since BC is inclined at 45° (i.e., less than $(45°+\phi_b/2)$), Rankine's pressures can be calculated as done in equation 7-23b. The second mode is for the wedge ABC

where BC is within the inferior backfill. In this case, the lateral force can be estimated using limiting-equilibrium considerations (e.g., Perloff and Baron (1976), pp. 594-596). For design, the higher pressure value must be selected.

7-4-4-2. SLIDING

Figure 7-34 is the freebody diagram of the reinforced wall. The load induced on the rigid block by the free draining backfill may cause the wall to slide along its base or, in some special cases, above it; i.e., along one of the geotextile sheets interface.

The assumptions regarding the forces acting on the rigid block, presented in paragraph 7-4-4-1, are applicable here as well. Hence, the horizontal force tending to cause slide along the base is

$$R = K_a H(q + \frac{\gamma H}{2}) \qquad (7\text{-}24a)$$

The maximum horizontal resisting force is

$$R_{max} = (W_1+W_2)\tan(\frac{2}{3}\phi_F) + \frac{2}{3} c_F(\ell+\ell_e+H/m) \qquad (7\text{-}24b)$$

where (W_1+W_2) is the weight of the reinforced wall -- see figure 7-34, ϕ_F and c_F are the friction and adhesion, respectively, of the foundation material at the base interface. It should be pointed out that for a permanent structure, a free draining

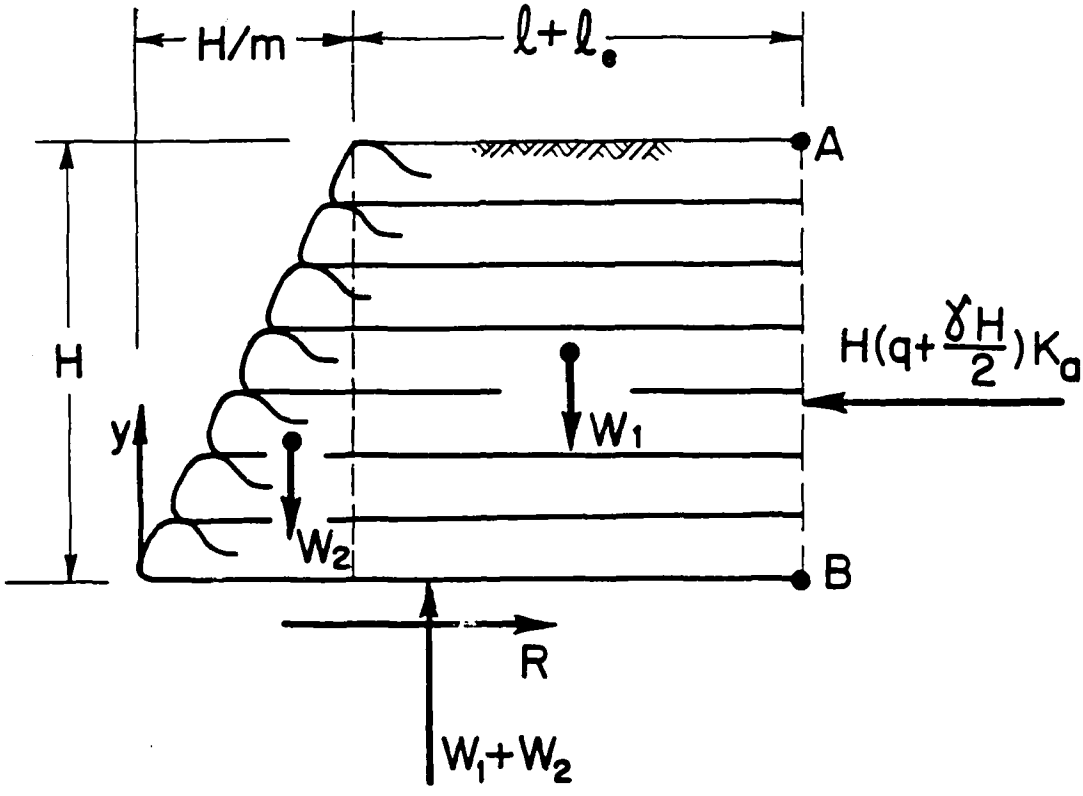

Figure 7-34. Freebody diagram of an externally stable wall

foundation soil is required -- see paragraph 7-4-1. Subsequently, the adhesion c_F is likely to be zero.

The factor of safety against sliding along the base is defined as

$$(F_s)_s = \frac{R_{max}}{R} \qquad (7\text{-}25)$$

Checking the sliding stability of Example III in paragraph 7-4-3-3 (fig. 7-32), one can calculate R = 0.27•10•120•10/2 = 1620 lb/ft. The maximum available resistance is R_{max} = (10800)•tan(2•20/3) = 2560 lb/ft. Hence, $(F_s)_s$ = 2560/1620 = 1.6.

The recommended minimal values for $(F_s)_s$ are 1.5 if the foundation material is granular and 2.0 if cohesive. If the minimum $(F_s)_s$ value is not exceeded, two typical remedies are possible: (1) increase $(\ell+\ell_e)$ so as to increase (W_1+W_2), and (2) construct a concrete footing with properly designed key and high surface friction -- see foundation handbooks for guide.

As was stated before, there are special circumstances where slide may occur through the inner structure. These cases are:

1) The value of R_{max} between the geotextile at the bottom and the foundation material is larger than R_{max} between the same geotextile and the retained soil. In this case, R_{max} in equation 7-25 should be approximated as

$$R_{max} = (W_1 + W_2)\tan(\frac{2}{3} \cdot \phi) \qquad (7\text{-}26)$$

and $(F_s)_s$ should be, at least, 1.5.

2) A point, line or strip surcharge load is acting to the right of $(\ell+\ell_e)$, inducing large lateral pressures along the upper portion of the interface AB in figure 7-34. Consequently, there is a possibility that an inadequate factor of safety against sliding of the upper portion of the structure will result. To ensure a $(F_s)_s = 1.5$ everywhere, first one has to determine the induced lateral pressures using techniques presented in most foundation handbooks (e.g., Winterkorn et al. (1975)). Then, at every geotextile sheet interface, R and R_{max} need to be determined using $(H-y_j)$ instead of H in equations 7-24a and 7-26. Subsequently, $(F_s)_s$ can be calculated now at any interface.

7-4-4-3. SLOPE STABILITY

Figure 7-35 illustrates two typical cases of general slope failure. The potential for deep seated failure increases significantly when the underlying material is weaker than the retained cohesionless soil or if it contains weak layers near the wall's foundation.

It is recommended to assess the overall stability using the simplified Bishop analysis method. However, if a weak thin layer is located near the wall's base, it is recommended to assess the stability using also the wedge method, dividing the mass to three

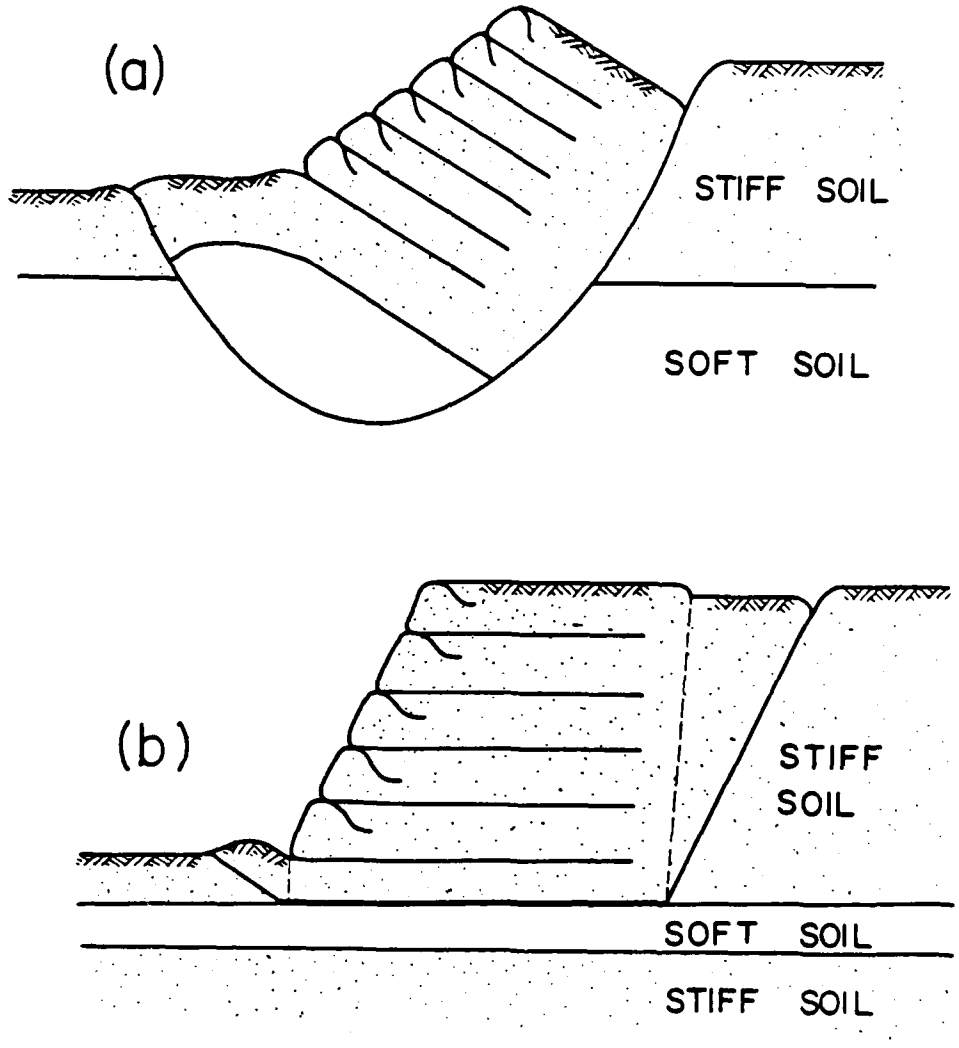

Figure 7-35. Illustration of typical overall slope failures

blocks. The wedge method should be used also when the foundation soil contains a thick layer of stiff soil near the wall's base. In this case it is likely that the potential slip surface will propagate along the interface with the hard layer. It should be noted that in the stability analysis the reinforced wall is typically considered as a rigid gravity wall.

When applicable, the short- and long-term stability should be checked. It is recommended to attain, in all times, a minimum factor of safety of 1.5 against general slope failure. If the safety factor is less than 1.5, decrease in the wall's face inclincation, or its height (if possible), may help resolve the problem.

7-4-4-4. BEARING CAPACITY

Figure 7-36 shows the pressures considered in estimating the bearing capacity of the base of the reinforced wall. Notice that the following assumptions are incorporated:

1. The stress distribution over the wall's base is trapezoidal.
2. Rankine's lateral earth pressures are acting on the rigid block over segment AB.
3. The passive resistance, that may develop in front of the wall, is ignored.
4. The surcharge load, acting to the right of point A, is uniform.

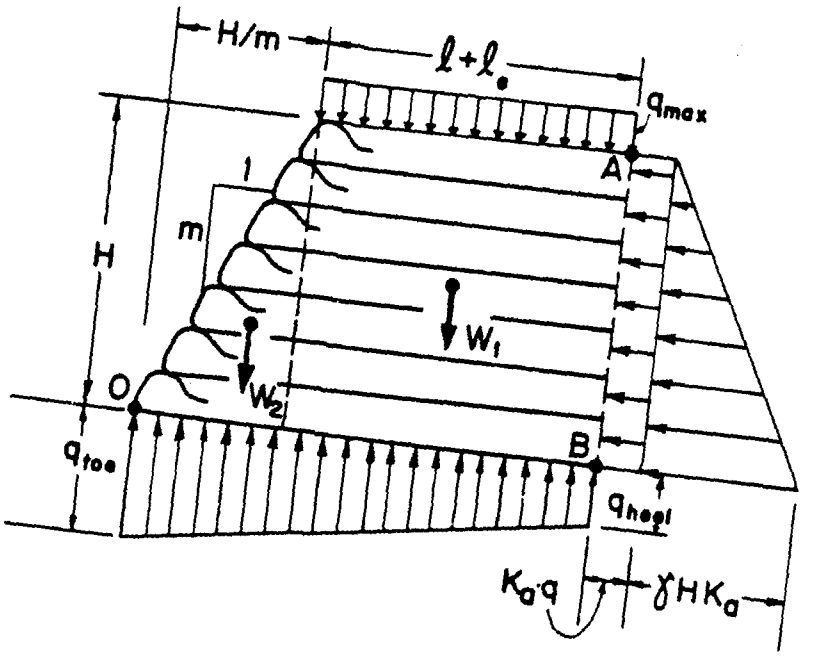

Figure 7-36. Pressures considered in the bearing-capacity evaluation

5. The surcharge load q_{max}, acting over $(\ell+\ell_e)$, is uniform.

In estimating the bearing capacity it is recommended to use Meyerhof's method (1953) for shallow foundation subjected to inclined and eccentric load. Taking moments about point O (see fig. 7-36), one can show that the eccentricity e is

$$e = \frac{\ell+\ell_e}{2} + \frac{H}{m} - \frac{\frac{2}{3}\frac{H}{m}W_2 + (\frac{\ell+\ell_e}{2} + \frac{H}{m})[W_1 + q_{max}(\ell+\ell_e)] - K_a(q+\frac{\gamma H}{3})\frac{H^2}{2}}{W_1 + W_2 + q_{max}(\ell+\ell_e)} \quad (7\text{-}27)$$

Note that to comply with assumption (1) above, e must be less than $(\ell_e+\ell)/6$. Using Meyerhof's (1953) definition, the effective foundation width is

$$\bar{B} = (\ell + \ell_e + \frac{H}{m}) - 2e \quad (7\text{-}28)$$

For a foundation of effective contact width $\bar{B}$, it is assumed that the load acts centrally, exerting average pressure of

$$q_{av} = \frac{W_1 + W_2 + q_{max}(\ell + \ell_e)}{\bar{B}} \quad (7\text{-}29)$$

The ultimate bearing capacity load is

$$q_{ult} = c\,N_c + \frac{1}{2}\gamma B N_\gamma \quad (7\text{-}30)$$

where N_c and N_γ are the bearing capacity factors for centrally loaded strip foundation. These factors are available in most foundation handbooks (e.g., Winterkorn et al. (1975)).

The factor of safety against bearing capacity failure is defined as

$$(F_s)_{bc} = \frac{q_{ult}}{q_{av}} \qquad (7\text{-}31)$$

The minimum required value for $(F_s)_{bc}$ is 2.0.

It should be noted that a uniform surcharge load q_{max} (see fig. 7-36) should be taken as equivalent load for strip load as explained in paragraph 7-4-3. Using Example III in paragraph 7-4-3-3 (see also fig. 7-32) for q_{max} = 840 lb/ft, one can calculate e = 0.3 ft; hence $\bar{B}$ = 9-2·0.3 = 8.4 ft and q_{av} = (10800+9·840)/8.4 = 2186 lb/ft^2. The ultimate bearing capacity of the foundation soil, q_{ult}, must be greater than 2.0·2186 = 4372 ≅ 2.2 ton per square foot. It can be verified that if Example II in paragraph 7-4-3-3 is considered (q = 840 lb/ft^2 acting over large area), then the resulted eccentricity is e = 0.9 ft, $\bar{B}$ = 7.2 ft and q_{av} = 2550 lb/ft^2. Consequently, q_{ult} must be greater than 2.6 ton/ft^2.

There may be cases where $(F_s)_{bc}$, for the initial design, will be less than the required value. Increasing $(\ell+\ell_e)$ may help somewhat; in extreme cases, however, special types of foundations (e.g., piles) or special treatment (e.g., soil stabilization) might be needed.

It should be noted that if the soil immediately underneath the wall's base is comprised of a thin layer (say, less than $\bar{B}$)

of high strength soil, underlaid by weaker soil, $(F_s)_{bc}$ should be assessed using a bearing capacity method for layered soil. If the thickness of the strong thin layer is less than 0.2 $\overline{B}$, ignore its existance when assessing the ultimate bearing capacity (i.e., assume that the foundation soil entirely comprise of the weaker foundation soil).

7-4-4-5. SETTLEMENT

Satisfaction of the above stability criteria does not guarantee tolerable settlements. Therefore, this subject, which may affect the geotextile reinforced wall serviceability but will not cause catastrophic failure, deserves special attention.

Unlike most other walls, the immediate settlement, rendered by the weight of the reinforced structure, is not of major concern, unless the natural soil is fairly loose. Typically, the retained and backfill soils are placed simultaneously, layer by layer, as the wall construction progresses. Consequently, if the geometry of the wall is properly monitored during construction, slight deviation, rendered by immediate settlement can be corrected with the placement of the next layer. If the natural soil is loose, however, large differential settlements will probably develop. Moreover, part of these "immediate" deformations will develop at a rate slower than construction. As a result, it may not be possible to correct structural geometrical deviations during construction and, therefore, the settlements must be

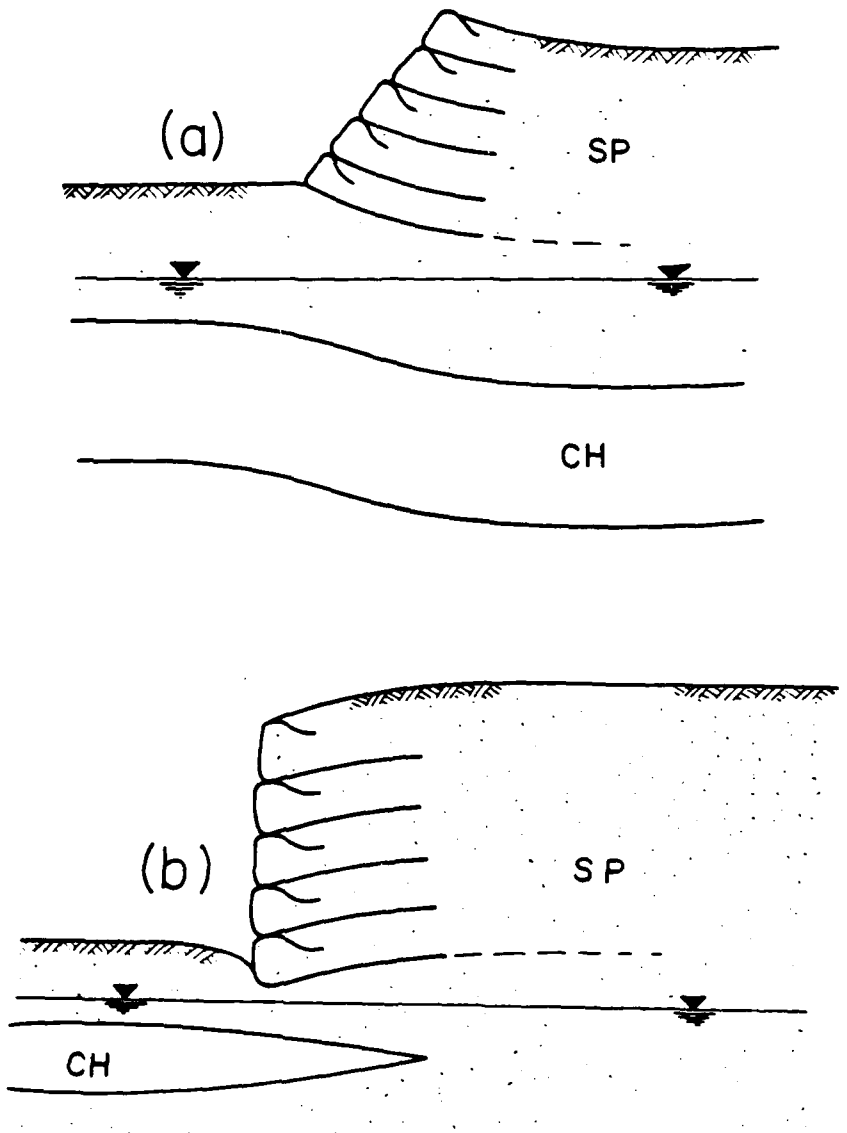

Figure 7-37. Illustration of typical consolidation settlements

considered in the design process and later on, properly monitored. Furthermore, if a permanent structure is to be constructed on top of the wall (e.g., bridge abutment), it may be necessary to predict the immediate settlement due to this structure, regardless of the natural soil. Immediate settlement (of wall and foundation) can be estimated using pseudo-elastic methods given in various foundation handbooks (e.g., Winterkorn et al. (1975)) or using a finite-element analysis.

In many cases a significant concern may arise from settlements due to consolidation. Figure 7-37 presents two such typical cases. To reasonably predict this settlement, first a reliable subsurface exploration is necessary. Second, the stress distribution within the consolidating layers, basically resulting from embankment's load, can be evaluated using, for example, Perloff's charts (1975). Combining the stress distribution, the various clays' properties and the 1-D consolidation theory, one can estimate the ultimate settlements and the approximated deformed profile of the reinforced wall. Depending on the structure significance, one can refine the predictions by using a more sophisticated analysis such as the finite-element for 2-D consolidation.

7-5. CONSTRUCTION

Site preparation should start with clearing and grubbing of all vegetation. Generally, it is recommended to replace at least

one foot of the natural soil below the wall base elevation with free-draining material (see paragraph 7-4-1). Before placement of the free-draining material, the surface of the excavated natural soil should be smooth, free of boulders, roots or cavities. If the natural foundation soil is clayey or silty, it is recommended to place a filter fabric on top of it. The free-draining material (preferably, crushed-stone) should be placed over the filter, up to the wall base elevation and compacted to its specified density.

The construction procedure of the wall is as suggested by the U.S. Forest Service, described and used by Bell et al. (1983) and Douglas (1982). Figure 7-38 illustrated the construction sequence after Bell et al. (1983). This figure is self explanatory. Figure 7-39 shows the details of the form system. Working with this type of temporary form system does not require special equipment. Bell et al. (1983) report that a new construction crew will develop the necessary technique for properly utilizing this form system within 3 to 4 lifts.

The wall face inclination, as well as its alignment, should be frequently surveyed to ensure that geometry is within specifications. Deviations can occur due to inadequate construction procedure and due to excessive settlement of the natural soil supporting the flexible wall. Attempt must be made to remedy

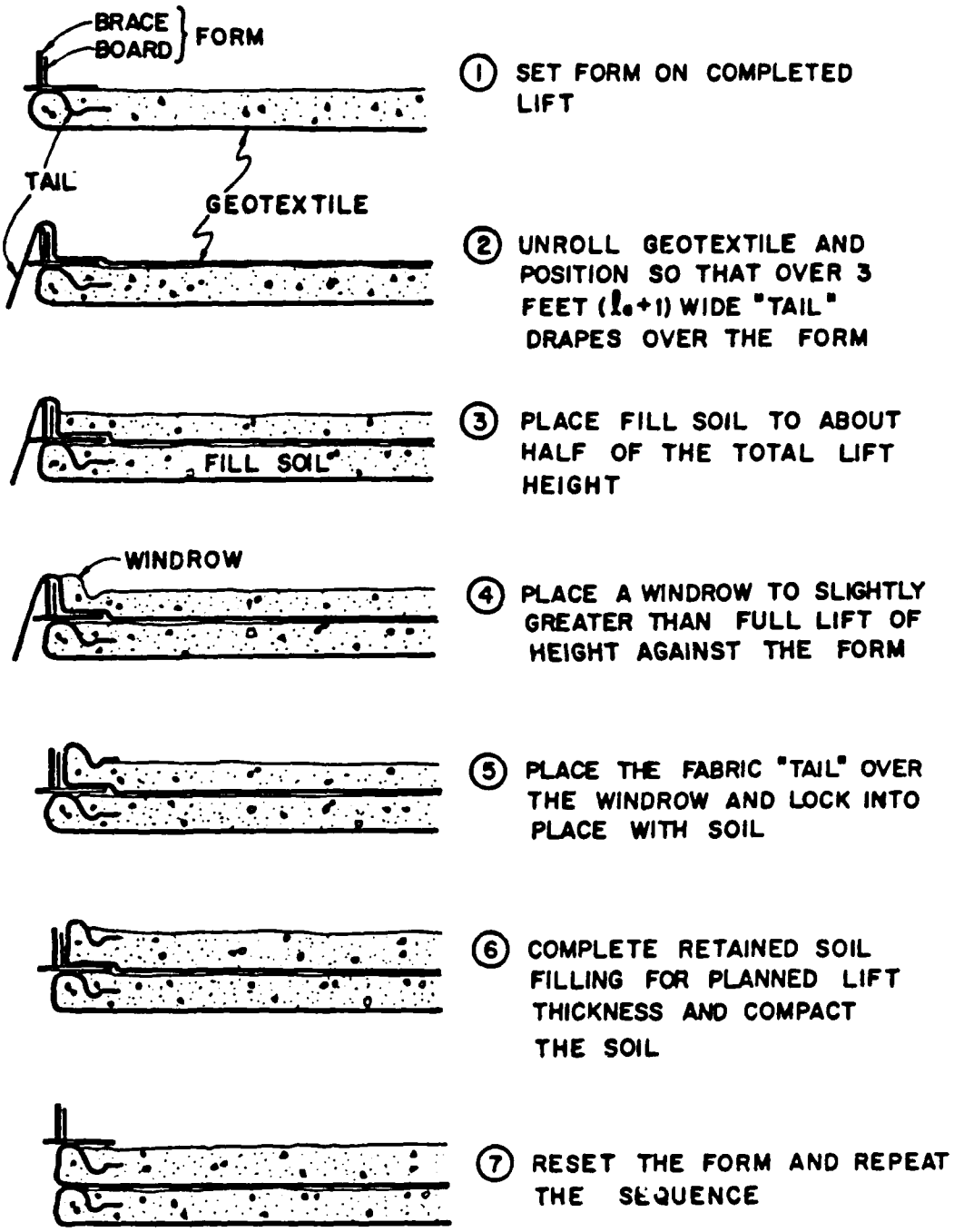

Figure 7-38. General procedure for the construction of a geotextile reinforced wall (Bell et al (1983))

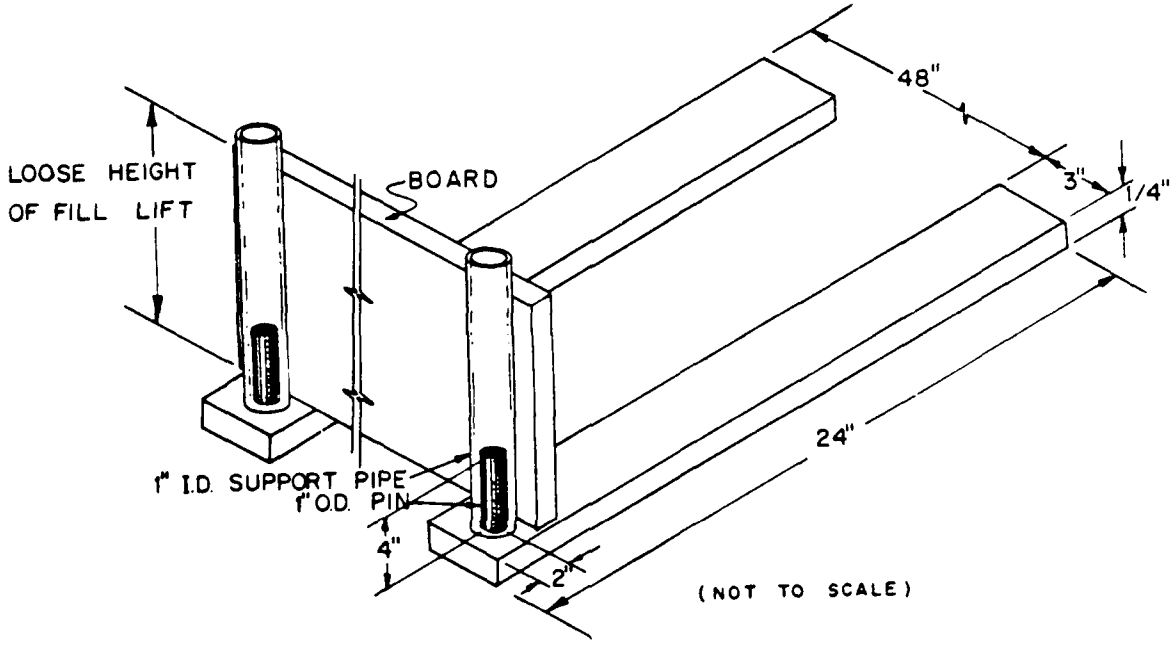

Figure 7-39. Details of the form system

these deviations with the next layers. In extreme cases, a re-design may be necessary.

During construction the geotextile sheets are susceptible to puncture and, possibly, abrasion damage. Special care, therefore, must be exercised when the fill material is placed over the geotextile. Inspectors should be instructed to watch for puncture or tear damages. Damaged geotextiles must be repaired or replaced. The type of construction equipment for dumping, spreading and compacting the fill is restricted by the geotextile puncture resistance, as explained in paragraph 7-4-2-3.

Each geotextile sheet should be continuous in the direction normal to the wall face. Overlapping or sewing of geotextiles in a direction parallel to the wall face must be avoided. If the geotextile sheet width is less than the length of the wall, several sheets may be placed next to each other, until their total width surpasses the wall's length. Each two adjacent sheets must lap over a minimum of 2 feet. Alternatively, if the required geotextile length (i.e., $\ell+\ell_a+\ell_e+d+1$, see para. 7-4-3) is smaller than the width of the geotextile roll, it may be placed parallel to the wall face. This will minimize overlapping and facilitate construction. It should be noted that the fact that a geotextile may have different tensile strength in each of the above principal directions, is already accounted for in the design (para. 7-4-2-3).

Since geotextiles are sensitive to UV light, their storage on site must protect them from such exposure. The protective cover must not be removed from the geotextile roll until the day it is to be installed. Immediately following the placement of a geotextile sheet, it should be covered with the fill material. Overnight exposure of the geotextile, however, is harmless. Immediately after the completion of the wall construction (if construction takes less than two weeks), the exterior wall face must be sprayed by a UV protective layer of, for example, asphalt or water-cement mixture (see para. 7-4-1). If the construction extends over a period longer than two weeks, a protective layer over the newly exposed geotextiles at the wall face must be sprayed every two weeks. Construction of the final facing and external structures can proceed now at a different pace.

7-6. MAINTENANCE

As is the case with most permanent retaining structures, water must drain freely. This is attained by adequately designed drainage system. To ensure that this system is continuously functioning, one has to inspect it periodically. Indications of excessive moisture on the exterior wall face should be investigated as to their origin.

Trees or any other type of deep rooted vegetation on top of the wall must be avoided. With time, deep roots will decrease the permeability of the retained soil. More importantly, roots

may puncture the geotextiles, decreasing their reinforcement potential. It is recommended to control vegetation by mechanical means or by using a herbicide that would not seep into the retained soil and possibly damage the geotextiles. It should be noted that, generally, excavation on top of the wall should not be permitted.

Since geotextile-retained soil wall is relatively a new type of structure, its performance over the long-run is founded on a speculative basis. It is extremely important, therefore, to monitor, as part of scheduled maintenance, signs indicating creep or progressive failure. Unusual cracks or deformaties on the coated wall face may indicate excessive geotextile creep. Wall face deformation or heaving soil away from the toe, possibly accompanied by severe deformations away from the top, imply that a progressive failure may take place. If any of these signs are observed, immediate investigation to the cause must be carried out.

Unless specifically designed for, all types of chemical or biological contaminants must not seep through the wall. Therefore, if water, suspected to be polluted, is seeping through the wall structure (e.g., from an adjacent drainage ditch), a water sample should be taken for a laboratory chemical analysis.

APPENDIX 7-A

REFERENCES

Al-Hussaini, M. M. (1977), "Field Experiment of Fabric Reinforced Earth Wall", Proceedings of the International Conference on the Use of Fabrics in Goetechnics, April 20-22, Paris, Vol. 1, pp. 119-121.

Al-Hussaini, M., and Perry, E. B. (1978), "Analysis of A Rubber Membrane Strip Reinforced Earth Wall", Soil Reinforcing and Stabilizing Techniques in Engineering Practice, Proceedings of a Symposium Jointly Organized by the New South Wales Institute of Technology and The University of New South Wales, Sydney, Australia, October, pp. 59-72.

Andrawes, K. Z., McGown, A., Wilson-Fahmy, R. F., and Mashhour, M. M. (1982), "The Finite-Element Method of Analysis Applied to Soil-Geotextile Systems", Proceedings of the 2nd International Conference on Geotextiles, August 1-6, Las Vegas, USA, Vol. 3, pp. 695-700.

Baker, R. (1981), "Tensile Strength, Tension Cracks and Stability of Slopes", Soils and Foundations, Journal of the Japanese Society of Soil Mechanics and Foundations Engineering, Vol. 21, No. 2, pp. 1-17.

Baker, R., and Garber, M. (1977), "Variational Approach to Slope Stability", Proceedings of the 9th International Conference on Soil Mechanics and Foundation Engineering, Tokyo, Vol. 2, pp. 9-12.

Baker, R., and Garber, M. (1978), "Theoretical Analysis of the Stability of Slopes", Geotechnique, Vol. 28, No. 4, pp. 395-411.

Barrett, R. K. (1985), "Geotextiles in Earth Reinforcement", Geotechnical Fabrics Report, March/April, Vol. 3, No. 2, pp. 15-19.

Bell, J. R., Barrett, R. K., and Ruckman, A. C. (1983), "Geotextile Earth-Reinforced Retaining Wall Tests: Glenwood Canyon, Colorado", Transportation Research Record, 916, pp. 59-69.

Bell, J. R., and Steward, J. E. (1977), "Construction and Observation of Fabric Retained Soil Walls", Proceedings of the International Conference on the Use of Fabrics in Geotechnics, April 20-22, Paris, Vol. 1, pp. 123-128.

Bell, J. R., Stilley, A. N., and Vandre, B. (1975), "Fabric Retained Earth Walls", Proceedings of the 13th Annual Engineering Geology and Soils Engineering Symposium, University of Idaho, Moscow, April 2-4, pp. 271-287.

Bell, J. R., Szymoniak, T., and Thommen, G. R. (1984), "Construction of a Steep Sided Geogrid Retaining Wall for an Oregon Coastal Highway", Symposium on Polymer Grid Reinforcement in Civil Engineering, March 22-23, The Institution of Civil Engineering, London, England, Paper #6.3.

Broms, B. B. (1978), "Design of Fabric Reinforced Retaining Structures", Proceedings of the Symposium on Earth Reinforcement, ASCE, Pittsburg, PA, April 27, pp. 282-304.

Chassie, R. G. (1984), "Geotextile Retaining Walls: Some Case History Examples", Paper Prepared for Presentation at The 1984 NW Roads and Streets Conference, Corvalis, OR, February 8th.

Chen, W. F. (1975), Limit Analysis and Soil Plasticity, Elsevier Pub., Amsterdam.

Christie, I. F., and El-Hadi, K. M. (1977), "Some Aspects of the Design of Earth Dams Reinforced with Fabric", Proceedings of the International Conference on the Use of Fabrics in Geotechnics, April 20-22, Paris, Vol. 1, pp. 99-103.

Christopher, B. R., and Holtz, R. D. (1984), Geotextile Engineering Manual, Draft Course Text, Prepared for FHWA, National Highway Institute, Washington, D.C., Contract No. DTFH61-80-C-00094.

Douglas, G. E. (1982), "Design and Construction of Fabric-Reinforced Retaining Walls by New York State", Transportation Research Record, 872, pp. 32-37.

El-Fermaoui, A., and Nowatzki, E. (1982), "Effect of Confining Pressure on Performance of Geotextiles in Soils", Proceedings of the 2nd International Conference on Geotextiles, August 1-6, Las Vegas, USA, Vol. 3, pp. 799-804.

Fowler, J. (1982), "Theoretical Design Considerations for Fabric-Reinforced Embankments", Proceedings of the 2nd International Conference on Geotextiles, August 1-6, Las Vegas, USA, Vol. 3, pp. 665-670.

Ingold, T. S. (1982), "An Analytical Study of Geotextile Reinforced Embankments", Proceedings of the 2nd International Conference on Geotextiles, August 1-6, Las Vegas, USA, Vol. 3, pp. 683-688.

Jewell, R. A. (1982), "A Limit Equilibrium Design Method for Reinforced Embankments on Soft Foundations", Proceedings of the 2nd International Conference on Geotextiles, August 1-6, Las Vegas, USA, Vol. 3, pp. 671-676.

Jones, C. J. F. P. (1985), Earth Reinforcement and Soil Structures, Butterworth and Co. (Publishers) Ltd.

Lee, K. L., Adams, B. D., and Vagneron, J-M. J. (1973), "Reinforced Earth Retaining Walls", Journal of the Soil Mechanics and Foundations Division, ASCE, Vol. 99, No. SM10, October, pp. 745-764.

Lee, K. L., Adams, B. D., and Vagneron, J-M. J. (1975), "Reinforced Earth Retaining Walls", Discussion Closure, Journal of the Geotechnical Engineering Division, ASCE, Vol. 101, No. GT3, March, pp. 345-346.

Leshchinsky, D. (1984), Geotextile Reinforced Earth, Part I & II, Research Report Nos. CE 84-44/45, Department of Civil Engineering, University of Delaware, Newark, DE, July.

Leshchinsky, D., Baker, R., and Silver, M. L. (1985), "Three Dimensional Analysis of Slope Stability", International Journal for Numerical and Analytical Methods in Geomechanics, Vol. 9, pp. 199-223.

Leshchinsky, D., and Reinschmidt, A. J. (1985), "Stability of Membrane Reinforced Slopes", Journal of the Geotechnical Engineering, ASCE, In Press.

Leshchinsky, D., and Volk, J. C. (1985), "Stability Charts for Geotextile Reinforced Walls", Transportation Research Record, In Press.

McGown, A., Andrawes, K. Z., and Kabir, M. H. (1982), "Load-Extension Testing of Geotextiles Confined In-Soil", Proceedings of the 2nd International Conference on Geotextiles, August 1-6, Las Vegas, USA, Vol. 3, pp. 793-798.

Meyerhof, G. G. (1953), "The Bearing Capacity of Foundations Under Eccentric and Inclined Loads", Proceedings of the 3rd International Conference on Soil Mechanics and Foundation Engineering, Zurich, Vol. 1, pp. 440-445.

Mitchell, J. K. (1984), "Earth Walls", TR News, Transportation Research Board, National Research Council, No. 114, September-October, pp. 24-31.

Mohney, J. (1977), "Fabric Retaining Wall-Olympic N. F.", Highway Focus, May, Vol. 9, No. 1, pp. 88-103.

Murray, R. T. (1980), "Fabric Reinforced Earth Walls: Development of Design Equations", Ground Engineering, Vol. 13, No. 7, pp. 29-36.

Murray, R. T. (1981), "Fabric Reinforced Earth Walls: Development of Design Equations", Supplementary Report 496, Structures Department, Transport and Road Research Laboratory, Crowthorne, Berkshire.

Murray, R. (1982), "Fabric Reinforcement of Embankments and Cuttings", Proceedings of the 2nd International Conference on Geotextiles, August 1-6, Las Vegas, USA, Vol. 3, pp. 707-713.

Perloff, W. H. (1975), Pressure Distribution and Settlement, Chapter 4 in Foundation Engineering Handbook, Edited by Winterkorn and Fang, Van Nostrand Reinhold Company.

Perloff, W. H., and Baron, W. (1976), Soil Mechanics: Principles and Applications, John Wiley & Sons.

Rowe, R. K. (1984), "Reinforced Embankments: Analysis and Design", Journal of the Geotechnical Engineering, ASCE, Vol. 110, No. 2, February, pp. 231-246.

Steward, J., Williamson, R., and Mohney, J. (1977), Guidelines for Use of Fabrics in Construction and Maintenance of Low-Volume Roads, Chapter 5, USDA, Forest Service, Portland, Oregon, June (Also Revised Version June, 1983).

Stilley, A. N. (1974), "A Model Study of Fabric Reinforced Earth Walls", A Thesis Submitted to Oregon State University in Partial Fulfillment of the Requirements for the Degree of Master of Science, 64 pp.

Szymoniak, T., Bell, J. R., Thommen, G. R., and Johnsen, E. L. (1984), "A Geogrid-Reinforced Soil Wall for Landslide Correction on the Oregon Coast", Transportation Research Record, 965, pp. 47-55.

Terzaghi, K., and Peck, R. B. (1967), Soil Mechanics in Engineering Practice, 2nd Edition, John Wiley & Sons, Inc.

Volk, J. C. (1984), "Analysis and Design of Geotextile Reinforced Walls", A Thesis Submitted to the Faculty of the University of Delaware in Partial Fulfillment of the Requirements for the Degree of Master of Civil Engineering, December.

Winterkorn, H. F., and Fang, H-Y (1975), Foundation Engineering Handbook, Van Nostrand Reinhold Company.

APPENDIX 7-B

STABILITY CHARTS FOR FAILURE MECHANISMS ASSUMING

THE GEOTEXTILE SHEETS TO BE HORIZONTAL AT THE SLIP SURFACE

The following set of charts is founded on the analysis presented in section 7-3. The difference between the mechanisms used for generating these charts and the design charts introduced in section 7-4 is in the assumed inclination of the geotextile sheets at the slip surface (para. 7-3-2-3). The failure mechanisms used for the charts here are similar to those shown in figure 7-8; however, the geotextiles here are assumed to be horizontal at the slip surface.

The purpose of including appendix 7-B is to enable full investigation of the analytical solution. This appendix permits a comprehensive comparative study of the effect of different assumed failure mechanisms concerning geotextiles (para. 7-3-2-3). It demonstrates that deviations in results (i.e., potential slip surface and the corresponding factor of safety) predicted based on the two different mechanisms are rather small for granular soil.

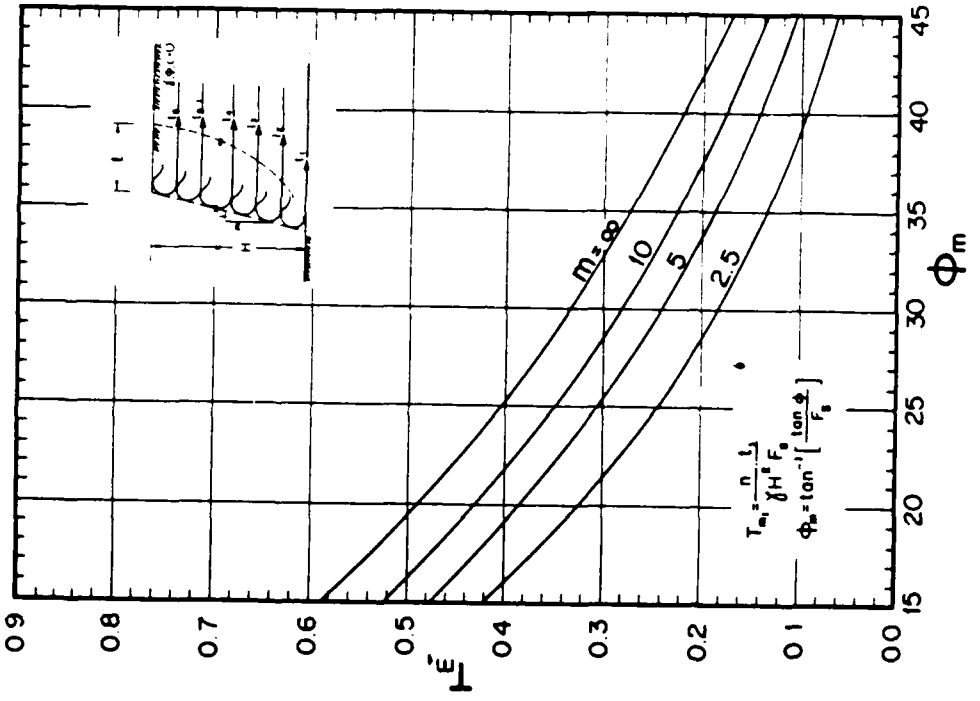

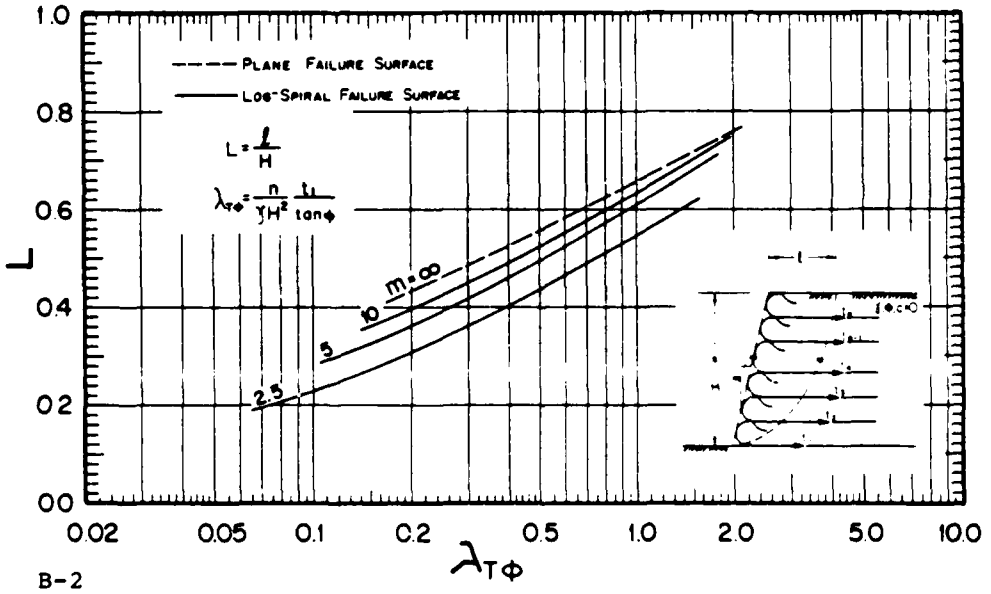

B-2

Figure 7-B-1. Stability chart

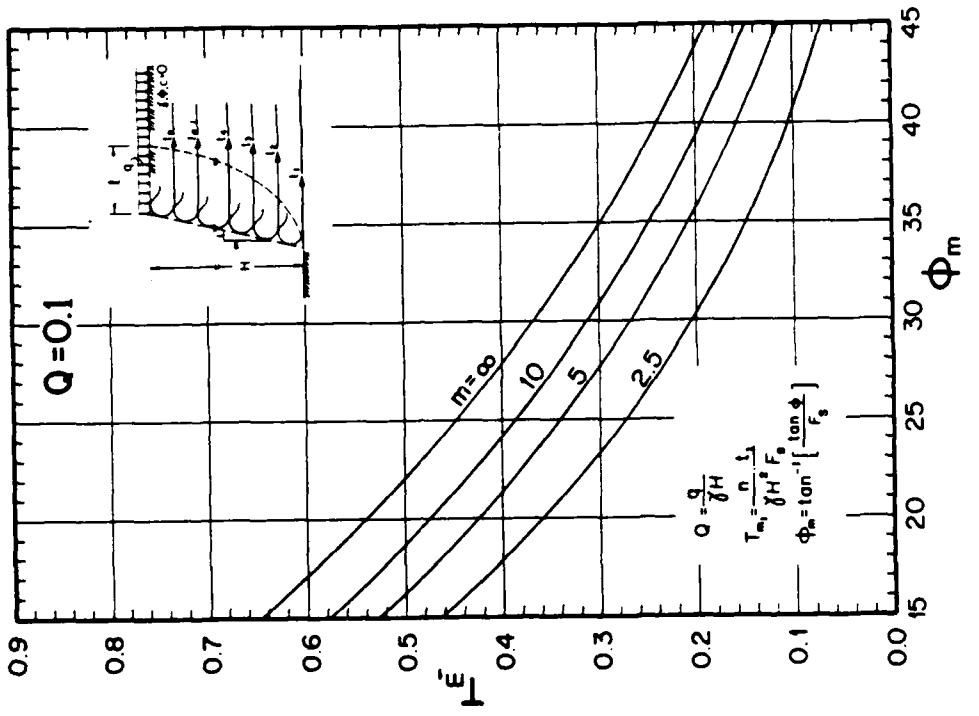

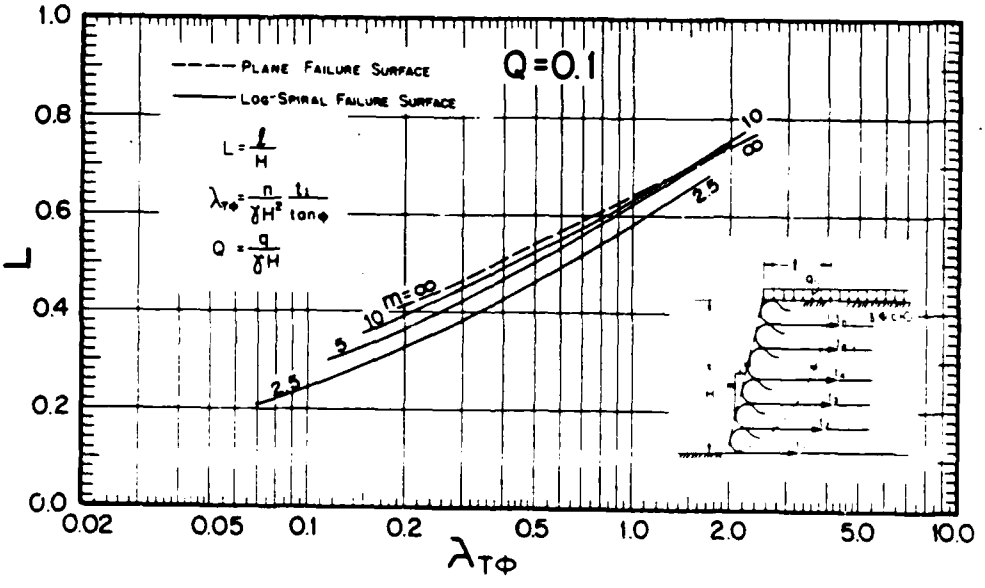

Figure 7-B-2. Stability chart
(uniform surcharge load of Q = 0.1)

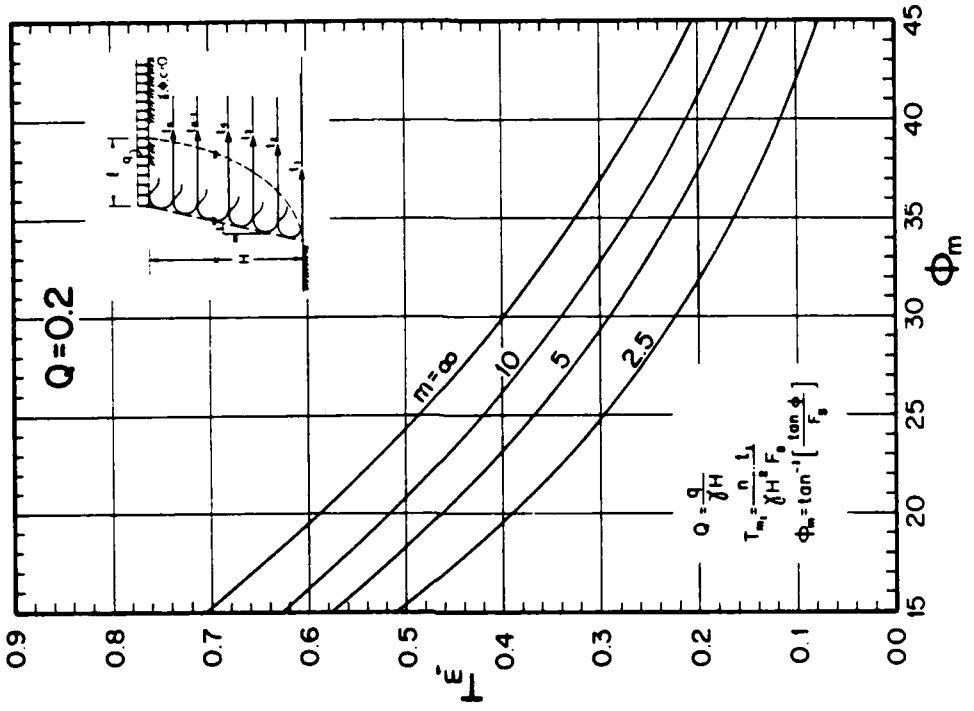

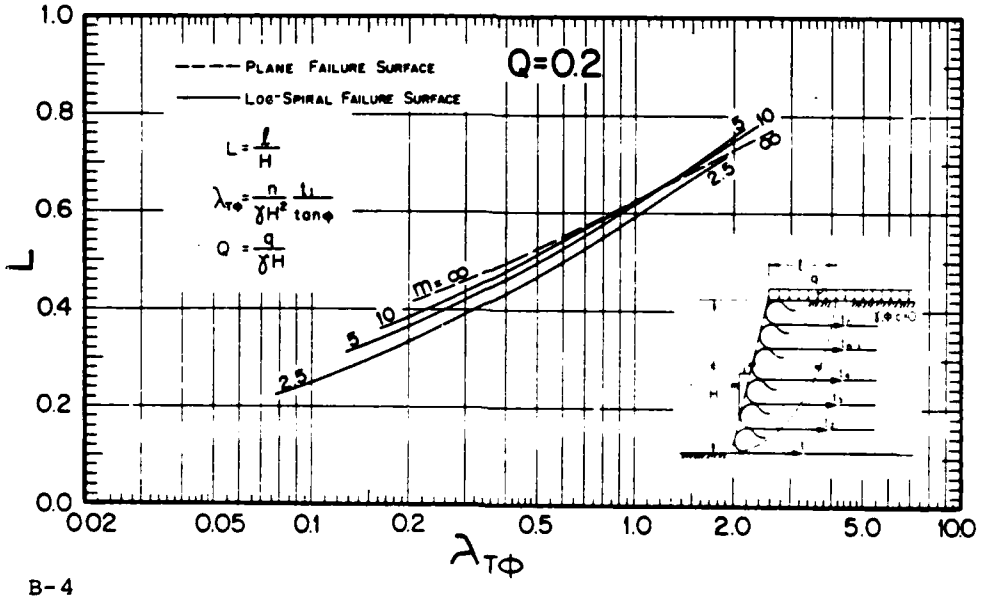

Figure 7-B-3. Stability chart
(uniform surcharge load of Q = 0.2)

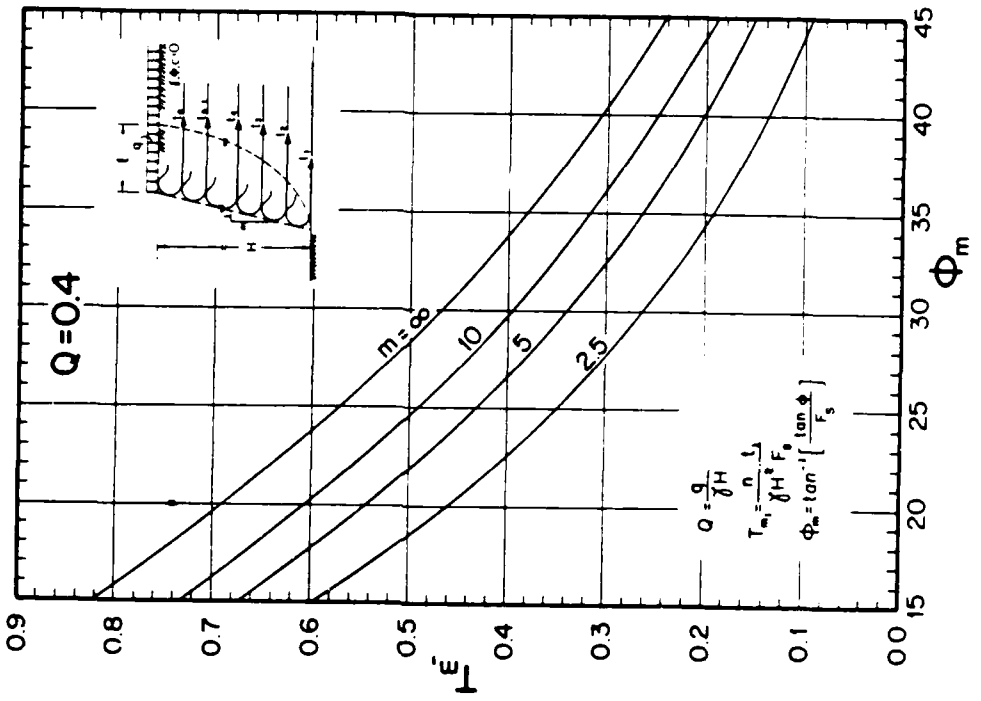

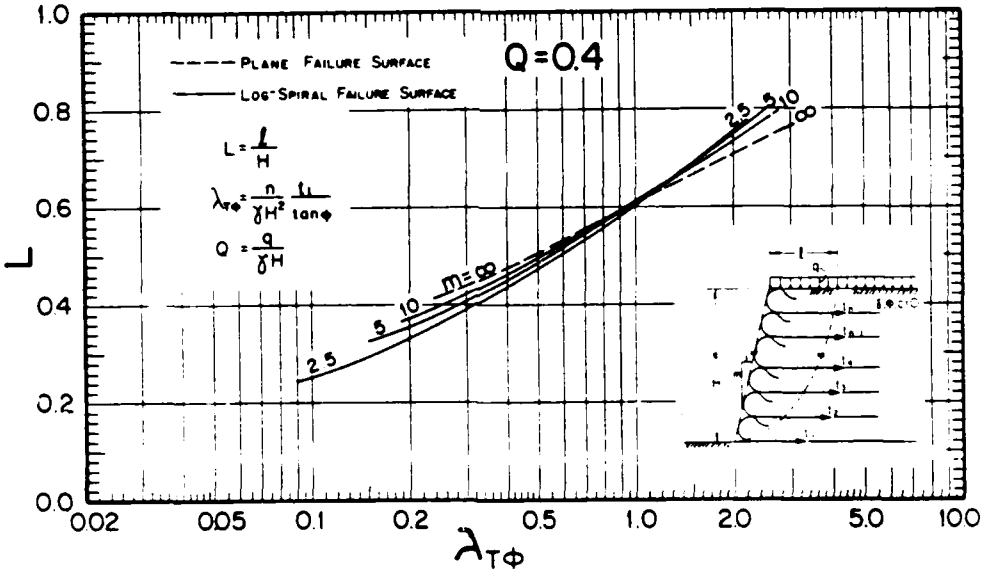

Figure 7-B-4. Stability chart
(uniform surcharge load of Q = 0.4)

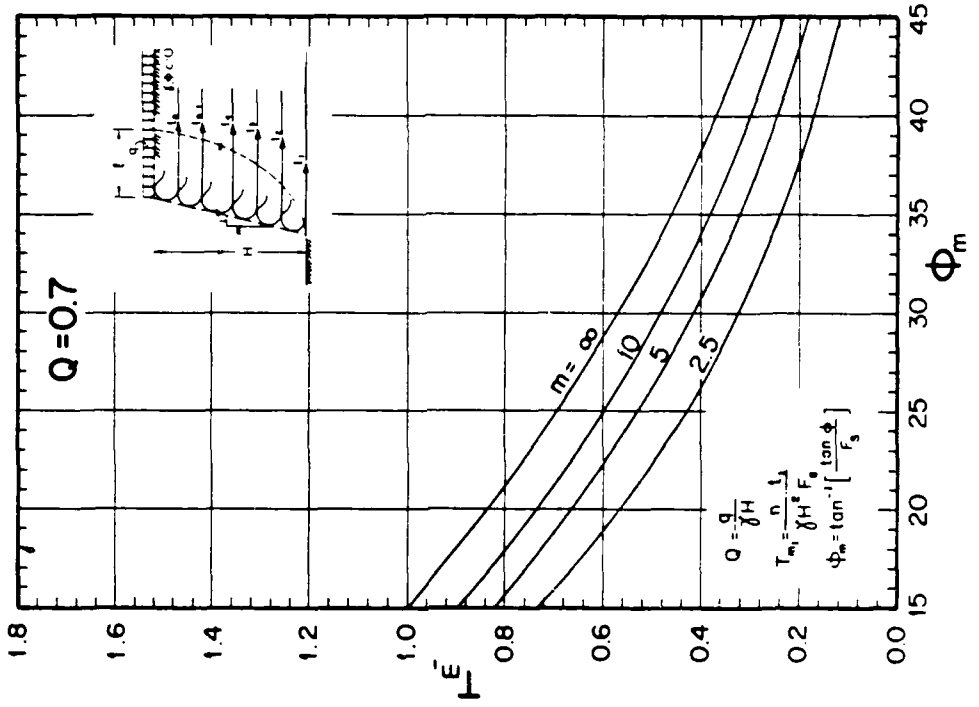

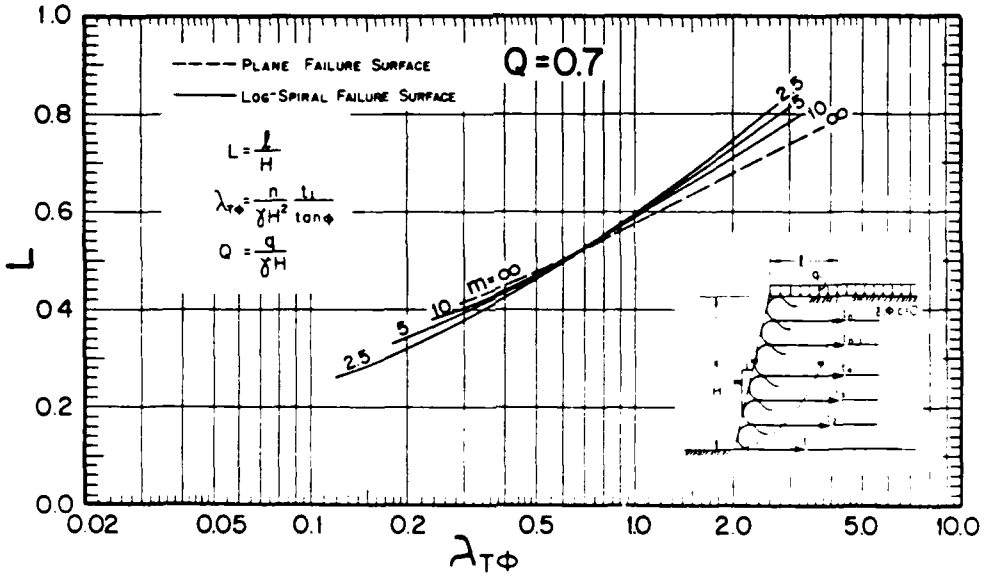

Figure 7-B-5. Stability chart
(uniform surcharge load of Q = 0.7)

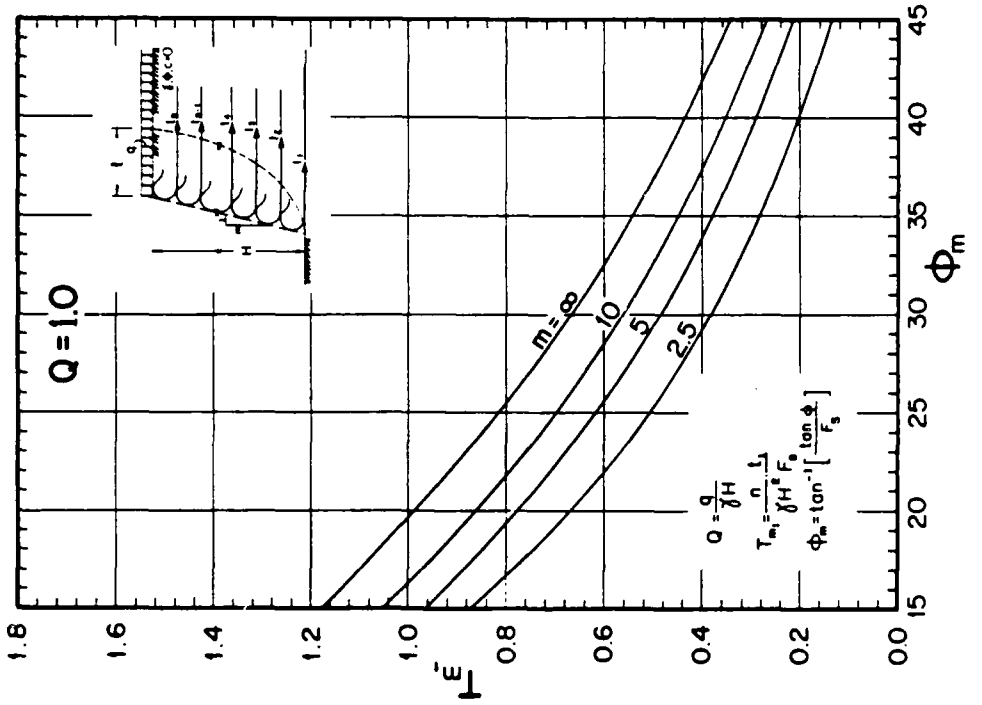

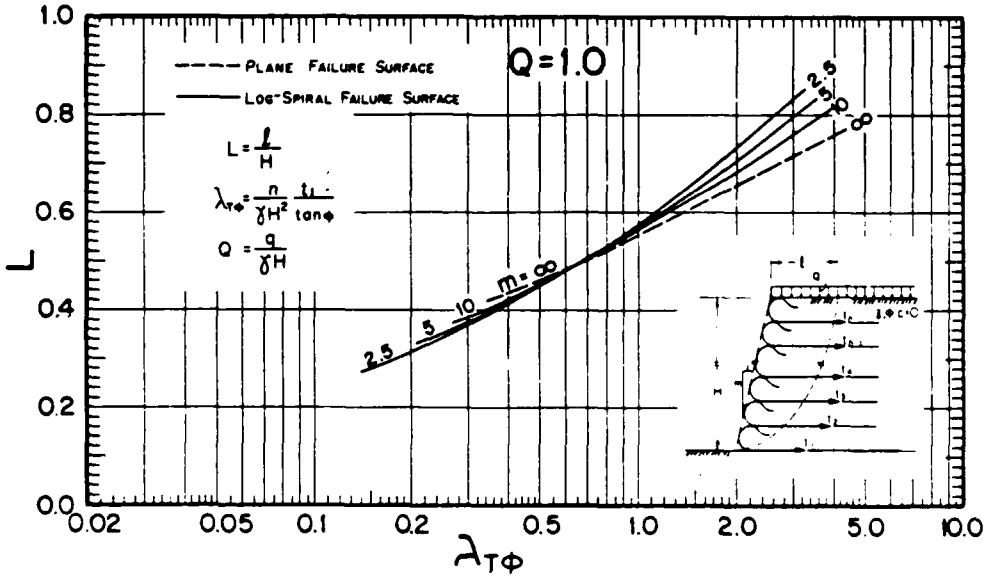

Figure 7-B-6. Stability chart (uniform surcharge load of Q = 1.0)

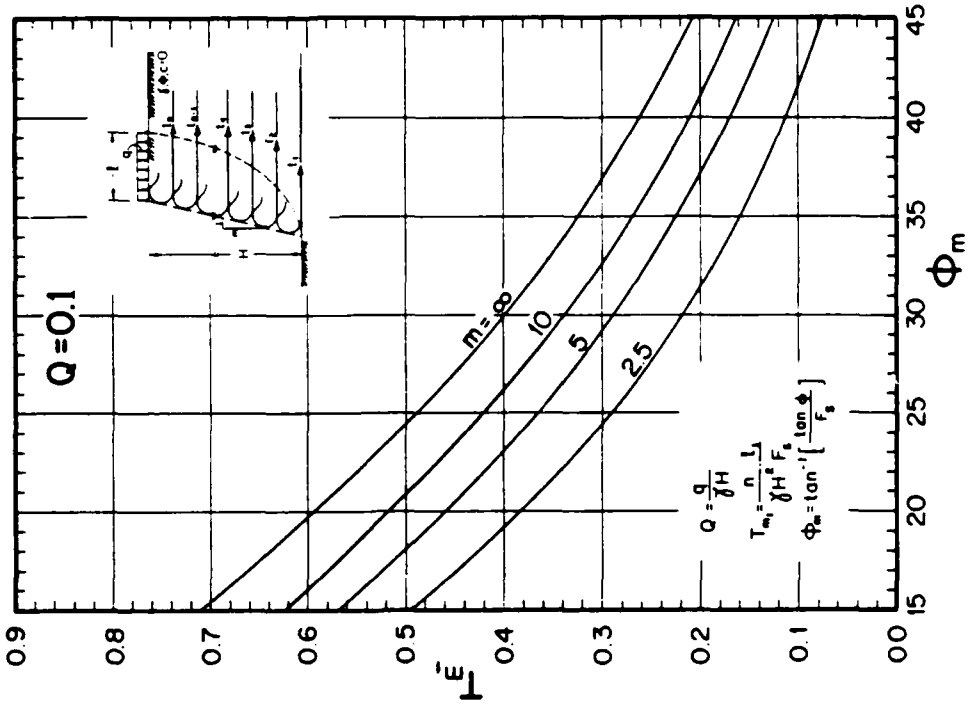

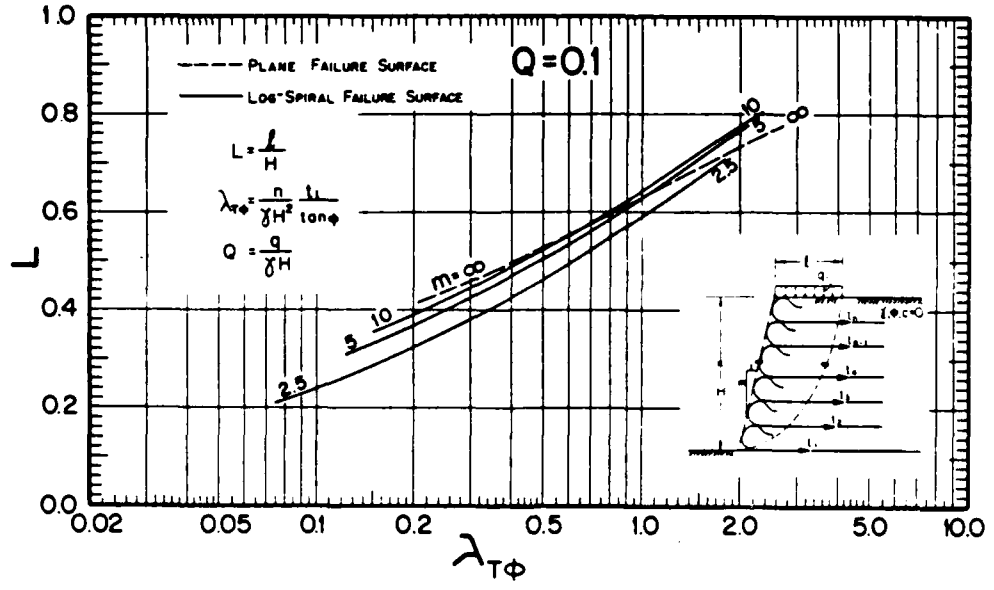

Figure 7-B-7. Stability chart
(strip surcharge load of Q = 0.1)

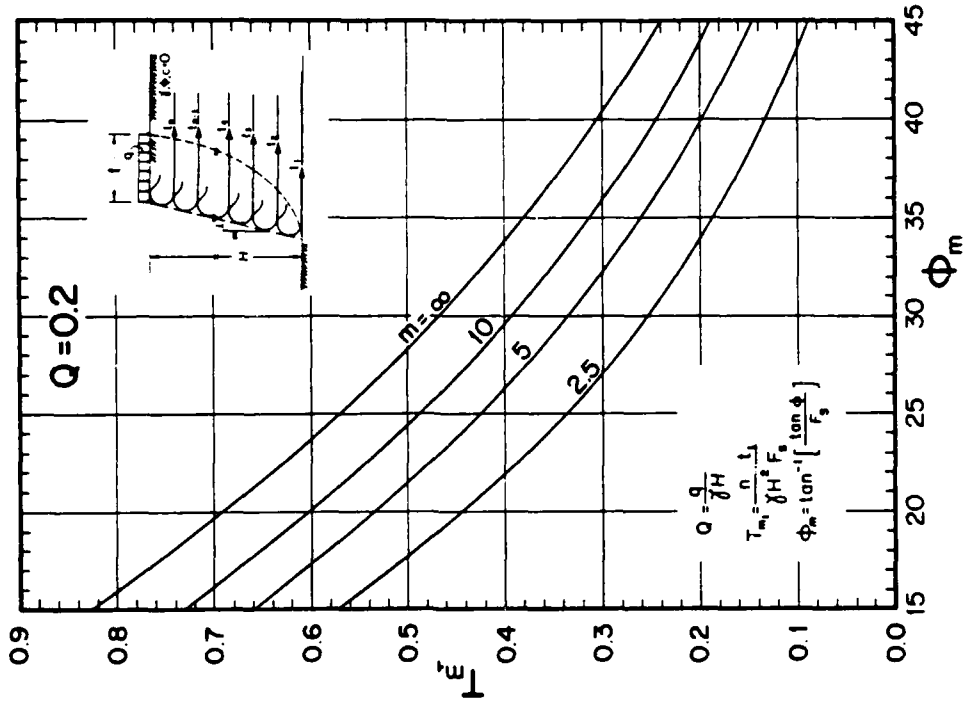

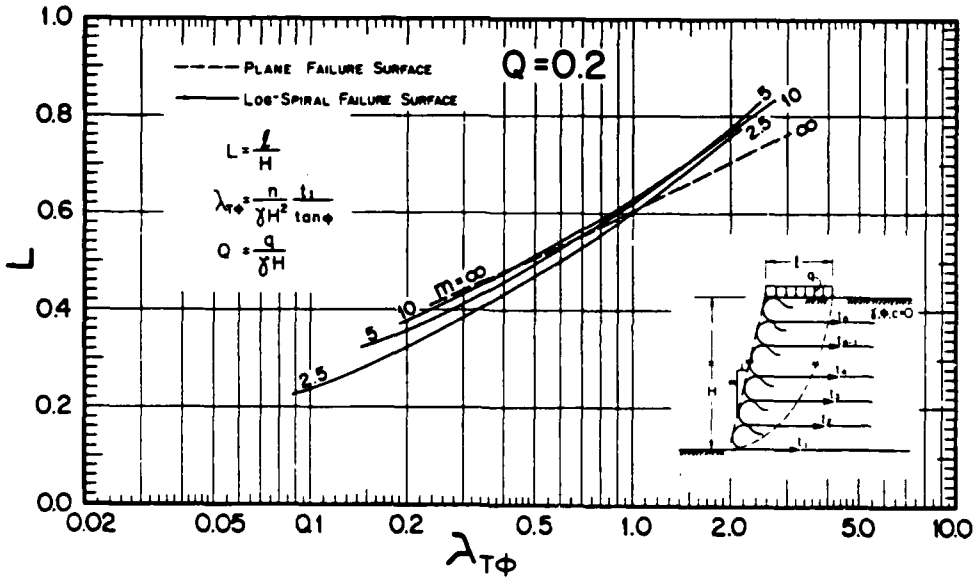

Figure 7-B-8. Stability chart (strip surcharge load of Q = 0.2)

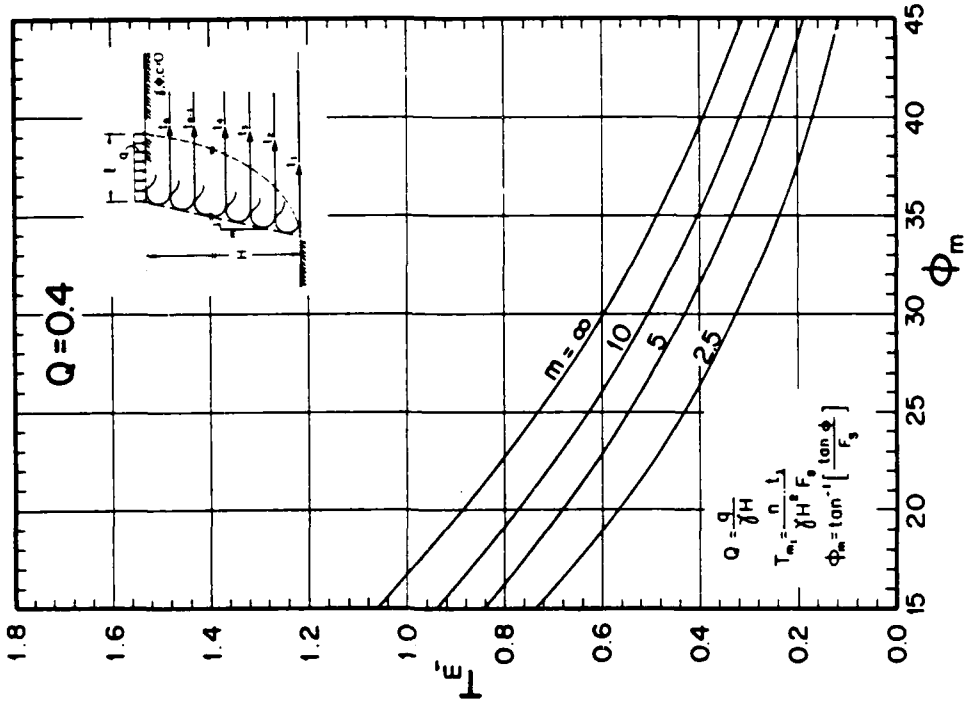

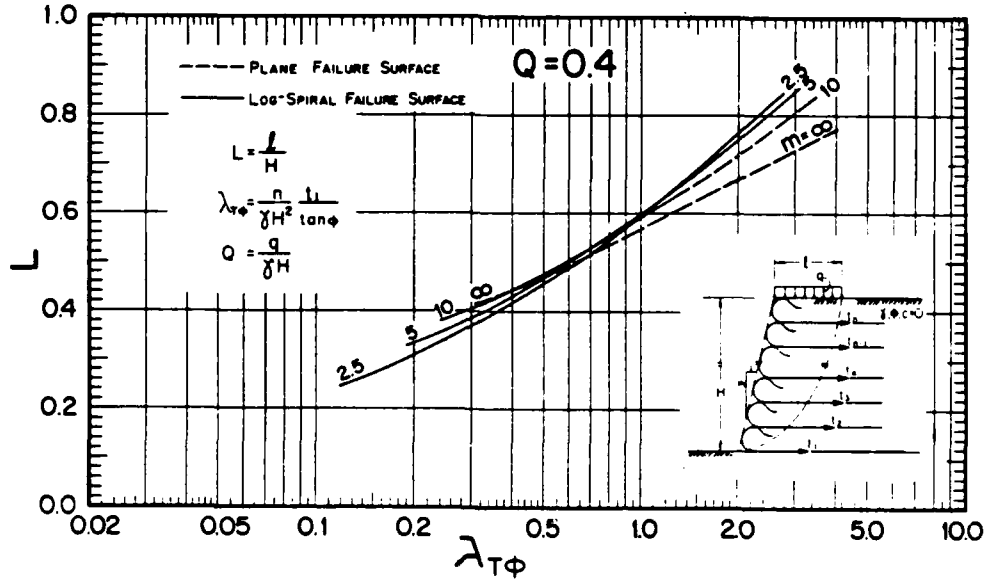

Figure 7-B-9. Stability chart
(strip surcharge load of Q = 0.4)

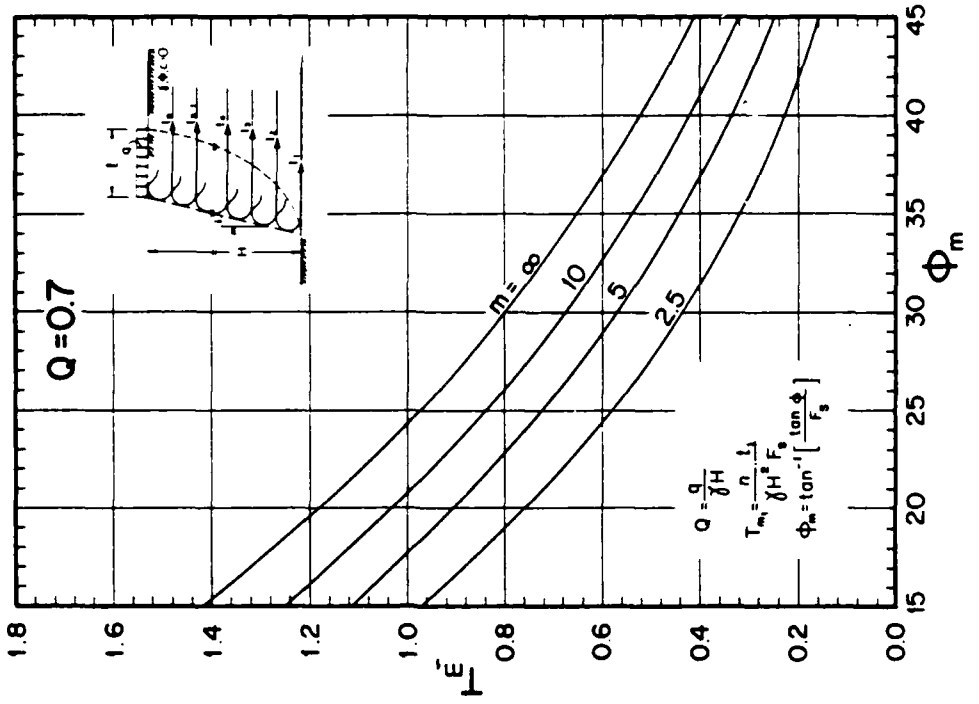

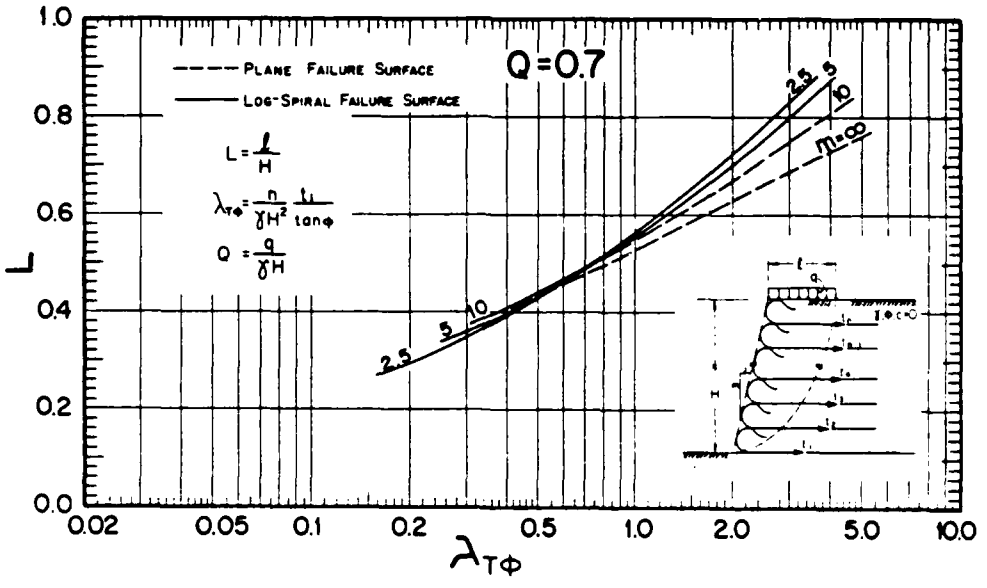

Figure 7-B-10. Stability chart
(strip surcharge load of Q = 0.7)

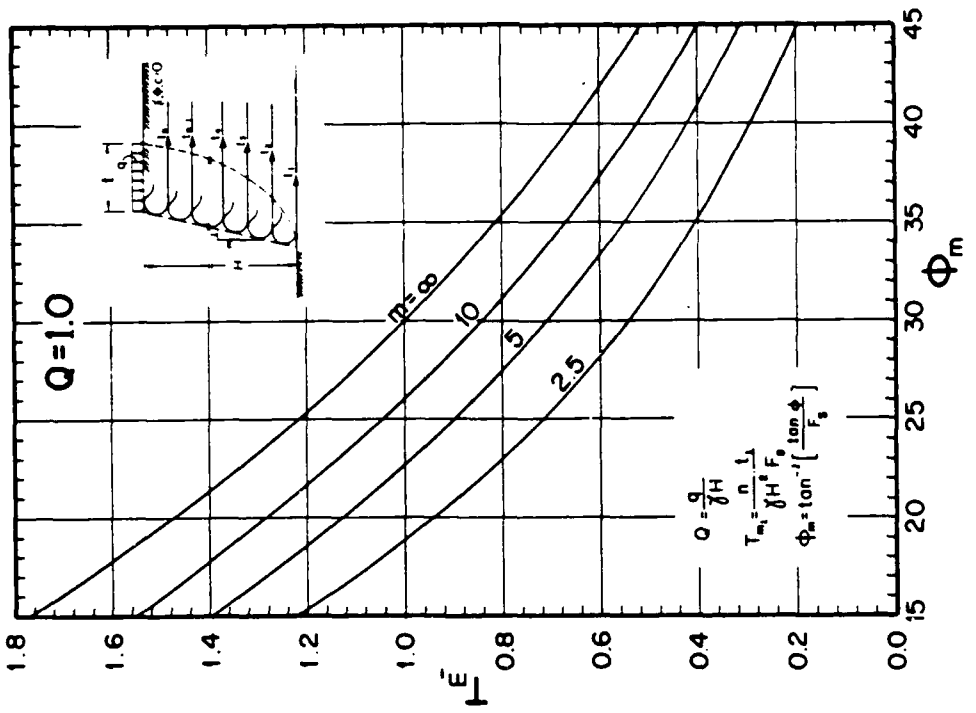

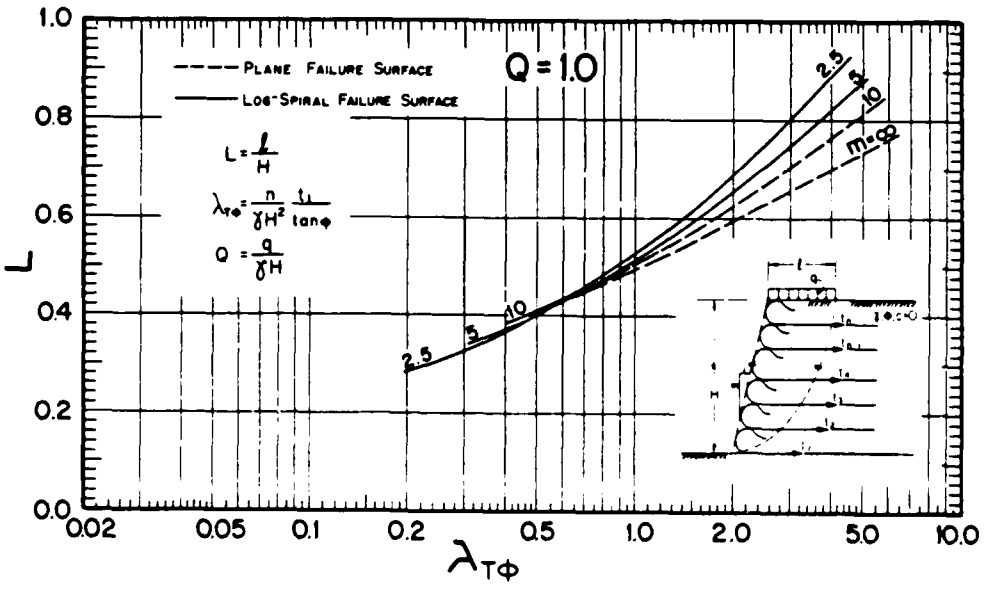

Figure 7-B-11. Stability chart
(strip surcharge load of Q = 1.0)

APPENDIX 7-C

NOTATION

The following symbols are used in sections 7-1 through 7-6:

A,B = constants;

$\bar{B}$ = effective foundation width;

c = cohesion;

d = geotextile sheets spacing;

e = eccentricity;

F_g = factor of safety with respect to a geotextile tensile resistance ($= t_j/t_{m_j}$);

F_s = overall factor of safety;

H = net height of wall;

i = inclination angle of the wall face;

K = lateral earth pressure coefficient;

ℓ = distance between the slip surface and wall face at the top of the wall;

ℓ_a = re-embedment length of a geotextile at the wall face;

ℓ_e = the embedded portion of a geotextile sheet along which tensile resistance develops;

ℓ_{e_1} = same as ℓ_e but for the first geotextile sheet (i.e., at the toe elevation);

M_R, M_E = moment resisting and tending to cause overturning of the wall, respectively;

m = wall face inclination ($m = \tan i$);

N = normalized cohesion ($= c/\gamma H$);

n = number of equally spaced geotextile sheets;

Q = normalized surcharge load ($= q/\gamma H$);

q = surcharge load acting on top of the wall;

q_a = surcharge load acting over ℓ_a;

q_e = surcharge load acting over ℓ_e;

R = normalized slip surface in polar coordinates or force reactions;

S = normalized stress ($= \sigma/\gamma H$);

T_j = normalized tensile resistance of geotextile sheet number j ($= nt_j/\gamma H^2$);

t_j = required tensile resistance of geotextile sheet number j;

t_{ult} = tensile strength of a geotextile;

W = weight of the reinforced wall;

X,Y = normalized cartesian coordinates ($= x/H$, $= y/H$);

X_c,Y_c = origin of the polar coordinate system;

y_j = elevation of geotextile sheet number j as measured up from the toe;

β = polar ordinate;

γ = soil unit weight;

θ_g = inclination of T;

$\lambda_{T\phi}$ = $(nt_1)/(\gamma H^2 \tan \phi)$;

μ_t, μ_b = coefficient of friction on top and bottom of a geotextile sheet, respectively;

σ = stress normal to the slip surface;

τ = stress tangential to the slip surface;

$\overline{\tau}$ = normalized shear stress (= $\tau/\gamma H$);

ϕ = internal angle of friction; and

ψ = $\tan(\phi)$.

Subscripts

b = backfill soil (applied to γ and ϕ only);

bc = bearing capacity (applied to F_s only);

F = foundation soil (applied to γ, ϕ and c only);

j = geotextile sheet number;

m = mobilized strength component (applied to ϕ, ψ, τ, N and T);

ot = overturning (applied to F_s only);

s = sliding (applied to F_s only).

END

DATE

FILMED

5-88

DTIC